The Late Quaternary paleoenvironmental changes in the high latitude North Atlantic based on foraminiferal record

A Thesis submitted in partial fulfillment for the Degree of

DOCTOR OF PHILOSOPHY

in the school of Earth, Ocean and Atmospheric Sciences
Goa University

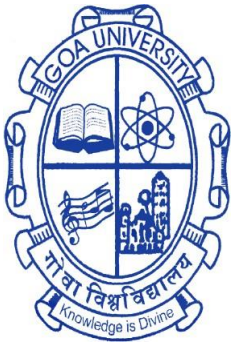

By

Nibedita Sahoo

National Centre for Polar and Ocean Research
Headland Sada, Vasco-da-Gama
Goa, India-403804

February *2023*

DECLARATION

I, Nibedita Sahoo hereby declare that this thesis represents work which has been carried out by me and that it has not been submitted, either in part or full, to any other University or Institution for the award of any research degree.

Place: Goa University.
Date : 07-02-2024 Nibedita Sahoo

CERTIFICATE

I hereby certify that the above declaration of the candidate, Nibedita Sahoo, is true and the work was carried out under my supervision.

Dr. Rahul Mohan
Group Director & Scientist
NCPOR, Goa

Acknowledgment

First and foremost, I would like to thank my supervisor, Dr. Rahul Mohan for his constant guidance and support throughout the research work. His words of motivation and encouragement to develop scientific curiosity were added to this research. I am indebted to his utmost patience and positive attitude in the ups and downs of this Ph.D. journey. The research also benefited from his broad knowledge in the field of micropaleontology and paleoclimate.

My sincere thanks go to the Directors of NCPOR, Dr. Ravichandran (Former Director), Dr. Javed Beg (Former Director-in-charge), and Dr. Thamban Meloth (Director) for supporting my research and providing the opportunity to carry out my research work in NCPOR. I am thankful to NCPOR, Ministry of Earth Sciences for supporting my research fellowship and the funding for radiocarbon analyses for the research work.

I express my gratitude to Dr. Rajiv Saraswat and Prof. C. U. Rivonker for their valuable suggestions and for assessing the research work throughout my Ph.D. course. Thanks to the faculty members and the administration of Goa University for assisting me in the Ph.D. process.

I cannot thank enough, Dr. Saalim Syed, for his mentorship and guidance in my Ph.D. The useful discussions in every aspect of the work have shaped this research. I am beholden to him for teaching me the grounding knowledge of ‘identification of foraminifera’ and ‘data interpretation’. His moral support and advice during the work boosted my motivation.

I am grateful to Dr. Alexander Matul for providing me with the samples for my Ph.D. His expertise in North Atlantic oceanography contributed to my understanding of the regional hydrography of the region. I would like to express my gratitude to Dr. Sanjeev Kumar for the analysis of the oxygen isotopic composition of planktic foraminifera. Special thanks to Dr. Ralf Schiebel and Lena Wurtle for the Mg/Ca measurement of planktic foraminifera.

I would like to express my sincere thanks to the entire team of the ‘Polar Micropaleontology and Past Climate’ group for their invaluable support and friendly working environment. The Gup-Shup sessions with Dr. Mahesh, Dr. Abhilash, Dr. Cheryl, Dr. Shabnam, and Dr. Shramik have integrated my perception of research in oceanography. Many thanks to Sahina, Vailancy, and Akshaya for the Scanning Electron Micrograph analyses of planktic foraminifera. Pallavi, Pooja, Hari, and Nuruzzama are to be specially mentioned for easing out everything with their informative and fun-filled conversations during and off the lab hours. I thank Ankita and Sweta for making all the strenuous paperwork and other official procedures effortless. I extend my thanks to Dr. Ravidas Naik, Dr. Shubham, Tarique, Tariq, Alok, Sunil and everyone from the institute for helping me in various ways during my Ph.D.

Appreciation for the people who made my Ph.D. life a memorable one outside the lab hours and were always available to hear me out and grab a coffee with me. Thanks to these wonderful people Rahul, Priyesh, Padma, and Kalpana who lessened the feeling of being away from home. Special thanks to my friends and my support team Jayashree, Farhin, Priya, Parag, and Vikram for always being there.

Above all, I thank my parents and family for their unconditional love and support throughout the years. Special mentions to my sisters and brothers for their encouragement and faith.

Dedicated to
My family and Friends

Abstract

The Subpolar North Atlantic (SPNA) Ocean plays a vital role in the global climate system as it is associated with deep-water formation, modulating the Atlantic Meridional Ocean Circulation (AMOC). AMOC is the term used for circulation involving the transformation of warm surface Atlantic water to cold deep water. The SPNA ocean displays a surface hydrographic variation by the interaction of various surface and deep water currents such as the North Atlantic Current, East Greenland Current, Labrador Current, Deep western boundary current, etc. Moreover, the North Atlantic Oscillation and subpolar gyre dynamics shape the upper watermass structure through complex ocean-atmosphere interactions. These variations in SPNA hydrography have been linked to the variation in AMOC strength both from modern observations and paleo studies. Hence, the SPNA ocean carries substantial significance in moderating the global climate and thus is the requisite for understanding past hydrographic variations in the SPNA. Since modern conditions are a continuation of the Holocene epoch, it provides the best framework to study the hydrographic variability of the SPNA and the associated factors. Due to their omnipresent characteristics, good preservation, sensitivity to subtle environmental changes, and preference for specific watermass habitats, planktic foraminifera are among the best paleo-proxies for surface hydrography reconstruction. In the present study, Holocene SPNA hydrographic variations have been reconstructed using planktic foraminifera proxies from a sediment core in the SPNA ocean, southwest of Iceland. Additionally, the modern distribution of the planktic foraminifera assemblages in the region has been explored using surface sediment samples collected along an east-west transect at 59.5°N.

This study documents a significant variation in the planktic foraminiferal assemblages in the SPNA ocean from east to west, influenced by the regional hydrography. A clear gradient has been displayed especially in the percentages of *Neogloboquadrina pachyderma* and *Neogloboquadrina incompta* along the transect, governed by the upper watermass attributes, temperature, and salinity. The SPNA assemblages were distributed into three major groups based on their occurrence and relation with the environmental parameters.

The Holocene hydrographic variations in the SPNA were documented in three major phases during the Holocene. An early warm phase with retreating meltwater influence at the site and increasing North Atlantic Current influence was recorded with increasing warm and subpolar planktic foraminiferal species at the site. Additionally, near-surface warming was recorded at the site during the early Holocene phase. The mid-Holocene was a cooling phase as reflected in the near-surface temperature, explained by a decreased warm NAC influence at the site. The late Holocene was unstable as compared to the early and mid-Holocene variations. This period was characterized by oscillating temperature and salinity variations, complied with the enhanced EGC strength and advance and retreat of the subpolar water over the studied region. The 8.2 ka event from the early Holocene, indicating the final discharge of the Laurentide Ice sheets was recorded in our near-surface temperature and salinity data. When compared to deep water mass variability records from the Holocene, the decline in the NADW formation was reflected in the surface hydrography, explained by complex subpolar dynamics. Hence, the surface hydrography in the SPNA ocean could be linked to the variations in AMOC strength.

Abbreviations

AMOC	Atlantic Meridional Overturning Circulation
BP	Before Present
DSOW	Denmark Strait Overflow Water
DWBC	Deep Western Boundary Current
EGC	East Greenland Current
ENAW	Eastern North Atlantic Water
IC	Irminger Current
IFSC	Iceland-Faroe-Shetland Channel
ISOW	Iceland-Scotland Overflow Water
LC	Labrador Current
LSW	Labrador Sea Water
MNAW	Modified North Atlantic Water
NAC	North Atlantic Current
NADW	North Atlantic Deep Water
NAO	North Atlantic Oscillation
SPF	Subpolar Front
SPG	Subpolar Gyre
SPMW	Subpolar Mode Water
SPNA	Subpolar North Atlantic
SSS	Sea Surface Salinity
SST	Sea Surface Temperature
STG	Subtropical Gyre
TPF	Total Planktic Foraminifera
WGC	West Greenland Current
WNAW	Western North Atlantic Water

TABLE OF CONTENTS

List of Tables

List of Figures

Chapter 1

1. Introduction

The post-industrial period has posed the most 'what-if' questions about the vulnerability of the global climate to increasing warming due to anthropogenic activity (IPCC, 2022). The few most critical questions are, (a) what happens if the global temperature continues to rise at the same rate and those projected at different Representative Concentration Pathways (RCP) scenarios (IPCC, 2020); (b) what happens if the Arctic ice completely disappears? ; (c) what happens if the glacial ice sheets on the larger land masses, such as Greenland and Antarctica experience excessive melting and (d) How the global oceans and climate will respond if the Atlantic Meridional Overturning Circulation slows down etc. Previously, several efforts have been made to answer these questions based on in-situ observations and using climatic models. However, the sensitivity of such climate models relies on the climatic records collected since the 18^{th} century using in-situ instruments and satellites and utilizing paleoclimatic information, reconstructed using various land-ocean proxies. However, these data sets are limited and there is a need to obtain high-resolution information to improve the climate models for better climatic predictions. The previous observations revealed that the changes occurring in the polar regions (e.g. Arctic) not only impact the regional environment but also show effects on the other climatic processes (e.g. Indian Monsoon) through atmospheric teleconnection (Burke et al. 2017; Francis et al. 2017). Thus, it is critical to understand the factors underlying these high-latitude climatic changes and the extent to which they would impact the other geographic regions.

1.1. The Northern high latitude regions: present climatic scenario

The increased atmospheric temperature and CO_2 concentrations are responsible for increased extreme weather events, increasing sea-level rise, increased sea ice extent, decreasing polar ice sheets, etc. which already have affected the global economy, public health, and land-ocean ecosystem. Recent investigations also reveal that in the past few decades, the polar regions have become more vulnerable to the increased rate of CO_2 and warming (IPCC, 2022). For instance, Antarctica is losing more ice sheets (Shepherd et al., 2018) with the unusual temperature rise

(Vaughan et al., 2003), whereas the Arctic is experiencing a three-times increase in its surface temperature than the global average in the last 40 years (polar amplification) (Serreze et al., 2009; AMAP 2021). This, in turn, amplifies global climate change through a positive feedback loop (Winton 2006; Serreze et al. 2009).

The sea-ice extent in the Arctic has come to a record minimum on 17th September 2012 (arctic summer) measuring 3.39 million square kilometers, with an average loss of 10-15 % per decade based on the last 40–50 years' data (Comiso and Nishio, 2008; Cavalieri and Parkinson, 2012; Comiso, 2012; Meredith et al. 2022). Greenland is also losing its ice sheets in an unprecedented manner since 1990 (Hanna et al., 2013). The freshwater from the melting Arctic Sea ice adds to the watermass of the Nordic Seas and the high-latitude North Atlantic Oceans through the Fram Strait, the Canadian Arctic Archipelago, and the Greenland-Scotland ridge (Li and Federov, 2021). Additionally, Greenland has contributed significantly to the North Atlantic's freshwater budget since 1960 (Dukhovskoy et al., 2019). The long-term freshening events in the North Atlantic reorganize the upper watermass structure in these regions and impact the necessary pre-conditioning process for deep water formation. Deep water formation in Nordic seas and the high latitude North Atlantic Ocean is associated with Atlantic Meridional Overturning Circulation (AMOC), an integral part of the Global thermohaline circulation. AMOC helps the redistribution of heat and carbon to the global oceans (Srokosz and Bryden, 2015; Buckley and Marshall, 2016). Thus, these changes in sea ice and ice sheets have the potential to impact the global climate through the Atlantic Meridional Overturning Circulation (AMOC) trend (Aagaard et al., 1985; Aagaard & Carmack, 1989; Haak et al., 2003; Jungclaus et al., 2005; Jahn & Holland, 2013; Boning et al., 2016; Nummelin et al., 2016; Sévellec et al., 2017; Thornalley et al., 2018). Climate models have predicted that if the present warming continues to occur at the same rate, there will be consequences on various climatic elements based on different emission scenarios (Representative Concentration Pathways, RCPs; IPCC 2022). These models suggest that the Arctic would be ice-free in the summers as early as the 2030s (Wang & Overland, 2012). In addition, the AMOC has been predicted to decline in the 21st century (IPCC, 2001).

1.2. Role of Subpolar North Atlantic Ocean in Global Climate (SPNA)

The potential drivers in the SPNA as identified in various studies are AMOC, NAO, and Subpolar Gyre. These are closely linked and affect the variability of one another.

1.2.1. Atlantic Meridional Overturning Circulation (AMOC)

Since AMOC has been closely associated with abrupt climate change (Broecker et al., 1985; Rahmstorf, 2002) and SPNA is the main component of AMOC, hence understanding the SPNA hydrography variability, its factors and its impacts on AMOC is an essential requisite.

Global ocean circulation is driven by processes comprising wind-driven surface currents and density gradient-driven deep ocean currents (Fig. 1.1). The warm and saline surface currents from the tropics and subtropics are carried by the wind system toward the poles, where they gain density by losing heat to the atmosphere. This dense water sinks to the bottom, forming a mass of deep water and the deep water then circulates to other oceans following the topography. This ocean conveyor belt distributes heat and salt to the global oceans and controls the climate system. In the Atlantic Ocean, part of this conveyor belt is known as the AMOC. In the Atlantic Ocean, AMOC accounts for a net equatorward ocean heat transport in the Southern hemisphere (0.5 PW Dong et al., 2009; Trenberth et al., 2019) while at northern midlatitudes, this explains around two-thirds of the oceanic northward heat transport (Johns et al., 2011; Trenberth et al., 2019). Moreover, a change in AMOC has been cited to be a critical global climate modulator, especially when an ‘abrupt climate transition’ has been recorded in the geological past (Rooth, 1982, Broecker et al. 1985, 1988, 1989, 1990; Broecker & Denton, 1989; Broecker 1994, 1997, 1998).

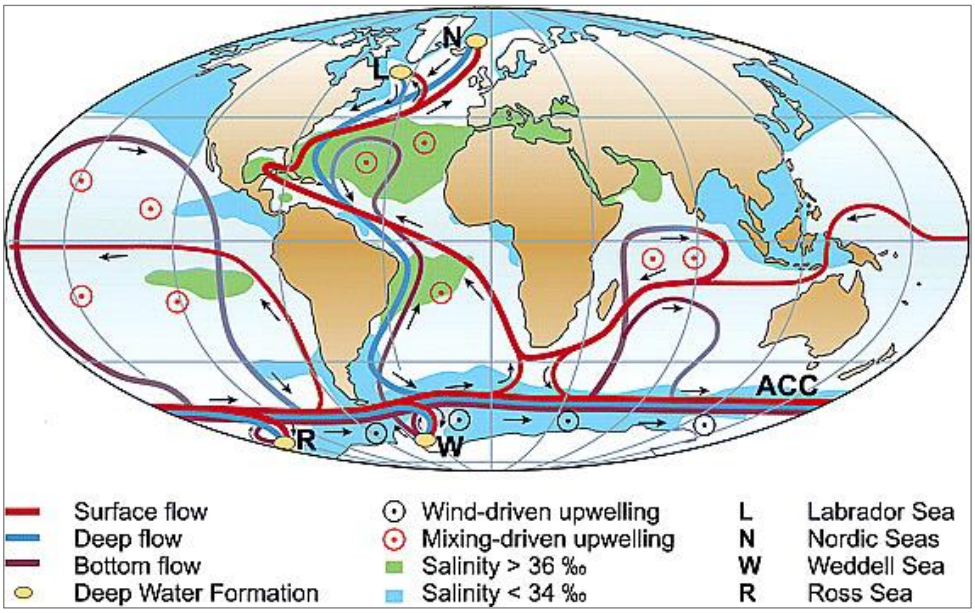

Fig. 1.1. Map showing global thermohaline circulation. Source: Kuhlbrodt et al., 2007 (after Rahmstorf, 2002)

The warm saline surface current and the cold deep current comprise the upper and lower limbs of AMOC, respectively. As Subpolar North Atlantic paves the way for the exchange of warm saline surface water from subtropics to the convection sites and contains one of these major convection sites in the Labrador Sea, hence forms an important part of the AMOC. The SPNA is a region between 45°N to 65°N latitude and 0 to 75°W longitude. This region plays a crucial role in global thermohaline circulation. The eastern SPNA receives warm water through the North Atlantic Current, an offshoot of the Gulf Stream, which makes the upper limb of AMOC in SPNA (Fig. 1.2). This water loses heat by continuous ocean-atmospheric interaction and mixing with the surrounding water mass along its way to the Labrador Sea. Also, cold freshwater from the Arctic enters the Labrador Sea via the East Greenland Current along the eastern coast of Greenland. By winter convection, this upper water mass forms the intermediate water mass, Labrador Sea water (LSW). The deep water mass formed in the Nordic seas enters SPNA as overflow water mass through Greenland-Scotland Ridge and Denmark Strait. The LSW, together with these overflow watermass, forms the North Atlantic Deep Water (NADW) and flows southward as a deep western boundary current. This deep water mass forms the lower limb of AMOC. LSW significantly contributes to the NADW (de Carvalho Ferreira and Kerr, 2017) and thus modulates the strength

of AMOC. An increase in the freshwater influx from the Arctic decreases the density of the upper water mass and therefore has an impact on the LSW formation. Moreover, the Atlantic water influx to the eastern SPNA is governed by the relative contribution of the subpolar and the subtropical waters (Hatun et al., 2005; Holliday et al., 2008; Sarafanov, 2009).

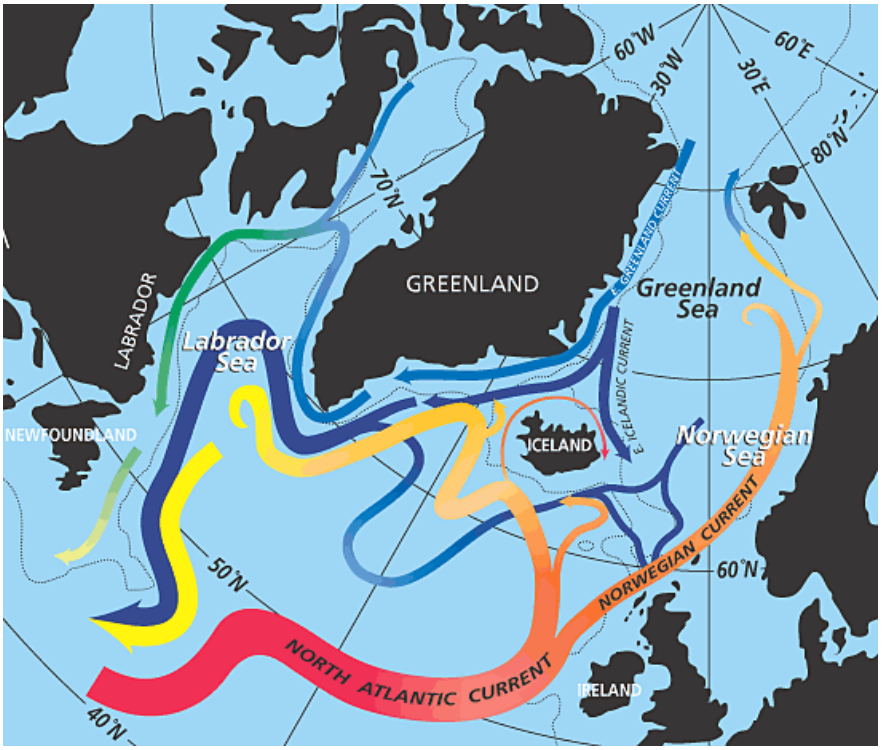

Fig. 1.2. Components of Atlantic Meridional Overturning Circulation in Subpolar North Atlantic Ocean**. Source:** https://www.whoi.edu/oceanus/feature/north-atlantics-transformation-pipeline-chills-and-redistributes-subtropical-water/

1.2.2. North Atlantic Oscillation (NAO)

The boreal winter (December-March) sea level pressure gradient in the North Atlantic accounts for a major part of the North Atlantic climate variability. This dominant atmospheric pattern over the North Atlantic is known as North Atlantic Oscillation (NAO) (Hurrell, 1995). The winter NAO alone accounts for the interannual variation of the mean winter surface temperature in the Northern Hemisphere (Hurrell, 1996). This oscillation arises due to the sea level pressure difference between the Icelandic low and the Azores high. The variability in NAO is described in two phases, a positive and a negative phase. When the sea level pressure difference in both regions is higher than usual, a positive NAO (NAO^{+})

prevails, and a lower difference, in the case of negative NAO (NAO^-). NAO^+ brings stronger westerlies over the subpolar oceans and is responsible for a warmer winter and more storminess in northwest Europe, whereas NAO^- is related to weakened westerlies with cooler winters and less storminess over northwest Europe (Fig. 1.3).

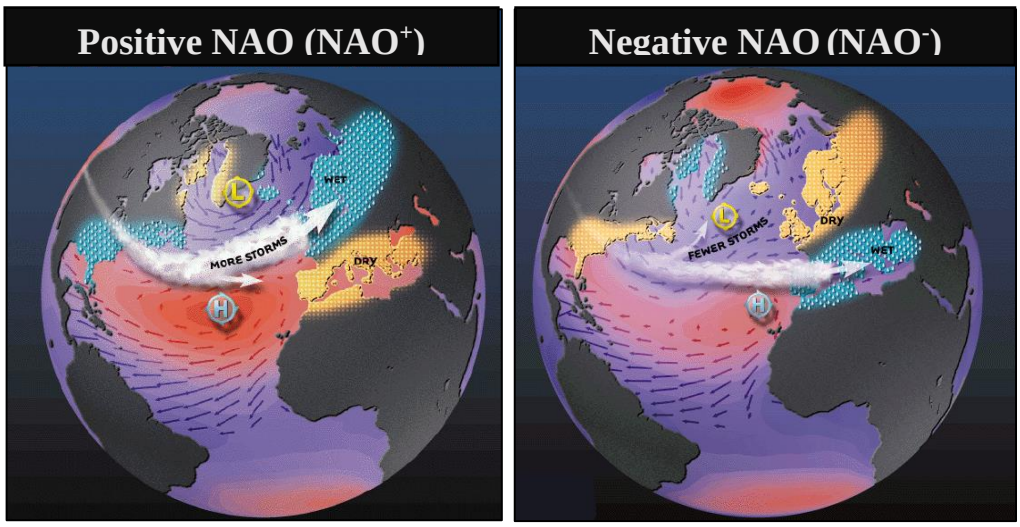

Fig. 1.3. The positive (left) and negative (right) phases of the North Atlantic Oscillation illustrate the weather patterns experienced over the Northern hemisphere region for each phase. Source: https://www.ldeo.columbia.edu/res/pi/NAO/

The origin of the NAO variability has been ascribed to external factors like stratosphere-tropospheric interaction (Scaife et al., 2005), volcanic aerosols (Fischer et al., 2007), solar activity (Shindell et al., 2001) and the internal factors in the extratropical atmospheric dynamics (Woolings et al., 2008). Changes in sea-ice and land snow cover (Deser et al., 2010), ocean-atmospheric feedback (Lau, 1997; Visbeck et al., 2003), SST in the North Atlantic Ocean (Marshall et al., 2001) also are closely related to the trends in NAO. The SSTs in the tropical Indian Ocean and Pacific are also likely to affect the NAO pattern (Hoerling et al., 2001; Müller et al., 2008).

NAO phases have been monitored since the 1860s till today. The pattern has been seen to swing between the positive and negative modes. A prominent negative NAO was documented in the winters of 2009/10 and 2010/11 in the last 150 years (Cattiaux et al., 2010; Jung et al., 2011). Since then, a positive NAO mode has been leading the atmospheric pattern of the North Atlantic (Fig. 1.4).

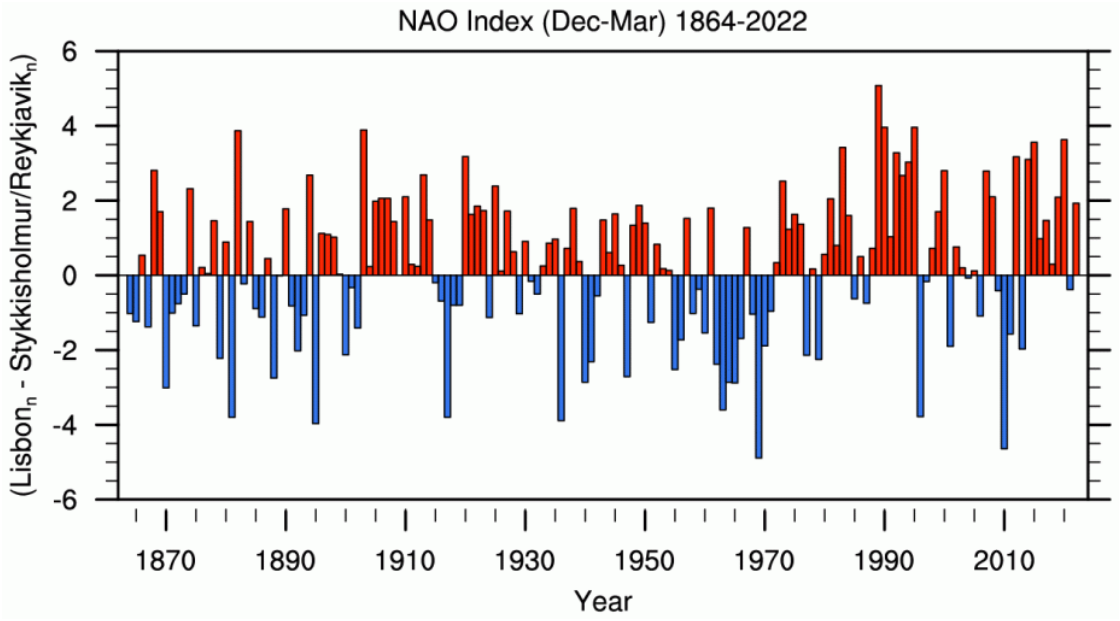

Fig. 1.4. A station-based winter (Dec-March) NAO index from 1864-2022. NAO index is measured as the sea level difference between Stykkisholmur/Reykjavik and Lisbon, Portugal. Source: https://climatedataguide.ucar.edu/climate-data/hurrell-north-atlantic-oscillation-nao-index-station-based

1.2.3. Subpolar Gyre (SPG)

The surface circulation in the SPNA ocean is driven by a cyclonic geostrophic gyre known as the Subpolar Gyre (SPG). North Atlantic Current (NAC) and Irminger Current (a derivative of the NAC) form the eastern part of the gyre. NAC brings warm and saline water from the Gulf stream to northeastern SPNA. The cold East Greenland Current (EGC), West Greenland Current (WGC), and the Labrador Current (LC) form the gyre's western part. The Gyre and the currents are believed to be governed by the combination of wind stress curl over the eastern SPNA region and the buoyancy forcing caused by heat flux over the Labrador Sea (Hakkinen and Rhines, 2004). The studies show that NAO^+ is related to a stronger SPG, which causes an eastward expansion of the SPG, decreasing the salinity of the water mass in the Northeast SPG. Whereas a negative NAO is related to a westward contraction of SPG, allowing more passage for the advection of subtropical water to the northeastern SPNA, thereby increasing the salinity of the inflow water. These variations are observed in a decadal to multi-decadal timescale. The subpolar front, which separates the subtropical warm water in the south from the cold subpolar water to its north, also shifts its position with the changing subpolar gyre strength.

Strengthening of SPG shifts this front to the southeast, with the subpolar water influencing the eastern SPNA region, and a retreat is caused by a weak SPG (Sarafanov et al., 2008; Núñez-Riboni et al., 2012).

SPG strength is also influenced by the influx of freshwater from the Arctic through EGC (Sundby and Drinkwater, 2007; Thornalley et al., 2009; Born et al., 2010). The addition of freshwater in the Labrador Sea alters the density structure in the SPNA region. This can cause a decrease in the northward heat flow via NAC.

Hatun et al. (2005) and Hakkinen and Rhines (2004) have recently suggested a link between the salinity of the NAC water in the eastern SPNA with the relative strength of both SPG and STG. A stronger SPG with an eastward expansion contributed to less saline NAC water in the northeastern SPNA, whereas a weak and contracted SPG resulted in a relatively more saline NAC water with a higher contribution from the STG water. An AMOC weakening is also a potential modulator of the strength of SPG by changing the heat balance.

The complex relation between AMOC, NAO, and SPG strength is responsible for the observed variability in the SPNA ocean including the sea surface temperature, salinity, and the faunal distribution pattern.

1.3. Observations of SPNA variability and related climatic factors from the Instrumental era

A negative temperature anomaly against the northern hemispheric trend has been observed in the subpolar oceans since 2005 which is termed the ‘warming hole’ (Rahmstorf et al., 2015; Robson et al., 2016; Thornalley et al., 2018; Ceasar et al., 2021). This cooling in the SPNA has been suggested to be related to the ongoing AMOC decline but also can be triggered by SPG dynamics (Jungclaus et al., 2014; Sgubin et al., 2017). A weakened AMOC restricts the northward heat distribution, which creates a cooling SPNA. This hypothesis also suggests an increase in the storage of heat south of the subpolar ocean in the Gulf Stream (Caesar et al., 2018), thus an out-of-phase relation between SPG and STG can be used as a fingerprint of AMOC (Caesar et al., 2018).

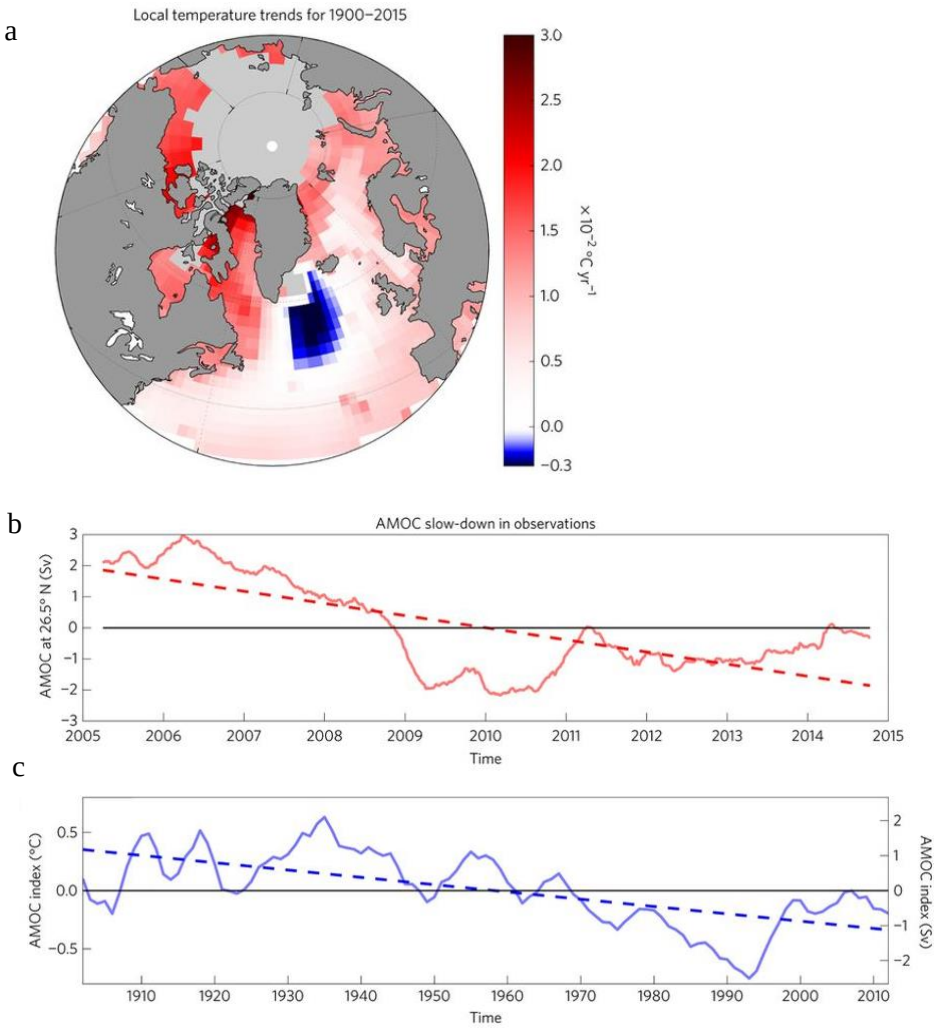

Fig. 1.5. a. The map shows a negative temperature anomaly in the subpolar ocean termed as a 'warming hole' in the local surface air temperature trend of the North Atlantic over 1900 to 2015. A decline in the AMOC strength was observed from **b.** AMOC index at 26.5°N from the RAPID array from 2005 to 2015 and **c.** reconstructed AMOC index (subpolar temperature minus Northern hemisphere temperature) from 1900 to 2010. Source: Sevellec et al., 2017

Given the IPCC projections of AMOC decline and its sensitivity to climate change, recently several observation systems have been deployed for direct monitoring of AMOC. Some of these effective programs are OSNAP (Overturning in the Subpolar North Atlantic Program, Lozier et al., 2017) at 53-60°N in the SPNA region since 2014, RAPID-MOCHA (Rapid Climate Change-Meridional Overturning Circulation and Heat flux Array, Cunningham et al., 2007) at 26.5°N in the subtropical North Atlantic since 2004, MOVE (Meridional Overturning Variability Experiment; Kanzow et al., 2006) at 16°N since 2000, SAMBA (the

South Atlantic MOC Basin-wide Array; Meinen et al., 2013) at 34.5°S in the South Atlantic since 2009. All these programs provide the necessary data to study AMOC variability. The RAPID-MOCHA at 26.5°N data indicates a mean AMOC strength of 17.7 ± 0.3 Sv between 2004 and 2018 (Smeed et al., 2019). Similarly, 14.6 Sv, 15.6 ± 0.8 Sv, and 2.1 ± 0.3 Sv of the mean AMOC strength have been estimated from the SAMBA, OSNAP East, and OSNAP West arrays, respectively (Frajka-Williams et al., 2019; Lozier et al., 2019). Besides this, Rahmstorf et al. (2015) have used an AMOC index based on the mean temperature difference between the subpolar region and the North Atlantic region to show a gradual decline in the strength of AMOC since 2004 (Fig. 1.5). A combined study of subpolar hydrographic changes and AMOC variability suggested no difference in AMOC strength despite the significant variability in the SPNA hydrography (Fu et al., 2020).

A strengthened SPG during 1995 was documented as a response to the persistent positive NAO forcings from 1989 to 1995. A consistent positive NAO results in a weakened SPG state after around 10+ years due to the warm water advection with the positive NAO forcing (Lohmann et al., 2009a). This created a difference in buoyancy forcing in SPG and combined with the negative NAO phase during 1995/96, where the SPG abruptly weakened (Lohmann et al., 2009b).

These modern observations disclose numerous anomalies in the SPNA in terms of subpolar gyre dynamics, AMOC strength, NAO patterns, and increased freshwater fluxes in a post-industrial climate change scenario. But whether these anomalies are solely exerted by the increased anthropogenic sources, or a part of the natural climatic variability is a challenging question and cannot be solved with the timescale of the modern dataset. The instrumental records are restricted only up to the last ~100-150 years, thus, we have only limited knowledge from these observations.

Therefore, it is essential to look at the proxy records before modern sample datasets which provide crucial information on how the climate has evolved in the geological record in response to the natural forcing. In addition, these proxy records provide a broader and long-term picture of how the SPNA hydrography has changed over time and to what extent these changes impact the global climate.

Among the past periods, the Holocene period is crucial to investigate due to its similar boundary conditions with modern-day e.g., the configuration of continents and ice sheets, sea level, atmospheric CO_2 levels, etc. (Vasskog et al., 2015; Bova et al., 2021; Farmer et al., 2021) which provides a suitable framework to understand the recent climatic changes.

1.4. Holocene: an overview

Though the Holocene has been described as a relatively stable period than the previous glacial and interglacial periods (Grootes and Stuiver, 1997), the emerging Holocene records have proved it to be a period associated with rapid climatic changes (RCCs, Mayewski et al., 2004), and Bond events of the 1500-year cyclicity (Bond et al., 1997). These abrupt changes contrary to the previously believed stable Holocene have been observed in marine records (Bond et al., 1997; Klitgaard-Kristensen et al., 2001; Andersen et al., 2004; Mayewski et al., 2004, Wanner et al., 2011), atmospheric records (O'Brien et al., 1995; Alley et al., 1997) and terrestrial records (Denton and Karlén, 1973). In the present interglacial, the Holocene is more peculiar to the North Atlantic, attributed to the complex feedback mechanisms involved with ice sheets, sea ice, and linked ocean-atmospheric dynamics (Rahmstorf, 1997; Clark et al., 2002). Majorly the Holocene has been classified into three major phases, (1) early progressive warming starting with deglaciation, (2) a mid-warm phase known as the Holocene Climatic Optimum, and (3) a relatively cold phase, the Neoglacial in the late Holocene (Walker et al., 2012). However, the temporal and spatial evolution of these Holocene changes is not homogeneous across SPNA. The early Holocene warm period has been justified by the increased orbital-driven solar insolation during the early Holocene (Leduc et al., 2010). However, the presence of the remnant ice sheets in the Northern Hemisphere caused a spatial difference across the North Atlantic through a complex behavior of insolation and ice-sheet feedback (Heikkilä and Seppä, 2003; Kaufman et al., 2004). This created a delay in the Holocene thermal Maximum in the western North Atlantic compared to the eastern Atlantic. When the Laurentide ice entirely retreated after 8-7 ka BP, the North Atlantic achieved a stable climate with a modern-like SPNA circulation pattern by establishing the formation of Labrador Sea water (Hillaire-Marcel et al., 2001; Hoogakker et al., 2011; Kissel et al., 2013). Whereas, with the decline in solar insolation in the northern hemisphere, a relatively

cold phase prevailed after 4 ka BP with glacial advances. These long-term phases in the Holocene have been explained by the variation in the orbital-driven solar insolation (Nesje and Johanssen, 1992).

Superimposed on these long-term trends, there have been millennial-scale oscillations in the North Atlantic e.g., 1500-year cycles as in Bond-events (Bond et al., 1997), and rapid climatic events of Mayewski et al. (2004). These events have been related to the solar irradiance variation (Bond et al., 2001; Hu et al., 2003; Renssen et al., 2006) with the internal ocean-atmospheric feedback (Wanner et al., 2011). In the late Holocene, there were centennial-scale oscillations across the North Atlantic, such as the warm Medieval climate anomaly and the cold Little Ice Age (LIA) (deMenocal et al., 2000; Andersson et al., 2003; Trouet et al., 2009; Ólafsdóttir et al., 2010). The most recent warm and cold events were preceded by post-industrial warming. The existence of these oscillations in the SPNA was mainly due to the advance and retreat of the cold fresh water in the North Atlantic associated with subpolar gyre dynamics and atmospheric oscillations (Thornalley et al., 2009; Staines-Urias et al., 2013; Moffa-Sanchez and Hall, 2017).

As there is not enough evidence to reconstruct the past NAO mode variability, only a few studies reconstructed the proxy-based NAO (Appenzeller et al., 1998; Cook et al., 1998; Trouet et al., 2009, 2012; Pinto and Raible, 2012). This lack of evidence from the past makes it difficult to track if there was an NAO-like atmospheric influence on the SPNA hydrography, and if present, how it has been varied. Based on the present data, some studies in the SPNA region have linked the variation in hydrography to today's NAO-like pattern (Rimbu et al., 2004; Staines-Urias et al., 2013). These studies suggested a strengthened gyre in a possibly positive NAO-like condition during the early phase of the Holocene and a negative-NAO-like forcing with the weakened SPG during the mid-Holocene. Similarly, the position of the Subpolar front has been used as a potential SPG strength indicator for the Holocene (Rasmussen et al., 2003; Moros et al., 2012). These studies show that the SPG strength dynamics have a bigger role in modulating the SPNA climate in addition to the insolation and volcanic forcings. Moreover, the studies from the east and the west SPNA yield non-uniform responses to the Holocene phases (Moros et al., 2004; Solignac et al., 2006; Renssen et al., 2009; Andersson et al., 2010) owing to

the regional climatic factors such as dominant surface currents influencing the region, SPG strength dynamics.

The AMOC change has been closely associated with climate shifts. As there is no direct tool available to reconstruct the past changes in AMOC, researchers have applied various means to evaluate the past changes such as water mass proxies (εNd (Gutjahr et al., 2008; Böhm et al., 2015; Lippold et al., 2016), Cd/Ca, $\delta^{13}C$ and $\delta^{18}O$ of benthic foraminifera (Oppo et al., 2003; Hall et al., 2004; Keigwin et al., 2005; Kleiven et al., 2008; Thornalley et al., 2010; Hoogakker et al., 2011)), proxies to reconstruct the bottom water strength (sortable silt size ($\overline{ss}$) (Bianchi and Mccave, 1999; Hoogakker et al., 2011; Ellison et al., 2006; Thornalley et al., 2013; Kissel et al., 2013), $^{231}Pa/^{230}Th$ (Gherardi et al., 2009; McManus et al., 2004; Böhm et al., 2015; Lippold et al., 2016) etc. Furthermore, there has been a continuous effort to improve the understanding of the AMOC strength from its influence on the upper ocean circulation in the high latitude North Atlantic. Hence, the upper water mass hydrography in the SPNA region has evolved as a prime zone to understand the AMOC variability given its liaison with the strength of AMOC. The changes in the AMOC have been cited to explain the abrupt climate changes in the past glacial and interglacial (Howe, Piotrowski, Noble, et al., 2016; Lippold et al., 2016; Lynch-Stieglitz, 2017; Marchitto & Broecker, 2006; McManus et al., 1999; Oppo et al., 2018; Praetorius et al., 2008; Roberts et al., 2010). Some major events such as Dansgaard-Oeschger, Heinrich events, and Younger Dryas have been closely associated with a variation in the AMOC (Lynch-Stieglitz, 2017; Praetorius et al., 2008). The Holocene has also been tied to AMOC variability. The early Holocene was observed with a decline in the AMOC followed by a strengthening in the mid-Holocene concurrent with the Holocene thermal maximum at the high latitude North Atlantic (Kissel et al., 2013; Thornalley et al., 2013). This early Holocene decline is tagged with freshwater discharge from remnant ice sheets. Moreover, the prominent 8.2 ka event in the early Holocene has been coupled with a major drop in the AMOC strength (Ellison et al., 2006; Kleiven et al., 2008). This event is coeval with the outburst of the proglacial lakes Agassiz and Ojibway (Ellison et al., 2006; Kissel et al., 2008). After the establishment of modern-like circulation conditions, AMOC declined during the mid-late Holocene. The late Holocene decrease has been correlated with an increase in the sea ice flux to the Nordic Seas

owing to the decreased orbital insolation (Thornalley et al., 2013). Some of the rapid millennial oscillations in the Holocene North Atlantic have also been linked with a variation in the AMOC strength. Nevertheless, centennial-millennial variation in NADW formation throughout the Holocene has been documented in few studies coinciding with the cold-water advance in the Subpolar North Atlantic Ocean (Oppo et al., 2003; Hoogakker et al., 2011; Kissel et al., 2013). Not all the proxies and the study sites reveal the same variation. They largely vary with the proxy sensitivity and the factors influencing the study site. Hence, one must take utmost care in interpreting this information.

The present assessment and future projections of a declining Atlantic Meridional Overturning Circulation (AMOC) in the current warming scenario emphasize the need for a deeper understanding of its driving factors. The anomalies in the Subpolar North Atlantic (SPNA), particularly in response to increased meltwater influx and a reduced AMOC offer a crucial region for comprehending cause-and-effect relationships in various climate scenarios. Holocene, the most recent geological period is marked by different climatic scenarios such as warming and cooling phases, and abrupt events like the 8.2 ka event and Bond events. Hence, the Holocene provides us with various climatic scenarios to gain insights from the SPNA. It is known from the previous studies that the Subpolar North Atlantic has not exhibited the same changes throughout its region during the Holocene (Eiríksson et al., 2000; Andersen et al., 2004; Berner et al., 2008; Balestra et al., 2010). Different eastern and western SPNA regional dynamics play a role in this contrast. Hence, these studies on Holocene SPNA evolution underscore the necessity for additional research to elucidate regional influences on SPNA Holocene variability. The Reykjanes Ridge, situated near the subpolar frontal region, becomes a favourable location for documenting regional SPNA variability. The frontal shift plays a pivotal role in hydrographic variations, determining the influx of cold and fresh water from the west or warm Atlantic Water from the east. This thesis investigates the Holocene dynamics of the region using planktic foraminifera proxies. Additionally, the distribution pattern of planktic foraminifera was studied to provide an overview of the species' response to the modern-day SPNA hydrography and related oceanographic elements such as temperature and salinity.

1.5. Objectives of the thesis:

The thesis aims to better understand the variability in Subpolar North Atlantic upper water hydrography and the factors influencing its variability. In this study, we used planktic foraminifera from the sediment core retrieved from the Reykjanes Ridge to reconstruct Holocene climatic changes at the Subpolar North Atlantic (SPNA) In addition, surface sediments from the region were studied to understand the distribution of the planktic foraminifera in the modern SPNA ocean and its response to recent environmental conditions.

The proposed objectives for the thesis are:

I. To document the variability in planktic foraminifera assemblages in the North Atlantic with respect to different water masses.

II. To reconstruct the Subpolar surface hydrography and its link to the strength of AMOC.

III. To document the response of the North Atlantic Current (NAC) and meltwater influx in subpolar water masses.

1.6. Outline of the thesis

In **chapter 1**, **Introduction,** background and importance of the study, the regional oceanography provided in detail. The aim and scope of the thesis, and proposed objectives have been elaborated at end of the chapter. In **chapter 2**, **Materials and methods,** the study area, and sample details and methodology adopted is described in detail. In addition, introduction and importance of the proxies used is presented in detail. This chapter also brief the statistical analyses used for the data representation. In **chapter 3**, The variation in planktic foraminifera assemblages associated with different surface hydrography from the Labrador Sea to Iceland-Faroe-Shetland Channel has been discussed in this chapter. In **chapter 4**, the paleoceanographic variations in the SPNA ocean have been reconstructed for the Holocene period, using the core AMK-410. The oxygen isotopic composition ($\delta^{18}O$) of *Globigerina bulloides* and *Neogloboquadrina pachyderma*, combined with the relative abundance of planktic foraminiferal species, have been used for this reconstruction of Holocene climatic changes. In **chapter 5,** The influence of

the North Atlantic Current and the meltwater influx from the Arctic on the SPNA hydrography have been discussed in detail. Further, in this chapter, the possible link between SPNA hydrography and AMOC strength is discussed. **Chapter 6**, **Summary and Conclusion**, documents all the key findings from the thesis.

Chapter 2

2. Materials and methods

Surface sediment samples used to fulfil the first objective were collected on-board R/V Akademik Ioffe 51st cruise (AI-51) during the summer of 2016. Whereas the sediment core used to fulfil the second and third objectives was collected from the eastern flank of the Reykjanes Ridge.

In the materials and methods chapter information about the study area and methodologies adopted are described in detail.

2.1. Regional oceanography

The SPNA Ocean is a complex setting that involves many surface and deep ocean currents. The Labrador Sea and the Irminger Sea (Pickart et al., 2003) located within the SPNA Ocean are crucial regions for the formation of Labrador Sea Water (LSW), the intermediate water mass, and North Atlantic Deep Water (NADW) which is an essential component of the deep water mass.

The SPNA Ocean consists of a complex system that interacts with the different types of surface and deep water masses (Fig. 2.1). A shoot-out of the Gulf Stream, the North Atlantic Current (NAC) has two main branches through which warm saline subtropical water reaches Nordic Seas through SPNA region (Daniault et al., 2016). It carries Western North Atlantic Water (WNAW) (Iselin, 1936; Pollard et al., 1996) (Temperature of ~ 9.5 °C, Salinity of ~ 35.2 PSU, Johnson et al., 2013). Out of these two, one branch travels Northeast through the Faroe-Shetland Channel (FSC), whereas the other branch splits into two sub-branches at the Iceland basin. Of the latter, one sub-branch enters the Nordic Sea through Iceland-Faroe Ridge, and the other sub-branch bends towards the west to form Irminger Current (IC) and forms a part of the Subpolar Gyre. The northern branch that goes through FSC carries a modified cooler watermass by mixing subpolar water and WNAW, known as Modified North Atlantic Water (MNAW) (Temperature 7.5-8.0 °C, Salinity 35.20–35.25 PSU (Read & Pollard, 1992)). Another water mass Eastern North Atlantic Water (ENAW) (Harvey, 1982; Pollard et al., 1996) (Temperature 10.5-11.0 °C, salinity 35.5- 35.6 PSU (Johnson et al., 2013)), is slightly warmer and more saline than WNAW, forms in the intergyre region of the Bay of Biscay and

dominates in the eastern region of Faroe-Shetland area. These water masses reach the Labrador Sea along the eastern coast of Greenland by East Greenland Irminger Current (EGIC). In addition, another cold water current, the East Greenland Current (EGC) brings cold and fresh water from the Nordic Seas to the Labrador Sea. At the south of the Cape Farewell, EGC and EGIC merge and form West Greenland Current (WGC), which moves northwest along the western coast of Greenland. The WGC along with the water coming from the Davis Strait and the Hudson Strait forms Labrador Current (LC) that flows along the Labrador Coast (Loder et al., 1998). The cold water mass, the Subarctic Intermediate Water (SAIW) mass is associated with the LC (Arhan, 1990). The water mass at the Labrador Sea forms an intermediate water mass Labrador Sea Water (LSW) by winter deep-convection. The deep watermass from the Nordic Seas, the Denmark Strait Overflow Water (DSOW) (Swift et al., 1980), and Iceland Scotland Overflow Water (ISOW) (Swift, 1984) join LSW to form the North Atlantic Deep Water (NADW). The NADW flows southward as a deep western boundary current. A major atmospheric pattern, North Atlantic Oscillation (NAO) is known to influence the hydrography of the SPNA region.

Annual average temperature and salinity at the eastern side of the studied transect (see section 2.2) was 10.33 °C (Avg. 0-50m depth) and 35.28 PSU respectively. The temperature and salinity decrease as we go westward from the Iceland basin towards the Labrador Sea. It reaches 8.12 °C, 35.00 PSU near Reykjanes Ridge, and a minimum of 4.6 °C, 34.57 PSU in the Labrador Sea. Thus, the water mass at the eastern side of the studied transect is much warmer (NAC water) than the westernmost section of the Labrador Sea, where the water gets modified by mixing and losing heat to the atmosphere throughout the transect. Thus, the studied transect shows a gradient from warmer to cooler water mass in its upper water column from east to west. Sub-polar Front (SPF) separates the warmer and saline subtropical water mass from the cooler and fresher subpolar water (Belkin and Levitus, 1996; Bersch et al., 2007). Shifting of this front has been reported from the SPNA region with the change in its hydrographic structure, and strength of SPG (Perner et al., 2018).

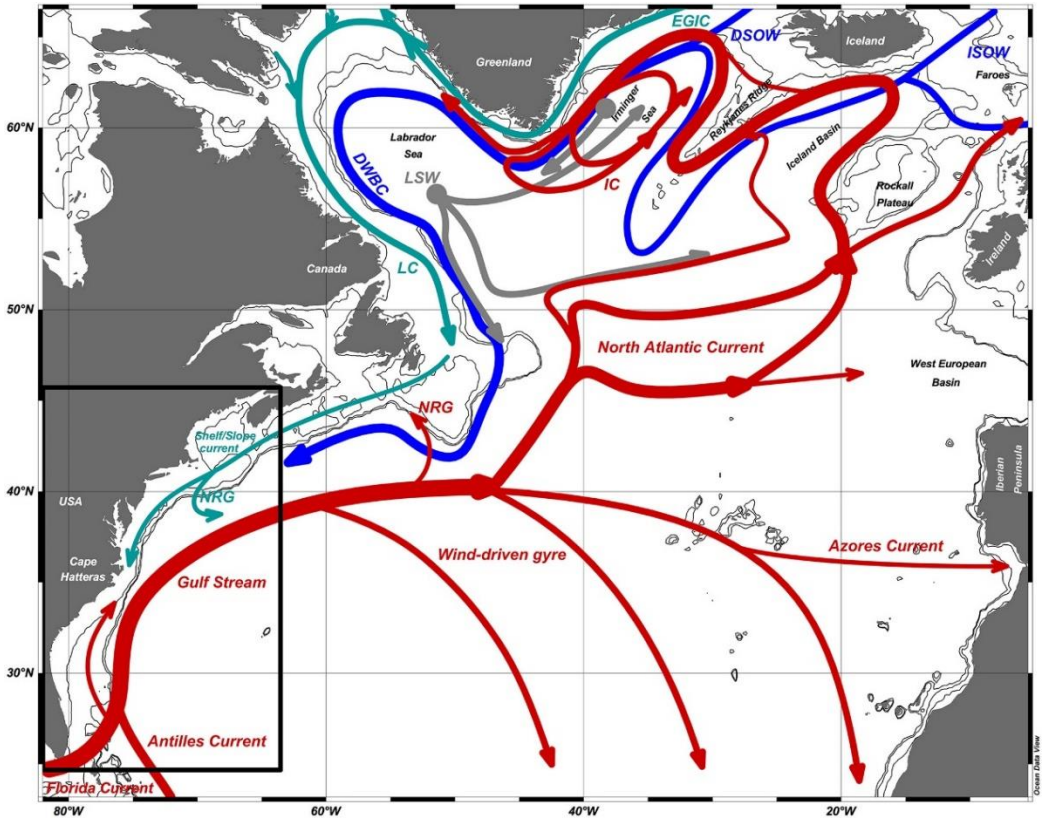

Fig. 2.1. Subpolar North Atlantic Circulation showing all the major currents in the region. The lines in red indicate warm surface currents, whereas the blue lines indicate cold deep currents. IC: Irminger Current; EGIC: East Greenland Irminger Current; LC: Labrador Current; DSOW: Denmark Strait Overflow Water; ISOW: Iceland-Scotland Overflow Water; LSW: Labrador Sea Water. (Source: Garcia-Ibanez et al., 2015).

2.2. Sample details

2.2.1. Surface sediments

Twenty-five surface sediment samples were collected along a longitudinal transect at 59.50 °N in the Subpolar North Atlantic (SPNA) Ocean using a Van Veen Grab. The surface sediment samples cover an area stretching from longitude -54.17°W to -3.87°E between the Labrador Sea and Iceland-Faroe-Shetland Channel. The sampling depths vary from 158.00 m at the shallowest station 22 to 3,477 m at station 3 (Table 2.1, Fig. 2.2).

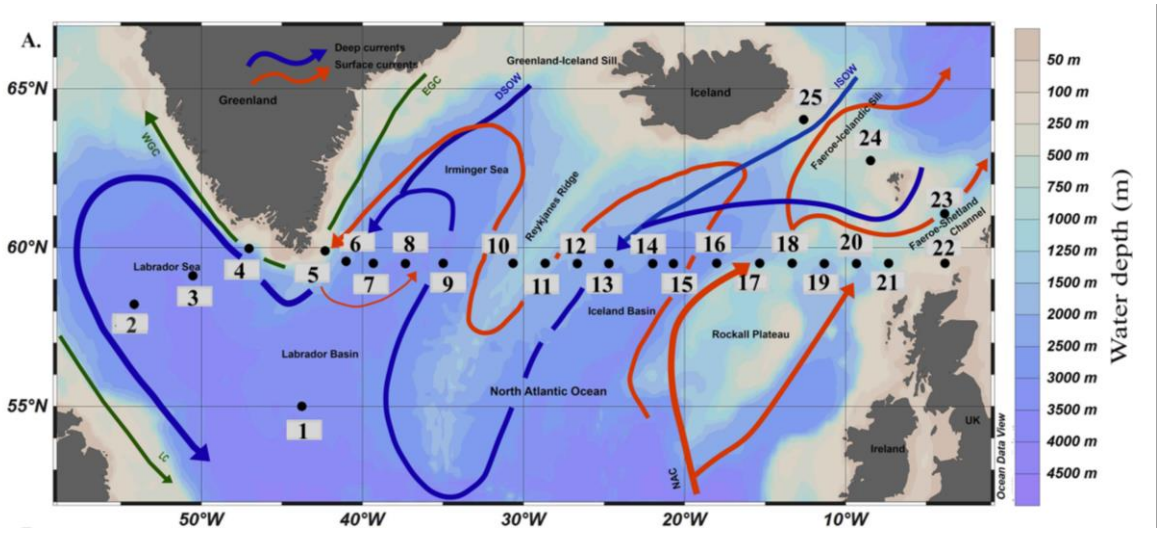

Fig. 2.2. Map showing locations of surface sediment samples (black dots) collected during AI-51 cruise; major oceanographic currents of the region are also shown (Schlitzer, 2015), warm surface currents, cold surface currents, and cold deep currents are shown by red, green, and blue arrows respectively; NAC: North Atlantic Current, EGC: East Greenland Current, WGC: West Greenland Current, LC: Labrador Current, ISOW: Iceland-Scotland Overflow Water, DSOW: Denmark Strait Overflow Water

2.2.2. Sediment core

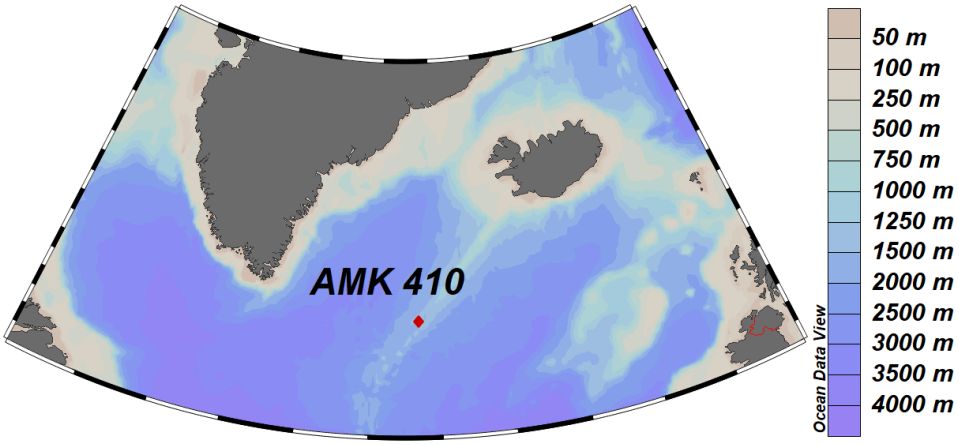

Fig. 2.3. Map showing the location of the sediment core AMK-410

The sediment core AMK 410, a gravity core was obtained from 58.33 °N latitude and 31.60 °W longitude at a depth of 1,580 m. The location was chosen to best fit to achieve our objectives. The area is influenced by the warm North Atlantic

Current from subtropics and the cooler subpolar water. The detailed oceanographic setting of the site can be found in the preceding subsection.

2.3. Sediment sample processing

Table 2.1. Location details of the surface sediment samples collected during the AI-51 cruise.

Station ***No.***	***Water depth (m)***	***Latitude (°N)***	***Longitude (°W)***
1	3346	55.00	-43.76
2	3393	58.22	-54.17
3	3477	59.11	-50.51
4	2389	59.97	-47.04
5	328	59.90	-42.32
6	2399	59.56	-41.01
7	2922	59.50	-39.33
8	3156	59.49	-37.32
9	3064	59.50	-34.98
10	1531	59.51	-30.66
11	1694	59.50	-28.67
12	2237	59.50	-26.66
13	2512	59.50	-24.71
14	2740	59.49	-21.99
15	2825	59.50	-20.69
16	2182	59.50	-18.00
17	1519	59.50	-15.33
18	1291	59.50	-13.33
19	1611	59.50	-11.33
20	1468	59.50	-9.33
21	1051	59.50	-7.33
22	158	59.50	-3.83
23	1150	61.07	-3.87
24	484	62.74	-8.46
25	567	64.03	-12.62

Same processing protocols were followed for both surface sediment samples and sediment core samples.

A small piece of sediment was weighed and freeze-dried. The dried samples were divided into two halves; one half was used for foraminiferal analyses, and the other was kept for sedimentological analyses. For foraminiferal analyses, the dried samples were soaked in de-ionized water for six hours, followed by wet sieving

over 63 µm mesh. The sieved samples were dried in an oven at 50°C. The coarse fraction (>63 µm) was then dry sieved through different size fractions for planktic foraminiferal assemblage analysis, and stable isotope and Mg/Ca analyses.

The other half of the dried sediment (only for surface sediment samples) were ground to a fine powder in an agate mortar-pastel for analysis of calcium carbonate content of the sediment.

2.4. Sediment sample analysis

2.4.1. Planktic foraminiferal assemblage analysis

For planktic foraminiferal counts, >100 µm size fraction was chosen for surface sediment samples, not to miss the smaller species like *Turborotalita quinqueloba* and *Globigerinita uvula*. The larger size fractions >150 µm and >125 µm, which are preferred for most of the planktic foraminiferal assemblage studies, are shown to understate the smaller species counts as compared to the >100 µm size fraction in the high latitude North Atlantic and Arctic Oceans (Kandiano and Bauch, 2002; Husum and Hald, 2012). Some recent studies also show a decrease in temperature estimation using the transfer function while considering the smaller size fraction over the larger ones (Husum and Hald, 2012). The >100 µm size fraction was split into two equal parts using a micro-splitter, and the process was repeated until a minimum of 300 planktic species were counted in the smallest split fraction. A tiny fraction was weighed, and 300-800 planktic foraminifera species were picked into a microscopic slide using Nikon SMZ 1500 stereo-zoom microscope and 112X magnification). The specimens were then identified to species level and counted following the taxonomic descriptions of Kennett and Srinivasan (1983) and Hemleben et al. (1989).

For the representation, total Planktic Foraminifera (TPF) absolute abundance and species relative abundance was calculated in each sample. The TPF represents total number of planktic foraminifera in the coarse fraction. Species absolute abundance is the contribution of the particular species to the total assemblage, presented in whole numbers per gram weight of sediment, whereas species relative abundance denotes the same in percentage relative to the total abundance. These parameters have been used in paleoceanography before the evolution of geochemical proxies.

They are used to interpret water mass structure and environmental conditions (Ufkes et al., 1998). Certain planktic foraminifera species abundance can be indicative of upwelling conditions and trophic environments.

2.4.2. Geochemical analysis of planktic foraminifera

Similar to the census counts, Planktic foraminifera shell morphology and their chemical composition (e.g., stable isotopes and trace metal composition), are extensively used in paleoclimate investigations. Planktic foraminifera forms their calcitic test in equilibrium with the surrounding water, thus, their isotopic and trace metal composition reflect information of ambient seawater chemistry. This makes them promising proxy to investigate past seawater composition. To fulfil the projected objectives, Carbon (C) and Oxygen (O) isotopes of specific foraminifera were measured. The principle and methods involved in these isotopic studies are summarised below.

2.4.2.1. Oxygen isotopic analysis of planktic foraminifera

Oxygen has three stable isotopes: ^{16}O (99.763 %), ^{17}O (0.0375 %), and ^{18}O (0.1995 %) (Garlick, 1969). The processes like evaporation, temperature, etc., cause oxygen isotope fractionation. For example, evaporation preferentially removes lighter isotopes (^{16}O) and makes the clouds and the water relatively richer in lighter (^{16}O) and heavier isotopes (^{18}O), respectively (Rayleigh fractionation). This leads to variation in the isotopic ratio ($^{18}O/^{16}O$) in components involved in the fractionation process. Generally, the ratio between ^{18}O and ^{16}O ($^{18}O/^{16}O$) represents the fractionation. For easy comparison between various components, it is presented in per mil (‰) relative to a standard known as isotopic composition, denoted with the notation "Delta" $\delta^{18}O$. The international standards for $\delta^{18}O$ are VPDB (Vienna PeeDee Belemnite) and VSMOW (Vienna Standard Mean Ocean Water) for carbonates and water, respectively. The $\delta^{18}O$ is expressed as the deviation in the Oxygen isotopic ratio of the sample with respect to the standard, expressed in per mil as shown in the following equation.

$$\delta^{18}O = \left[\frac{\left(\frac{^{18}O}{^{16}O}\right)_{sample} - \left(\frac{^{18}O}{^{16}O}\right)_{standard}}{\left(\frac{^{18}O}{^{16}O}\right)_{standard}} \right] \times 10^3 \ (‰) \text{ in VPDB}$$

The foraminiferal $\delta^{18}O$ is mainly governed by two factors: seawater $\delta^{18}O$ composition and temperature. Seawater $\delta^{18}O$ depends on the global ice volume (ice volume effect) and the local salinity effect such as evaporation-precipitation, sea ice melting, sea ice formation, advection, and mixing of water masses. Though, first $\delta^{18}O$ in carbonate was used to analyze the paleotemperature (Emiliani, 1955), later, it was confirmed that $\delta^{18}O$ in foraminifera is majorly determined by the global ice volume followed by other factors (Shackleton, 1967). The environmental factors influencing the foraminiferal $\delta^{18}O$ are shown in the schematic below (fig. 2.4), taken from Ravelo and Hillaire-Marcel (2007). Besides the environmental factors, dissolution, secondary calcification, and vital effects may alter the $\delta^{18}O$ in foraminifera. So, care should be taken while analyzing and interpreting the $\delta^{18}O$ data in foraminifera.

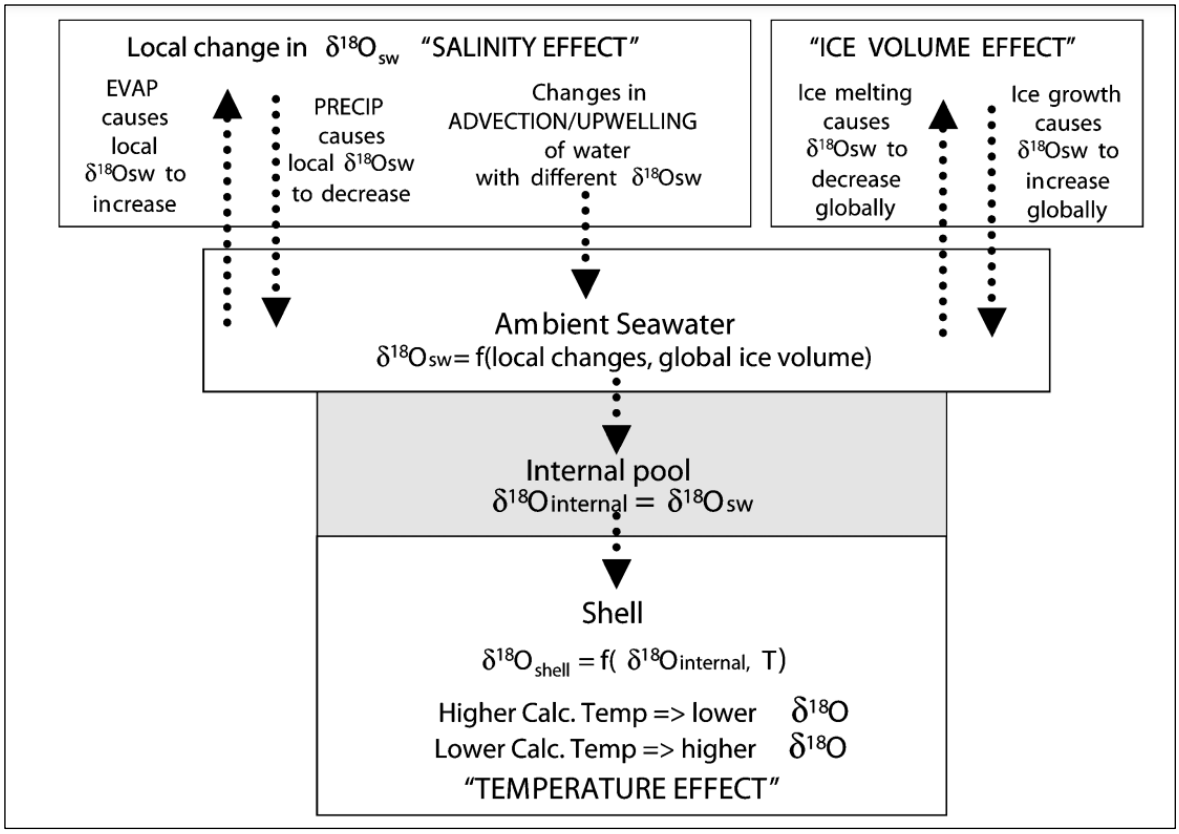

Fig. 2.4. Schematic showing the factors governing the foraminiferal shell $\delta^{18}O$; $\delta^{18}O_{sw}$: seawater $\delta^{18}O$. (Source: Ravelo and Hillaire-Marcel, 2007).

Procedure for stable isotopic analysis

For stable isotopic analysis, 15-20 specimens of surface water planktic foraminifera *Globigerina bulloides* and 35-40 specimens of *Neogloboquadrina pachyderma*

were picked from the size range of 250-350 µm and 125-250 µm, respectively. Only specimens with no secondary calcification and dissolution were chosen with the utmost care. The samples were processed and analyzed with an Isotopic Ration Mass Spectrometer (IRMS) in the Geosciences-Stable Isotope lab at the Physical Research Laboratory, India. NBS 19 and an in-house standard (Makrana marble) were used during the measurement. The standard deviation for $\delta^{18}O$ was found to be 0.04‰ for NBS-19 and 0.10‰ for Makrana marble.

2.4.3. Mg/Ca analysis in foraminifera

Ca^{+2} in the foraminiferal carbonate may get substituted by Mg^{+2} during the calcification due to its similar ionic radius and charge as Ca. This substitution is temperature dependent. Though Mg/Ca in foraminifera also depends on pH and salinity, the effect is small and linear. Further, Mg/Ca exhibits an exponential relationship with temperature. Chave (1954) and Blackmon and Todd (1959) first reported the temperature sensitivity of Mg/Ca by X-ray diffraction. Thermodynamic calculations reveal an exponential increase of 3% Mg/Ca uptake into calcite per ℃ (Rosenthal et al., 1997; Lea et al., 1999), which is also seen in the case of inorganic calcite precipitation (Oomoori et al., 1987). However, vital effects are responsible for the variation of Mg percentage in foraminiferal calcite from inorganic calcite and among different species. Hence, different calibrations have been adapted for specific species using sediment traps (Anand et al., 2003; Pak et al., 2004), culture (Nürnberg et al., 1996; Mashiotta et al., 1999), and core tops (Elderfield and Ganssen, 2000; Dekens et al., 2002). All these calibrations follow the exponential relation between Mg/Ca, and temperature expressed as,

$$^{Mg}/_{Ca} = B\exp(A\times T),$$

Where, T is temperature, and A and B are constants, specific to species. ‘A’ represents the temperature sensitivity which is consistently found to be 0.09±0.01 (Anand et al., 2003; Katz et al., 2010). The pre-exponential constant ‘B’ varies with different species (Anand et al., 2003). Since the calibrations are particular to some species and regions with a limited temperature range, one must be careful enough to apply these calibration equations for paleotemperature studies.

Procedure for Mg/Ca measurement

For foraminiferal Mg/Ca analysis, around 50 specimens of *G. bulloides* from the size range 250-350 µm were picked into a clean and dry vial. Random specimens were picked from each core section and fixed to glass slides with the umbilical side facing upward. The last four chambers of the *G. bulloides* were analyzed separately for Mg/Ca in an LA-ICPMS (Laser Ablation- Inductively Coupled Plasma Mass Spectrometer), Max Planck Institute for Chemistry, Germany. The Foraminifera were ablated on a 55 µm spot using an NWR femtosecond laser, NWRFemto from ESI (2), with a 200 nm wavelength. With a laser pulse repetition rate of 1 Hz, the generated aerosols were analyzed separately for every shot in the ICP-MS (Element2 double-focusing SF). The ICP-MS was used in low-resolution mode to measure $^{25}Mg^{+}$ and $^{44}Ca^{++}$.

2.5. Calcium carbonate content

A small amount of freeze-dried bulk sediment was ground to a fine powder with clean and dry agate mortar and pastel. The powder was then analyzed for total inorganic carbon (TIC) in a coulometer (UIC, Inc. CM5017, Geology Lab, NCPOR). This TIC was used in the Espitalie et al. (1977)'s equation to calculate the total $CaCO_3$ (%),

$$CaCO_3 = (TC - TOC) \times 8.33\ (\%),$$

and,

$$TC - TOC = TIC,$$

So,

$$CaCO_3 = TIC \times 8.33\ (\%),$$

Where TC is Total Carbon, TOC is Total Organic Carbon, and TIC is Total Inorganic Carbon.

2.6. Statistical analyses

Cluster and principal component analysis was used to better understand the data and interpretation.

2.6.1. Cluster analysis

Cluster analysis is a method of classification of the datasets into groups based on similarity and dissimilarity between the data. The Hierarchical cluster analysis performs multiple steps of partition by analyzing all similarities and dissimilarities between samples to group them into clusters. The Hierarchical cluster analysis is always represented by a dendrogram. The Bray-Curtis similarity index has been popularly used by ecologists as a measure to assign the samples of the population to different groups.

The Hierarchical cluster analysis was performed on the planktic foraminifera assemblages to delineate different groups of stations using the Bray-Curtis similarity index. Each group was represented by its characteristic foraminiferal assemblage. This analysis has been used previously to identify the relationship between the group of stations and different water masses based on their specific planktic foraminifera assemblages (Parker and Berger, 1971; Thunell, 1978; Ottens, 1991). The SIMPER (similarity percentages) analysis (Clarke, 1993) was also performed to determine the individual species contribution to each cluster group.

2.6.2. Principal Component Analysis

Principal Component Analysis (PCA) is one of the oldest and most widely used multivariate statistical techniques to visualize and interpret data. This is used to reduce the dimensionality of a dataset. A large dataset with multiple correlated variables is reduced to a set of smaller variables with PCA and allows us to see any trend or pattern in the data.

Principal Component Analysis (PCA) was performed on the environmental parameters such as temperature, salinity, water depth of sampling point; Chl-a with total planktic foraminifera abundances; and species percentages using STATISTICA v. 10 software. This method of statistical correlation was used to understand the role of environmental factors on distribution of planktic foraminifera assemblage at the study site (Mallo et al., 2017). The marked correlations are significant at a p-value < 0.05.

2.7. Core Chronology

The core chronology was established with the help of radiocarbon dating (Libby, 1955). The cosmogenic radioisotope of Carbon (^{14}C) is produced when Nitrogen (^{15}N) is bombarded with a neutron in the upper atmosphere by a process known as cosmic spallation. This ^{14}C is incorporated into the atmospheric $^{14}CO_2$ and thus becomes a part of the global carbon cycle. The organisms in the biosphere or the sediments maintain an equilibrium with the atmospheric ^{14}C percentage, and as soon as they disconnect from this equilibrium, the ^{14}C decreases through decay. Thus, by measuring the residual ^{14}C, the age of the object or fossil could be known. The half-life of ^{14}C has been calculated 5730 years (Godwin, 1962).

In case of marine sediments, this process becomes complex as some factors could alter the ^{14}C age of water. A 15‰ fractionation of ^{14}C (equals 120 years) is involved in the ocean-atmospheric exchange of CO_2. In the case of upper water, there could be a mixing of modern water with ^{14}C-depleted water involved with ocean circulation, which varies geographically. Moreover, mixing old water during upwelling and the presence of sea ice, limiting the ocean-atmospheric interaction, also affects the reservoir age. Hence, a reservoir correction specific to a particular region must be added. Besides this, the assumption of a constant atmospheric ^{14}C percentage is not valid, and there has been evidence of variations in atmospheric ^{14}C (Damon et al., 1978; de Vries, 1958). For this, the radiocarbon age is converted to calendar years by using calibrating curves (Stuiver, 1993; Reimer et al., 2009).

Table 2.2. Radiocarbon age and calibrated age for the core AMK-410

Depth(cm)	Radiocarbon Age	Error (1 sigma)	Calibrated Age (Cal BP)
5	1700	±30	1189
11	2450	±30	2053
31	3980	±30	3907
41	5700	±30	6052
56	7990	±30	8411
91	27230	±120	30936

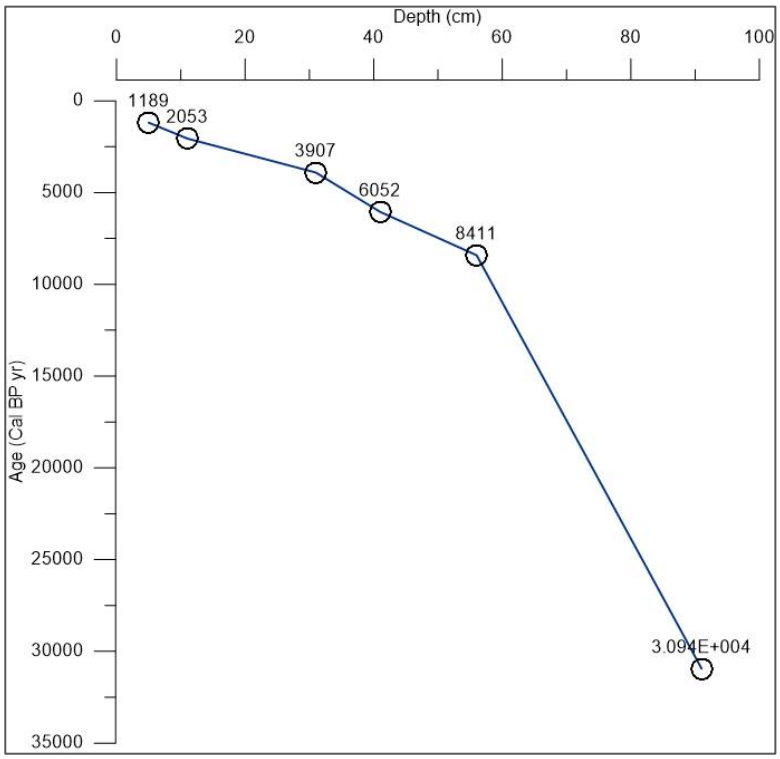

Fig. 2.5. Age-Depth model for the core AMK 410.

For Radiocarbon dating, about 10-12 mg of *G. bulloides* or *N. pachyderma* were picked from six core intervals. The samples were then analyzed in the Accelerated Mass Spectrometer (AMS) of Beta Analytic Inc., U.S.A. A local reservoir correction of 51±58 was applied to the radiocarbon dates. These corrected dates were then calibrated with CALIB.8 (Stuiver et al., 1993) using the marine ^{14}C calibration curve (Heaton et al., 2020). The intervals and the results are presented in the table 2.2. The age-depth model for the core is presented in the figure 2.5.

2.8. Ecology of the planktic foraminifera

Planktic foraminifera are dated back to the middle Jurassic. These are unicellular eukaryotic protists, mostly marine, with thick calcitic shells and are surface dwellers. They are ubiquitous in occurrence, populating the warm tropical to the cold polar oceans. These planktic foraminifera are depth-stratified as they prefer specific ecological parameters for living. They are constrained by various environmental parameters, especially water mass characteristics (temperature, salinity, nutrients, etc.) and food availability (Parker, 1960; Bé and Tolderlund, 1971; CLIMAP, 1976; Ortiz and Mix, 1992; Schiebel and Hemleben, 2005;

Rebotim et al., 2017; Schiebel and Hemleben, 2017). The foraminifera are very sensitive to any subtle change in these environmental conditions. They archive these ambient oceanic conditions such as temperature, and salinity in their shell chemistry. The calcitic shells hold good preservation potential, comprising a significant part of the oceanic sediments. These tiny shells are evolved as tools of paleoclimatology since the work by d'Orbigny (1826), Félix Dujardin (1835), Owen (1867), John Murray and Brady (1884) after the 1872-1876's HMS Challenger expedition. Since then, they have been widely used to infer paleoenvironments (Kucera, 2007; Schiebel et al., 2017). The depth stratification and ecological preferences of planktic foraminifera play a vital role in reconstructing paleoceanographic changes. However, the paleoenvironmental reconstructions rely on a better understanding of the modern foraminiferal ecology and factors governing their abundance in different water masses.

Table 2.3. List of planktic foraminifera identified in the study.

List of planktic foraminifera species
Globigerina bulloides (d'Orbigny 1826)
Globigerinita glutinata (Egger 1893)
Globigerinita uvula (Ehrenberg 1861)
Globorotalia inflata (d'Orbigny 1839)
Globorotalia scitula (Brady 1882)
Neogloboquadrina pachyderma (sensu. Darling et al. 2006; syn. *N. pachyderma* (Ehrenberg 1861) sinistral)
Neogloboquadrina incompta (Cifelli 1961; syn. *N. pachyderma* (Ehrenberg 1861) dextral)
Turborotalita quinqueloba (Natland 1938)
Orbulina universa (d'Orbigny1839)

The planktic foraminifera found in this study from both the surface study and the sediment core complies with the previously published literature on the region (Tolderlund and Bé, 1971; Ottens, 1991, 1992; Perner et al., 2018; Schiebel and Hemleben, 2000; Stangeew, 2001; Schiebel et al., 2001; Chapman, 2010; Staines-

Urias et al., 2013; Schiebel et al., 2017). A total of nine species of planktic foraminifera were identified in the AMK 410, of which only six are abundant and comprise more than 80% of the assemblages. The list of the species is given below in table 2.3 and figure 2.6. Additionally, detailed ecological knowledge of these species specifically from the region is simulated in table 2.4.

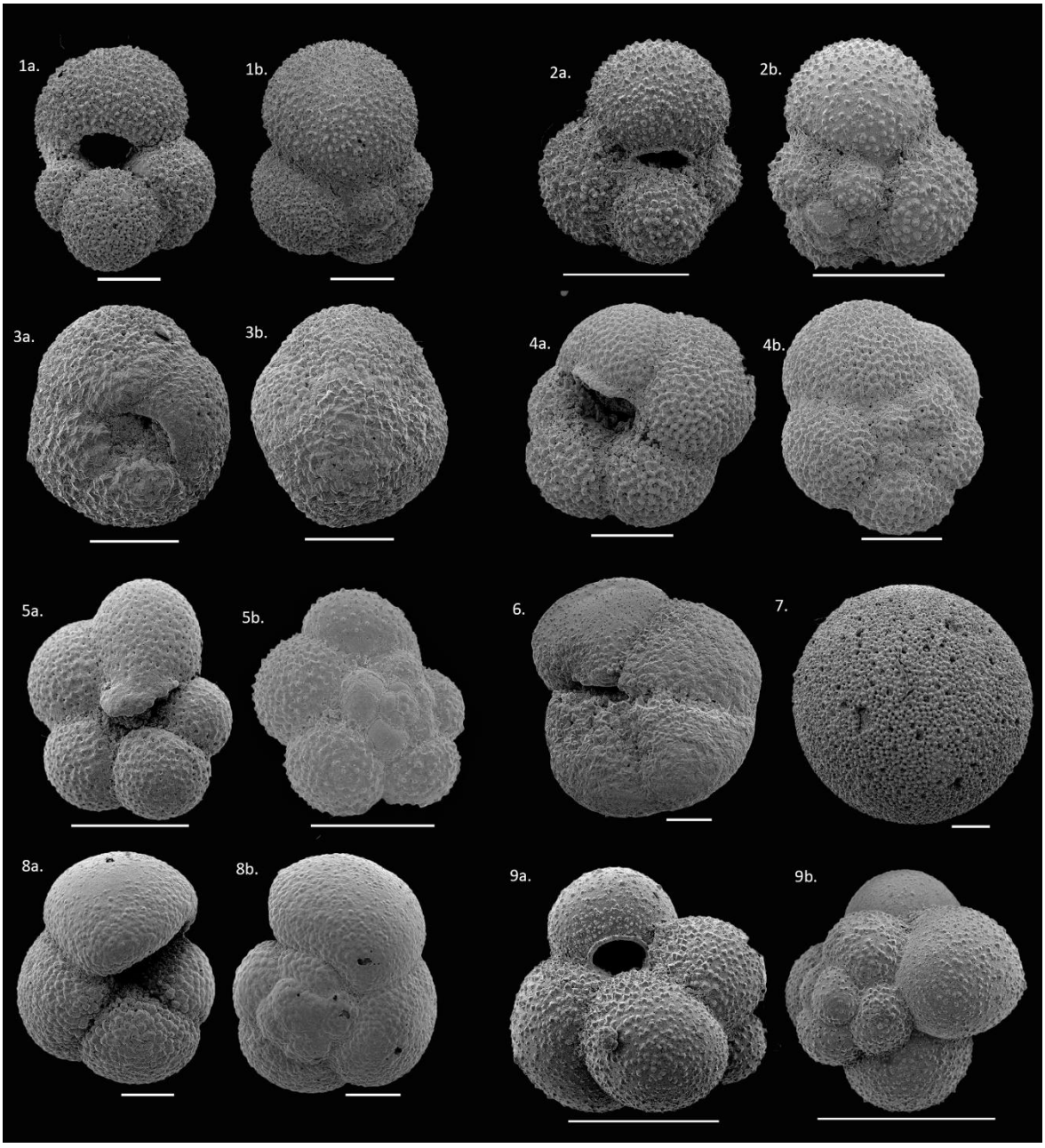

Fig. 2.6. Plate. SEM images of the planktic foraminiferal specimens from the surface sediments along 59.5°N transect on-board AI-51. 1(a,b). *G. bulloides* 2(a,b). *G. glutinata* 3(a,b). *N. pachyderma* 4(a,b). *N. incompta* 5(a,b). *T. quinqueloba* 6. *G. scitula* 7. *O. universa* 8(a,b). *G. inflata* 9(a,b). *G. uvula*. Scale bars 100 µm.

Table 2.4. Ecology of the planktic foraminifera species, with their depth habitat, geographical distribution, ecological information, and distribution in the SPNA (In the present study).

	Depth Habitat	Geographical distribution	Ecological Information	Distribution in SPNA (Present study)	References
N. pachyderma	Upper 100m (in EGC) 50-200m (when warm Atlantic water present)	Subpolar to polar	The abundance increases towards poles. It dominates the assemblage when summer SST < 9°C.	•Dominated in the west of Reykjanes Ridge •Also found in the Faroe-Shetland channel •Absent in the central Iceland Basin and at the eastern transect	Hemleben et al., 1989; Husum & Hald, 2012; Simstich et al., 2003; Toldurlund & Be, 1971, present study
N. incompta	60 - 150m	Temperate to subpolar	This species prefers warm and stratified water.	•Found maximum at the eastern transect. •Minimum in Labrador Sea	Toldurlund & Be, 1971; Fairbanks et al., 1982; Reynolds & Thunell, 1985; Schiebel & Hemleben, 2000; Kuroyanagi & Kawahata, 2004, present study
G. bulloides	Upper 50m (surface mixed layer)	Temperate to subpolar	The species abundance is enhanced with increased nutrients.	•Maximum in the Iceland basin	Be & Toldurlund, 1971; Ottens, 1992; Thunnel & Sautter, 1992; Ganssen & Kroon, 2000; Schiebel & Hemleben, 2000, present study
T. quinqueloba	10-60m (near surface)	Temperate to subpolar	This symbiotic species is related to presence of oceanic fronts. Abundance increases with primary productivity.	•Patchy in abundance •Maximum at the central Irminger Sea and the eastern transect	Reynolds & Thunell, 1985; Johannsen et al., 1994; Carstens et al., 1997; Volkmann, 2000; Husum & Hald,2012; Meilland et al., 2020, present study

G. uvula	40-100m	Temperate to polar	This species is associated with oceanic front and primary productivity.	•Constitutes only minor % •Maximum at the eastern near coastal region and in the central Irminger sea	Schiebel & Hemleben, 2002; Schiebel et al., 2002; Husum & Hald, 2012
G. glutinata	60-150m	Cosmopolitan	Its presence marks the onset of Spring bloom.	•Constitutes major % of the assemblage •Absent only in the Labrador Sea	Ottens, 1992; Volkmann 2000a, Schmuker & Schiebel, 2002; Schiebel & Hemleben, 2000; Chapman, 2010
G. inflata	100-400m (Near thermocline)	Temperate	Abundance of *G. inflata* in SPNA depends on the flux of advected warmer water.	•Present only in the central and eastern transect •Absent in the Irminger Sea and Labrador Sea	Hemleben et al., 1989; Ottens, 1992; Ganssen & Kroon, 2000; Pflaumann et al., 2003; Chapman, 2010
G. scitula	Below thermocline to 200-300m	Cosmopolitan	Presence of this species in SPNA indicates warm water entrainment from subtropics. Its abundance is related with primary productivity.	•Rare in this study •Only found in two stations	Hemleben et al., 1989; Schiebel & Hemleben et al., 2000; Schiebel et al., 2002; Chapman, 2010; Retailleau et al., 2011
Orbulina sp.	Upper 100m (euphotic zone)	Tropical to temperate	This symbiote bearing species can tolerate wide ranges of temperature and salinity. Presence of this species in high latitude indicates presence of warmer water from subtropics.	•Rare in this study	Berger, 1969; Fairbanks et al., 1982; Hemleben et al., 1989; Schiebel & Hemleben, 2017

Chapter 3

3. Planktic foraminiferal assemblages in the surface sediments from the Subpolar North Atlantic Ocean

This synthesis has been published in the peer-reviewed journal Frontiers in Marine Science (doi: 10.3389/fmars.2021.781675).

3.1. Introduction

The distribution and ecology of planktic foraminifera have been studied in the plankton tows, sediment traps and surface sediments from the world oceans (Berger, 1969; Thunnell and Reynolds, 1984; Schiebel and Hemleben, 2000; Schiebel et al., 2001; Jonkers et al., 2010; Meilland et al., 2020). The studies referred to are either confined to different basins or show regional heterogeneity. A complete ecological and spatial distribution of planktic foraminifera is understudied in the Subpolar North Atlantic (SPNA) ocean, an area influenced by the large-scale changes in the surface hydrography on both short and large timescale (seasonal, annual, interannual, decadal, etc.).

The SPNA exhibits significant west-to-east oceanographic gradients from the subarctic to temperate regions (McCartney and Talley, 1982; Read, 2000; Brambilla and Talley, 2008). In particular, SPNA hydrography is characterized by the presence and interaction of different warm and cold surface water currents (Read, 2000; García-Ibáñez et al., 2015). The strength and extent of Subpolar Gyre (SPG) influence the hydrography in the SPNA (Hátún et al., 2005; Staines-Urías et al., 2013). The hydrographic diversity strongly affects the distribution of modern planktic foraminifera in SPNA, resulting in the occurrence of several cold-, warm- and mixed-water planktic foraminifera associations (Bé and Tolderlund, 1971; Ottens, 1991; Schiebel et al., 2001).

The enhanced warming of the high latitude regions in recent decades has led to major oceanographic shifts and resulted in changing ecology of various planktic faunas (Fossheim et al., 2015; Oziel et al., 2017; Neukermans et al., 2018; Jonkers et al., 2019). Especially, planktic foraminiferal assemblages in high latitude oceans have shown a change in diversity, with an influx of temperate species (Stangeew,

2001; Jonkers et al., 2019; Schiebel et al., 2017; Meilland et al., 2020). As opposed to the single dominant species found in polar regions (Bé and Tolderlund, 1971), several plankton tow experiments reported a rise in warmer-water foraminiferal species in polar regions (Stangeew, 2001; Jonkers et al., 2019; Meilland et al., 2020). The distribution of modern planktic foraminifera reported from the SPNA ocean is mainly confined to either the western (Stangeew, 2001; Jonkers et al., 2010) or the eastern SPNA ocean (Schiebel and Hemleben, 2000). These studies are based mainly upon plankton tows and infer the planktic foraminifera populations with respect to seasonality. Several studies discuss the variations in planktic foraminifera assemblage structure in a latitudinal as well as a longitudinal transect, pertaining to a change in water mass structure in Nordic seas as well as in Subarctic Pacific (Stangeew, 2001; Kuroyonagi and Kawahata, 2004; Chapman, 2010; Mallo et al., 2010; Pados and Spielhagen, 2014; Meilland et al., 2020); but not in the SPNA ocean. Thus, the main objective of the present study is to assess the spatial distribution of planktic foraminiferal assemblages and their ecological preferences in the SPNA ocean. Moreover, this becomes interesting as SPNA has complex hydrography, showing an east-west gradient in its physiographic properties, which significantly modulates the planktic foraminiferal distribution. This study, covering the entire SPNA from west to east, would improve our understanding of planktic foraminifera distribution related to various environmental parameters of different water masses and significant shifts in high-latitude regions.

3.2. Oceanographic Context

The surface currents in the SPNA region (described in Chapter 2) and the associated water masses are controlled by the dynamics of cyclonic Subpolar Gyre (SPG). A strengthened and expanded SPG brings more subpolar water from the western SPNA to the eastern SPNA through the eastern limb of SPG. A weakened and contracted gyre brings subtropical warm water to east SPNA through the eastern limb of SPG (Staines-Urías et al., 2013). The upper water mass at east SPNA gets colder and denser as it travels downstream towards the Labrador Sea through mixing with the surrounding subpolar water mass and air-sea interaction (Read, 2000).

In general, alternating warm and cold-water currents create a prominent hydrological contrast along the studied transect at 59.50 °N (Fig. 3.1B, 3.1C and 3.1D). The annual average temperature and salinity of the surface water (averaged for a water depth of 0-100 m) vary from 10.33 °C and 35.28 PSU on the eastern side, through 8.12 °C and 35.00 PSU on the central part near Reykjanes Ridge, to 4.60 °C and 34.57 PSU in the Labrador Sea (WOA 2018, Locarnini et al., 2018; Zweng et al., 2018). The primary productivity in the region (chlorophyll-*a* concentration) ranges from 5.80 (ln (mg/L)) to 8.00 (ln (mg/L)) (Fig. 3.1D).

The hydrographic dynamics in SPNA is associated with different-scale eddies and hydrological fronts, bringing more nutrient-rich water to the region. The warm subtropical water from NAC and cold subpolar water are separated by the subpolar front, creating a highly productive region (Taylor and Ferrari, 2011b). The eddies associated with the Iceland Basin, and Irminger Sea, bring more nutrient-rich water to the surface (Mahadevan et al., 2012). This makes SPNA a highly productive region (Taylor and Ferrari, 2011b; Mahadevan et al., 2012). Also, the extent and strength of SPG circulation directly impact productivity changes in SPNA (Hátún et al., 2009). The increased freshening of SPNA and decreased Atlantic Meridional Overturning Circulation (AMOC) strength has a negative effect on primary productivity (Osman et al., 2019). The productivity of plankton communities in SPNA exhibits clear seasonal character peaking from spring to autumn after the shutdown of winter convection and the formation of stable surface stratification (Taylor and Ferrari, 2011a). Primary productivity, along with the other physical parameters, controls the distribution of planktic foraminifera assemblages (Bé and Tolderlund, 1971; Schiebel and Hemleben, 2017). The abundance of foraminifera species is also linked with chlorophyll-*a* (Chl-*a*) concentration (Schiebel et al., 2001; Kuroyanagi and Kawahata, 2004; Retailleau et al., 2011).

3.3. Material and Methodology

The details of sediment sample collection, processing, and analysis are described in chapter 2, ‘Material and Methods’ in detail.

3.3.1 Environmental parameters

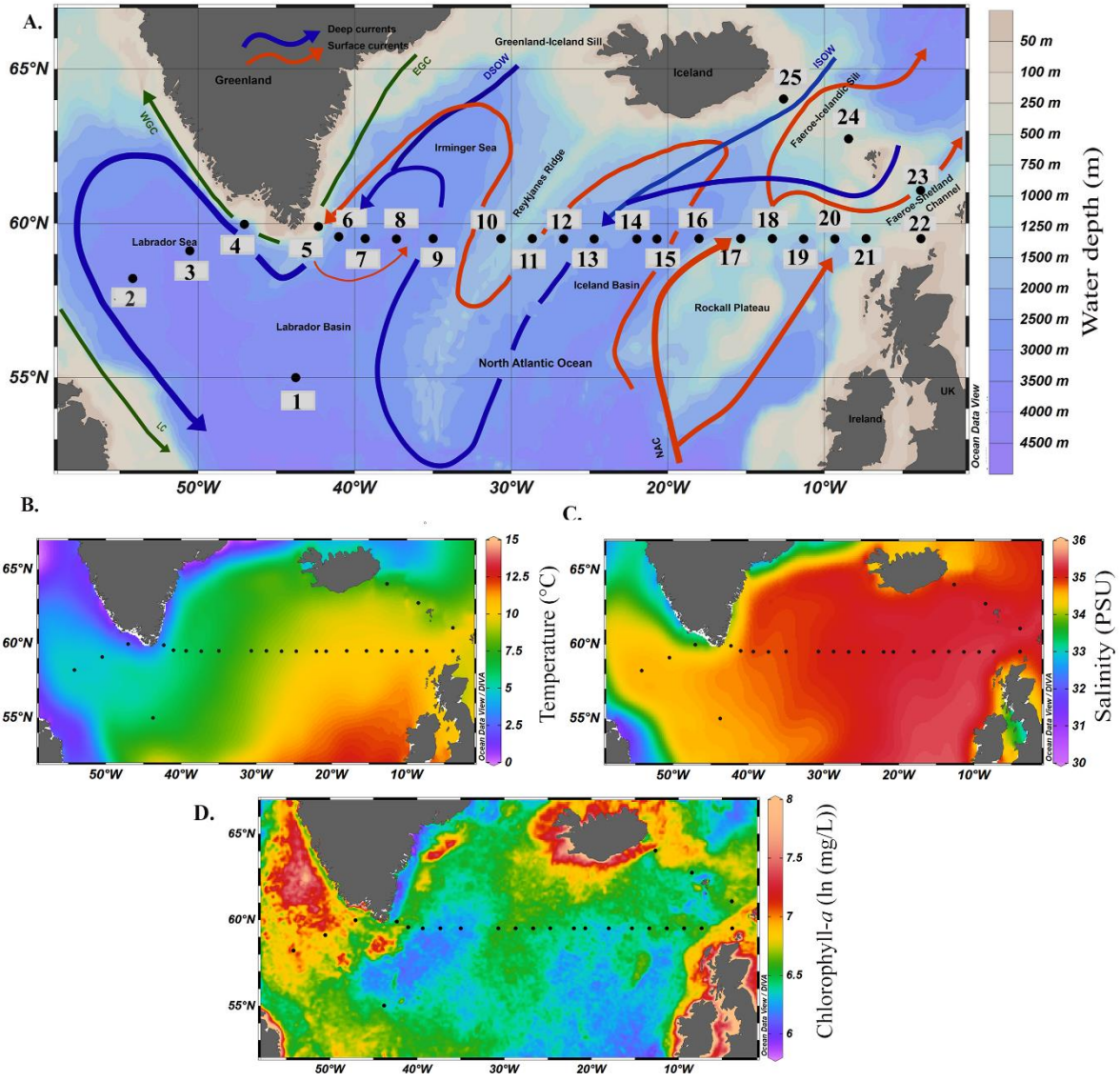

Fig. 3.1. (**A**)Map of locations of surface sediment samples with major ocean currents, has been taken from Fig. 2.2 of Chapter 2 and used here for reference; Map showing surficial distribution of, (**B**) Annual average Sea Surface Temperature (SST, ℃). (**C**) Annual average Sea Surface Salinity (SSS, PSU), and (**D**) Annual average Chlorophyll-a [ln (mg/L)] of the modern ocean.

The annual average temperature and salinity data were obtained from the World Ocean Atlas 2018 (WOA18, https://www.ncei.noaa.gov/access/world-ocean-atlas-2018/) from National Oceanic and Atmospheric Administration (NOAA) (Locarnini et al., 2018; Zweng et al., 2018). Both temperature and salinity data were

averaged over 0 to 100 m of water depth. This depth range was selected as the maximum abundance of planktic foraminifera has been reported in the upper 100 m of water in the northeastern Atlantic (Schiebel and Hemleben, 2000). Annual average Chl-*a* (mg m^{-3}) data was taken from Moderate Resolution Imaging Spectroradiometer (MODIS) Chl-*a* concentration Level 3 data (http://oceancolor.gsfc.nasa.gov/cgi/l3) from the year 2001 to 2018 (Fig. 3.1D). These data were used to analyze the relationship between planktic foraminifera distribution and the main environmental variables along the transect.

3.4. Results

3.4.1. Total planktic foraminifera and Calcium Carbonate

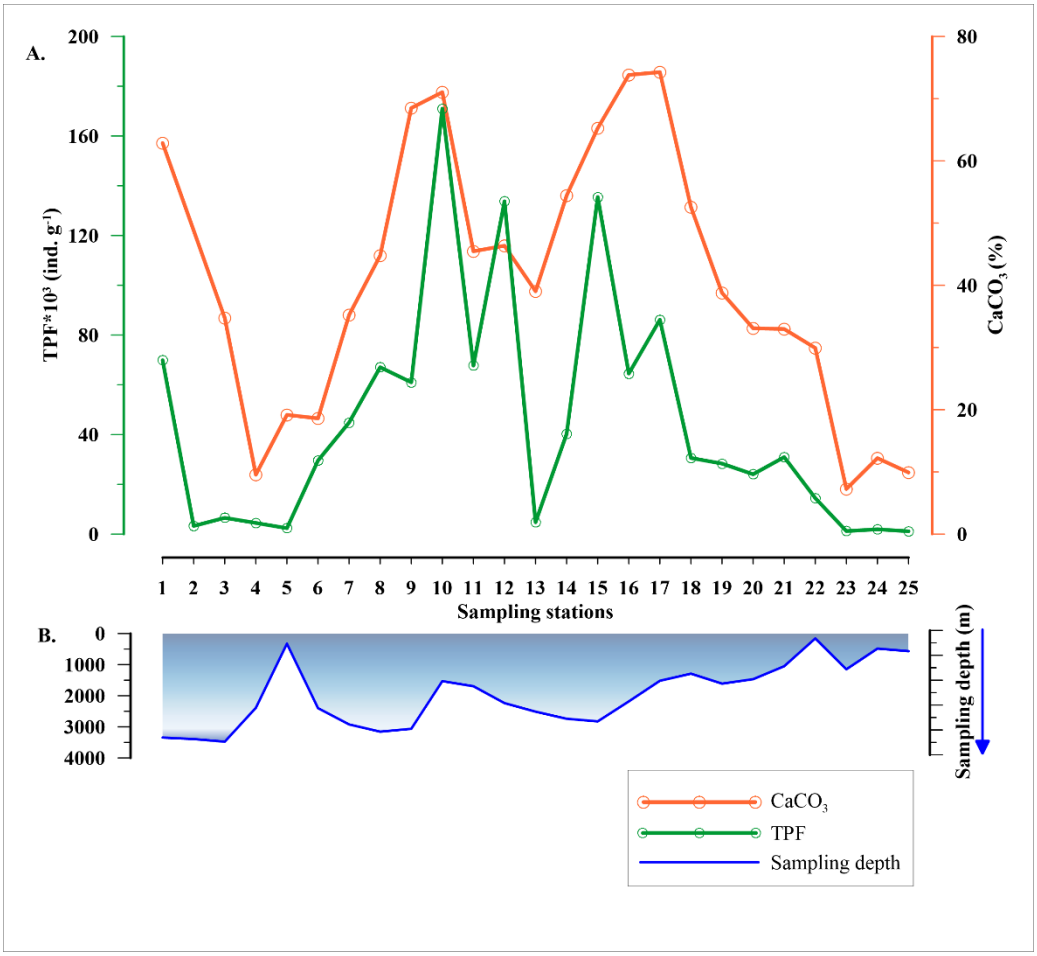

Fig. 3.2. (**A**) Variation in Total Planktic Foraminiferal (TPF) abundance in numbers per gram sediment (ind. g^{-1}) (in green) and calcium carbonate ($CaCO_3$) % (in orange) at different stations, and (**B**) the blue curve depicts the sampling depth (m) of the stations in the subpolar North Atlantic Ocean.

Total planktic foraminifera (TPF) varied between 1212 and 183557 ind. g^{-1}. The highest abundance occurred at station 10 (water depth of 1531 m) near the Reykjanes Ridge, while the lowest abundance was at station 23 (water depth of 158 m), in Faroe-Shetland Channel (FSC). Interestingly, few stations (2, 3, 4, 13) located at deeper depths in the Labrador Sea, east of Greenland and Reykjanes Ridge exhibited low TPF, along with the samples at shallow regions (5, 24, 25), which are generally marked by lowest TPF (Fig. 3.2A and 3.2B). Subsequently, the $CaCO_3$ content in the surface sediments varied from 9% at station 4 (water depth of 2389 m), near the southwest coast of Greenland, to 74% at station 17 (water depth of 1514 m), at the western side of Rockall Plateau. Furthermore, TPF and $CaCO_3$ content varied concomitantly (Fig. 3.2A).

Significant variations in the distribution of planktic foraminifera species was found along the transect. A total of nine species occurred in the samples: *Globigerinita glutinata*, *Neogloboquadrina pachyderma*, *Neogloboquadrina incompta*, *Turborotalita quinqueloba*, *Globigerina bulloides*, *Globigerinita uvula*, *Globorotalia inflata*, *Globorotalia scitula* and *Orbulina* sp. (Fig. 2.6 of chapter 2). The list of planktic foraminifera species and their ecological information can be found in Table 2.4 of chapter 2. Among all, the former six species were the most abundant. Together, they contribute at least 80% to the planktic foraminifera community.

The former five species were consistently present along the transect except at a few stations; whereas *G. inflata* was present only in the eastern part of the transect (absent towards the west of Reykjanes Ridge). However, in the western part of the transect, in the Labrador Sea and Irminger Sea, the sampled stations were dominated by *N. pachyderma*. Moreover, it is the only species found in the two sampling sites of the Labrador Sea, constituting 100% of the assemblage (Fig. 3.3A).

3.4.2. Variations in relative abundances of planktic foraminifera species

The relative abundance of planktic foraminifera species varied considerably from west to east along the transect (Fig. 3.3). *Neogloboquadrina pachyderma* was the most abundant species in the western part of the transect consisting of 100% of the assemblage in sediment fraction of > 100 μm in the Labrador Sea (Fig. 3.3A). This

species was more abundant in the Labrador and Irminger Seas, and its concentration decreased towards the eastern part of the transect. The species was absent from stations 15, 20, 21 and 22 in the eastern side of Iceland Basin. The average relative abundance of *N. incompta* was 22% in the transect with the highest value of 43% (station 20) near the Scottish shelf and nil in the Labrador Sea (stations 2 and 3) (Fig. 3.3B). Higher relative abundance was seen in IFSC (average 41%) followed by Iceland basin-Rockall Plateau (average 27%) and the lowest in the Irminger Sea (average 12%) and the Labrador Sea (average 2%). *Globigerinita inflata* was concentrated only in the eastern transect with the highest relative abundance of 5% at stations 25 and 14 in Iceland-Faroe Ridge and Iceland basin (Fig. 3.3C). The average relative abundance of *G. inflata* was 2% in the eastern part of the transect. Likewise, the average *G. glutinata* percentage along the transect was 19%, with the highest abundance of 45% (station 14) in the Iceland Basin, although absent in the Labrador Sea (Fig. 3.3D).

G. bulloides percentage was low in this area, with an average value of 4%. *G. bulloides* showed a maximum abundance of 20% at station 10 in the Reykjanes Ridge area. While the abundance of *G. bulloides* was nil at stations 2, 3, 22 and 23 in the Labrador Sea and near the Scottish shelf (Fig. 3.3E). Relative abundance of *T. quinqueloba* increased (> 25%) in specific sites in the Irminger Sea, Iceland Basin and off Scotland, with relatively lower percentages in other stations ranging between 0-21% (Fig. 3.3F). *G. uvula* was present in the samples with very low relative abundance, highest as 5% near the Scottish shelf (station 21). The occurrence of *G. uvula* was patchy in the transect. *G. scitula* and *Orbulina sp.* were very rare. *G. scitula* was found only in the eastern Iceland basin (stations 14, 15 and 16) at < 1% and near the east coast of Greenland (station 4) with 4%. *Orbulina* sp. was found only at two stations in the eastern Iceland basin and Iceland-Faroe Ridge (stations 14 and 23).

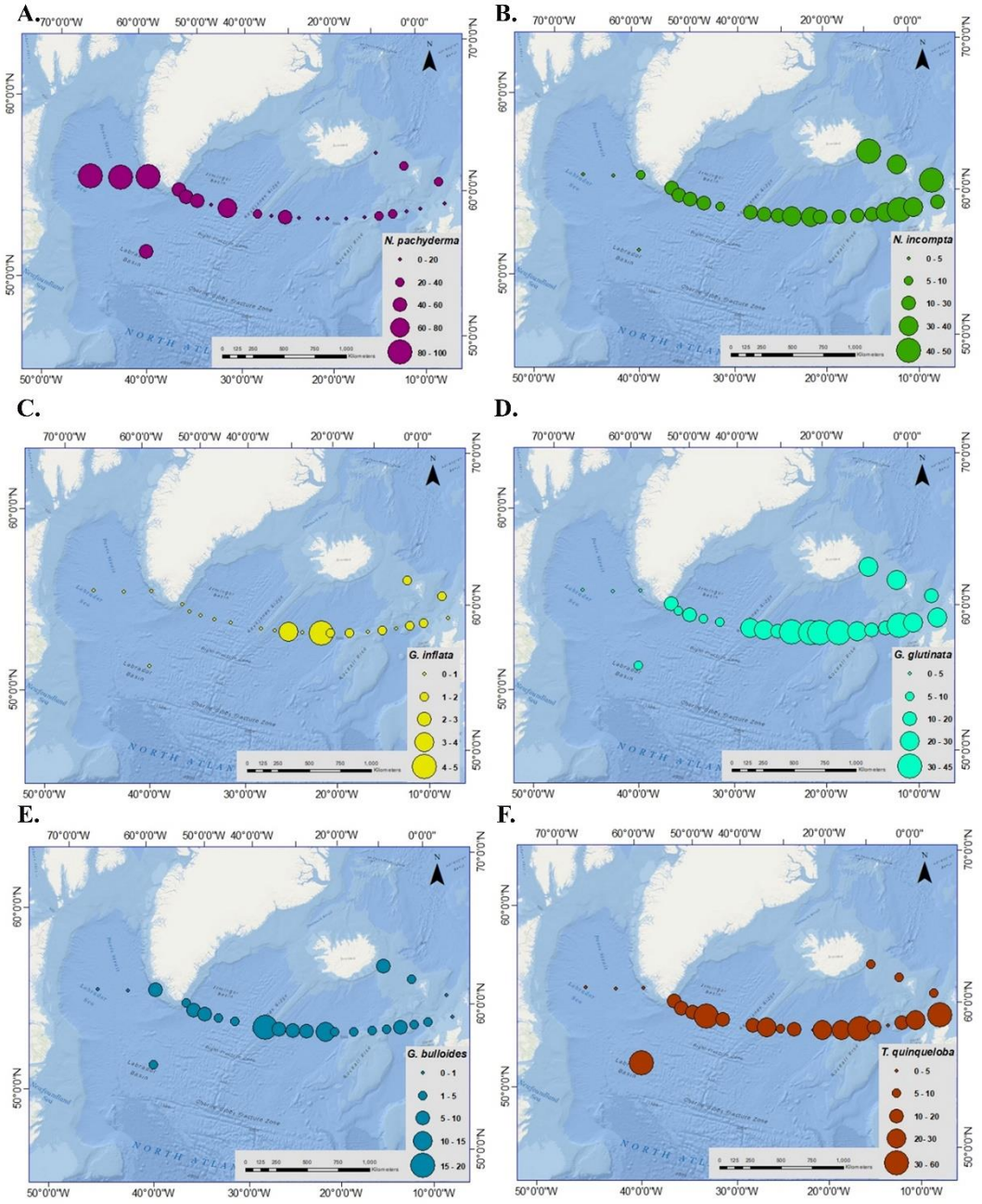

Fig. 3.3. Spatial variation in relative abundance (%) of planktic foraminiferal species (**A**) *Neogloboquadrina pachyderma* (*N. pachyderma*), (**B**) *Neogloboquadrina incompta* (*N. incompta*), (**C**) *Globorotalia inflata* (*G. inflata*), (**D**) Globigerinita *glutinata* (*G. glutinata*), (**E**) *Globigerina bulloides* (*G. bulloides*), (**F**) *Turborotalita quinqueloba* (*T. quinqueloba*) from Labrador Sea to Faroe-Shetland channel. Please note the percentage range for each species is different.

3.4.3. Ratio *N. pachyderma*/ *N. incompta* along E-W transect

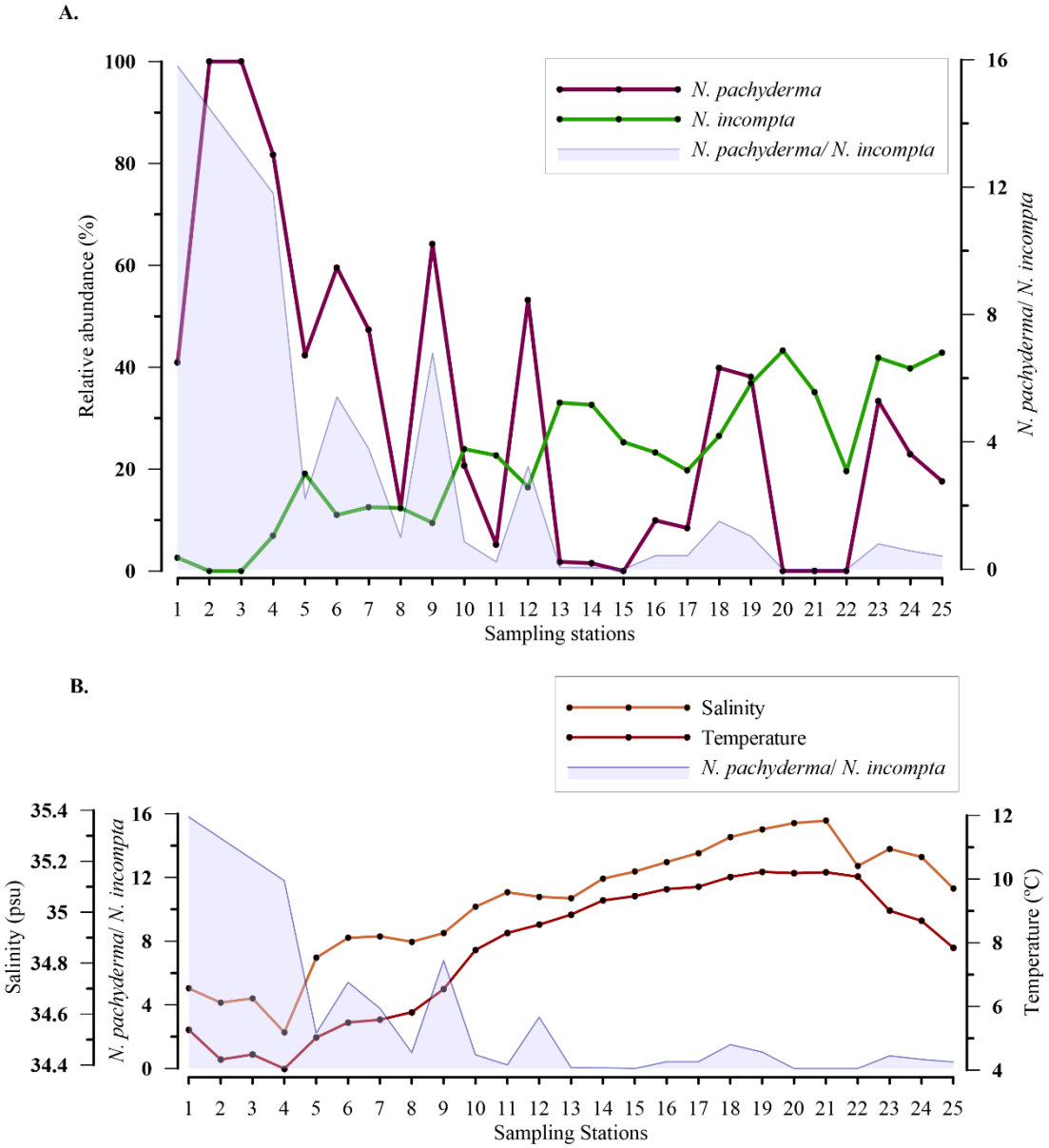

Fig. 3.4. (A) Variation in relative abundance (%) of *Neogloboquadrina pachyderma* (*N. pachyderma*) and *Neogloboquadrina incompta* (*N. incompta*) along the transect and variation in the ratio of *N. pachyderma*/*N. incompta* against the sampled stations is shown in blue; (**B**) Plot showing a relation between the ratio of *N. pachyderma* and *N. incompta* abundance with sea surface temperature and salinity.

The distribution of the species *N. pachyderma* and *N. incompta* is significantly influenced by the temperature and salinity of the region. Also, a change in the relative abundance of *N. pachyderma* and *N. incompta* is linked to specific summer SST values of the water mass (Žarić et al., 2005). Hence, to document the variation in water mass properties (temperature and salinity) from west to east along the sampled transect, the ratio of *N. pachyderma* and *N. incompta* was used. Along the transect, the relative abundance of *N. pachyderma* was observed to increase significantly from the eastern to the western part. However, *N. incompta* exhibited an opposite trend with *N. pachyderma* abundance from east to west (Fig. 3.4A). To better interpret the variation of these two species with respect to water mass (temperature and salinity) along the transect, we analyzed the ratio of the two species (Fig. 3.4). The ratio of *N. pachyderma*/*N. incompta* decreased towards the eastern side of the transect. Also, a higher ratio of > 2 was observed towards the western part of the transect, where lower temperature and salinity values were also observed (Fig. 3.4B).

3.4.4. Principal Component Analysis (PCA)

To assess the ecological preferences of the planktic foraminifera and their relation to the environmental parameters in the SPNA ocean, PCA was performed. The first two PCA factors explain 86.98% of the total variance. The first factor explains 60.71%, and the second factor explains 26.27% (Fig. 3.5). Factor 1 has positive loadings on temperature and salinity computed for the first 100 m (average) of the water column, whereas factor 2 has a positive loading with superficial Chl-*a*. In the PCA analysis, both temperature and salinity vary in the same trend. However, both the parameters have an individual influence on the abundance and distribution of planktic foraminiferal species in the studied area. From the correlation table (Table 3.1), *G. glutinata, N. incompta* and *G. inflata* exhibit positive values regarding temperature (0-100 m) with r values 0.75, 0.81 and 0.48 respectively and salinity (0-100 m) with r values 0.67, 0.86, 0.41 respectively. *N. pachyderma* shows a negative correlation with temperature (r = -0.76) and salinity (r = -0.73). *N. incompta* shows a negative correlation with water depth. Other species have no significant correlation with any of the environmental parameters.

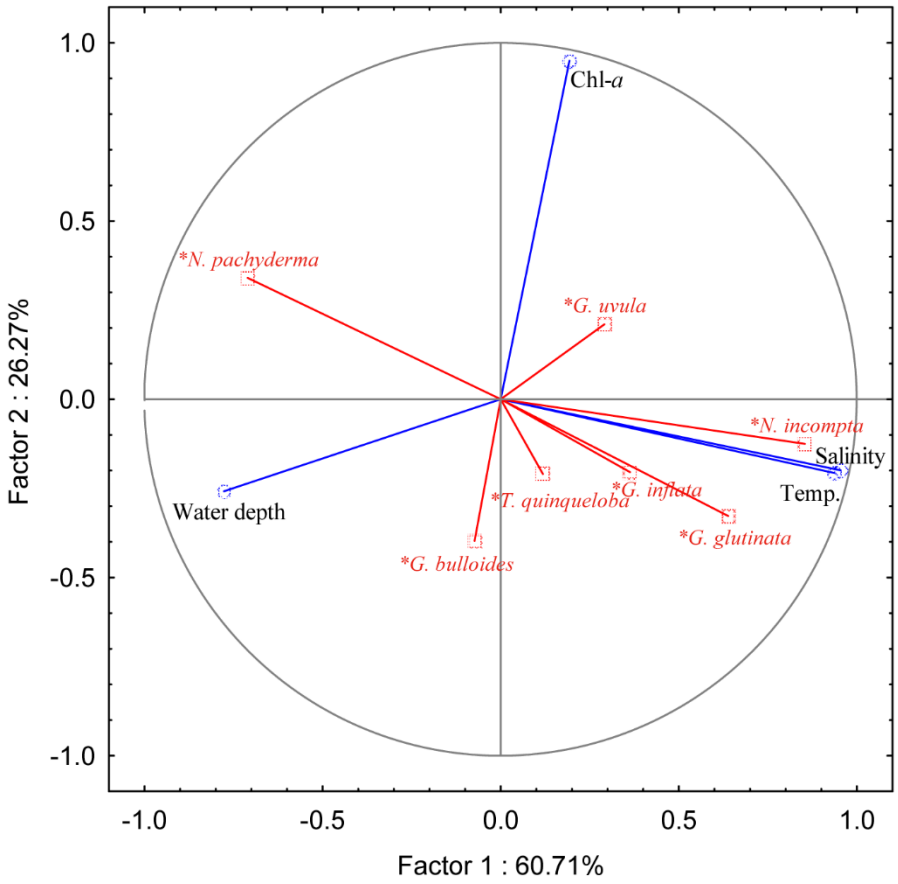

Fig. 3.5. Principal component analysis (PCA) plot of the relative abundance of the different species (*N. pachyderma*: *Neogloboquadrina pachyderma*; *N. incompta*: *Neogloboquadrina incompta*; *G. inflata*: *Globorotalia inflata*; *G. glutinata*: *Globigerinita glutinata*; *G. bulloides*: *Globigerina bulloides*; *T. quinqueloba*: *Turborotalita quinqueloba*; *G. uvula*: *Globigerinita uvula*) with different environmental parameters [average temperature (Temp., °C) and salinity (PSU) of the first 100 m of the water column, Chlorophyll-a concentration (Chl-a, mg m^{-3}) and water depth (m)].

Table 3.1. Correlation factors for relative abundance of planktic foraminifera (*N. pachyderma*: *Neogloboquadrina pachyderma*; *N. incompta*: *Neogloboquadrina incompta*; *G. bulloides*: *Globigerina bulloides*; *T. quinqueloba*: *Turborotalita quinqueloba*; *G. inflata*: *Globorotalia inflata*; *G. glutinata*: *Globigerinita glutinata*; *G. uvula*: *Globigerinita uvula)* with different environmental parameters (average temperature (Temp., ºC) and salinity (PSU) of the first 100 m of the water column, Chlorophyll-*a* (Chl-*a*, mg m^{-3}) and water depth (m). Numbers in red show significant correlations (p-value < 0.05).

	N. pachyderma	***N. incompta***	***G. bulloides***	***T. quinqueloba***	***G. inflata***	***G. glutinata***	***G. uvula***
Water depth	0.44	-0.62	0.08	-0.07	-0.07	-0.30	-0.37
Salinity	-0.73	0.86	-0.04	0.14	0.41	0.67	0.17
Temp.	-0.76	0.81	0.00	0.14	0.48	0.75	0.23
Chl-*a*	0.18	0.05	-0.43	-0.19	-0.05	-0.14	0.22

3.4.5. Cluster Analysis

A hierarchical cluster analysis was performed on the planktic foraminifera dataset to delineate different groups of stations having specific assemblages using the Bray Curtis similarity index (Fig. 3.6). Based on the similarity index, stations along the transect can be divided into three distinct cluster groups I, II and III. The species percentage discussed in this section refers to the individual species contribution (in %) to different clusters, further analyzed from SIMPER analysis.

Cluster group I

Cluster group I includes three stations, 2, 3 and 4, from the central and northeastern Labrador Sea (Fig. 3.6). The planktic foraminifera assemblages associated with this group are dominated by *N. pachyderma*. Other planktic foraminifera species *N. incompta*, *G. bulloides*, *T. quinqueloba* and *G. scitula*, though present in station 4, do not contribute to the similarity percentage of this cluster group. Only *N. pachyderma* contributes 100% to Cluster I. The average similarity between these samples was 76.63% in Bray Curtis similarity analysis.

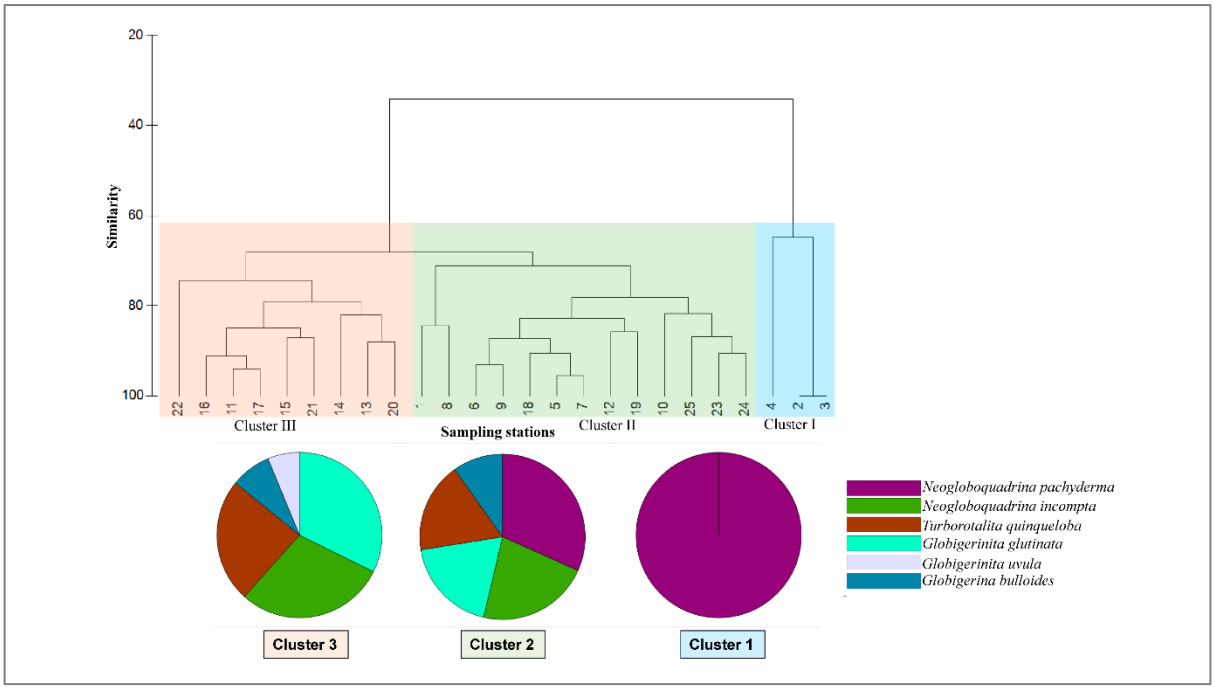

Fig. 3.6. Hierarchical cluster analysis of stations based on foraminiferal assemblages (Bray Curtis similarity). The pie charts show the contribution of different species to different clusters (by SIMPER analysis).

Cluster group II

Cluster group II includes 13 stations from two separate areas within the transect: (1) western half of transect from Reykjanes Ridge to Irminger Sea and central SPG (stations 1, 5, 6, 7, 8, 9, 10 and 12), (2) eastern/northeastern end of transect including the stations from northernmost Rockall Plateau and Iceland-Faroe-Shetland sill (stations 18, 19, 23, 24 and 25) (Fig. 3.6). Compared to monospecific planktic foraminifera associations of Cluster group I, assemblages from Cluster group II are mixed, consisting of almost all the species found in the study area. The most abundant species are *N. pachyderma* (30%), *N. incompta* (21%), *G. glutinata* (18%), *T. quinqueloba* (16%) and *G. bulloides* (9%). The average similarity of the Cluster group II was 78.81% in the samples.

Cluster group III

Cluster III groups nine stations (11, 13, 14, 15, 16, 17, 20, 21 and 22) on the eastern side of the transect from the Reykjanes Ridge to Rockall Plateau and off Scotland (Fig. 3.6). However, few stations from the eastern part of the transect (stations 12, 18 and 19) are included in Cluster group II. The planktic foraminiferal assemblages

in this region consist mainly of *G. glutinata* (30%), *N. incompta* (27%), *T. quinqueloba* (22%), *G. bulloides* (7%) and *G. uvula* (6%). The average similarity between the samples in this group is 80.71%.

3.5. Discussion

3.5.1. Distribution and abundance of planktic foraminifera in the SPNA

Planktic foraminifera distribution is majorly governed by the contrasting water mass characteristics in the SPNA ocean. Total planktic foraminifera co-varied with the calcium carbonate content in the surface sediments along the sampled transect from the Labrador Sea to Faroe-Shetland Ridge (Fig. 3.2A). A positive correlation r = 0.72 between the two suggests planktic foraminifera as the main contributor to the biogenic carbonate in the SPNA. A similar observation representing planktic foraminifera as a key component of bottom ocean carbonate was also reported by Honjo and Manganini (1993), Ziveri et al. (1995) and Retailleau et al. (2012). The distribution of planktic foraminifera is primarily based on sea-surface temperature and salinity of the region (Thunell, 1978). However, particularly in the North Atlantic Ocean, Sea Surface Temperature (SST) plays a dominant role (Stangeew, 2001). Along the transect in this study, the lowest planktic foraminifera abundances in the Labrador Sea can be attributed to persistent low annual average (0-100 m) temperature of 3-4 °C and salinity of 34.86 PSU. Such low temperature causes a low saturation state for $CaCO_3$ and accounts for a low pH in the Labrador Sea (Azetsu-Scott et al., 2010). These characteristic physical parameters (low temperature, salinity and pH) of the Labrador Sea are due to the influx of cold and fresh polar water by East Greenland Current (EGC), fresh Arctic water coming through the Canadian Arctic Archipelago (Melling et al., 2008) and the modified Atlantic water (relatively cooler than North Atlantic Water) coming through Irminger Current (IC) (Pollard et al., 2004). Furthermore, some parts of the Labrador Sea are influenced by relatively much lower pH water mass coming through the Canadian Arctic Archipelago (Azetsu-Scott et al., 2010). The low pH acts as an additional factor causing low planktic foraminifera abundances as it is detrimental to the calcitic foraminifera shells and limits planktic foraminiferal abundance. The decreasing rate of deep water formation, linked to the current climate change scenario (Rahmstorf et al., 2015; Thornalley et al., 2018), increases

the residence time of the cold deep water at the formation site. This also might cause the dissolution of the highly susceptible foraminiferal shells resulting in low planktic foraminifera abundance. Another area with low planktic foraminifera abundances is the shallow water region of Faroe-Shetland Ridge. Planktic foraminifera are more abundant in the open ocean than in neritic zones with shallow water depths (Schmuker, 2000; Retailleau et al., 2009). The water mass near Faroe-Shetland is entrained by a tongue of cold and fresh nutrient-poor Arctic water brought by East Iceland Current (EIC), which can additionally cause a decline in productivity in the region. The sites near the eastern flank of the Reykjanes Ridge show a reverse relation between the TPF and the $CaCO_3$. These deep-sea sites are very dynamic due to their position next to the Reykjanes Ridge slope, the Bjorn and Gardar drift (contourite drift at the eastern side of the Reykjanes Ridge) and also the deep water overflow ISOW. The sedimentation rate is very high at these drift sites (Bianchi and McCave, 2000). Also, these sites are highly influenced by sediment suspension and redistribution by the strong overflow currents north of 58.4 °N (Bianchi and McCave, 2000). However, Giraudeau et al. (2000) suggested that the biogenic carbonates should perfectly represent the upper water mass properties for a regional area. The drifts also contain detrital carbonates which might contribute to the total $CaCO_3$ % of the sediment from these sites. There also could be an effect of dilution due to the deposition of the fine fractions that come with the overflow water. Moreover, the cold ISOW can influence the preservation of the foraminiferal shells. However, ISOW water is well saturated with carbonate (García-Ibáñez et al., 2021) and the sites are much above the Carbon Compensation Depth in this region. Nevertheless, the deep sea sediments in the pelagic ocean consist of foraminifera, coccolithophores, calciferous dinocysts and pteropods. The average contribution of the latter two is minor to the Global carbonates in comparison with the foraminifera and coccolithophores (Baumann et al., 2000). Broerse et al. (2000) have suggested a major contribution of the coccolithophores in the finer fraction (<32 µm) of the carbonates in the NE Atlantic region. Also, major coccolithophore blooms were documented in the SPNA region following the NAC and IC pathways in the south of Iceland (Iglesias-Rodríguez et al., 2002). In another study from Baumann et al. (2000), this has been identified that a lower planktic foraminiferal productivity is associated with an increase in the coccolithophore abundance following a lower nutrient condition. Hence, a possible

difference between the TPF and $CaCO_3$ could be due to an increased contribution of coccolithophores. Lastly, the shell weights of planktic foraminifera fossils are also highly considerable in the total carbonate percentage of the sediments. These shell weights can be influenced by the ambient seawater conditions (surface carbonate, Barker and Elderfield, 2002; Bijma et al., 2002; Marshall et al., 2013), or bottom water conditions (Lohmann, 1995; Broecker and Clark, 2001), as well as by secondary influences like temperature, and nutrient conditions (Aldridge et al., 2012; Weinkauf et al., 2016). However, to understand which factor is responsible for the differences in TPF and $CaCO_3$ %, all these possible reasons need to be scrupulously assessed and studied further for the region.

Planktic foraminifera was most abundant in the middle of the transect covering the eastern Iceland Basin to the central Irminger Sea, which is influenced by the modified nutrient-rich Atlantic water. The presence of Subpolar Front (SPF) in this area near Reykjanes Ridge aids in enhanced planktic foraminiferal abundances in SPNA as frontal regions are characterized by the uplifting of nutrient-rich waters, which allows a greater abundance of phytoplankton and leads to higher primary productivity (Lutjeharms et al., 1985; Kimura et al., 2000). Further, eddy activity in the Irminger Sea and Iceland Basin is responsible for strong mixing at the surface, enriching the surface water with nutrients (Knutsen et al., 2005) which increases primary productivity and hence, the planktic foraminifera abundances in the region.

The planktic foraminiferal number is comparable with the sediment trap and plankton tow datasets previously reported in the SPNA ocean (Schiebel and Hemleben, 2000; Schiebel, 2002). The planktic foraminiferal shells vary from 1.20 x 10^3 to 1.80 x 10^5 g^{-1} (present study) with varying sampling depths. Samples from the open ocean at a depth of 2000 m exhibit comparable numbers with Lundgreen (1996), which represents 1.60 x 10^5 planktic foraminifera tests yr^{-1} (extrapolated tests day^{-1} in September from 47 ° 50´ N, > 100 µm (Table 3 in Schiebel, 2002)). However, a decrease in flux with depth is associated due to the biologically mediated dissolution of planktic foraminifera through the water column while settling (Schiebel and Hemleben, 2000). Further, the relative abundances found in the multinet samples from the BIOTRANS area and at 57 °N, 20-22 °W of Schiebel and Hemleben (2000) is comparable to the planktic foraminifera species

composition in our study. Hence, the species assemblage in the surface sediment in this area represents the upper water mass assemblages. Pados and Spielhagen (2014) also reported a similar observation from Fram Strait. Moreover, the mean lateral transportation for the smaller species *T. quinqueloba* and *N. pachyderma* is 50-100 km and 25-50 km in the Fram Strait, respectively (Gyldenfeldt et al., 2000). From this, we can suggest no significant effect of lateral transportation on planktic foraminifera assemblages in the SPNA ocean.

3.5.2. Species' ecological preferences

The polar to subpolar species *N. pachyderma* was found to be a single dominant species in the Labrador Sea in the present study. A significant increasing trend was observed in the relative abundance of *N. pachyderma* towards the western transect in the study area (Fig. 3.3A). Our data show a strong negative correlation of *N. pachyderma* relative abundance with both temperature ($r = -0.76$) and salinity ($r = -0.73$), marking its dominance in the cold fresh Polar water of Labrador and Irminger Seas (Table 3.1). Previous studies (Kohfeld, 1996; Greco et al., 2019) exhibited a number of environmental factors controlling the abundance and distribution of *N. pachyderma*. This species is observed abundantly in low temperature and low saline regions (Bé and Tolderlund, 1971), which is also evident in our study. Moreover, abundances of *N. pachyderma* of $\geq 95\%$ and $< 50\%$ correspond to a summer temperature of < 4 °C and ≥ 9 °C, respectively (Bé and Tolderlund, 1971). The occurrence of *N. pachyderma* has been reported to vary as a function of salinity, presence/absence of sea ice and deep chlorophyll maximum (Stangeew, 2001; Jonkers et al., 2010; Greco et al., 2019). Usually, *N. pachyderma* abundances show a two-way pulse in its flux in North Atlantic; one in summer at maximum stratification and another in spring (Toldurlund and Bé, 1971; Jonkers et al., 2010). Some studies reported that food availability (Chl-*a* concentration, as a proxy of phytoplankton biomass) also affects the distribution of *N. pachyderma* like other planktic foraminifera (Fairbanks and Wiebe, 1980; Kohfeld et al., 1996; Schiebel and Hemleben, 2005). However, our results for SPNA suggest a statistically validated relationship of *N. pachyderma* abundances with water temperature and salinity but weak dependence on Chl-*a* concentrations ($r = 0.17$ in Table 3.1). Although, it should be noted that the weak correlation of *N. pachyderma*

with Chl-*a* may be a result of considering only the most superficial layer in this statistical analysis.

In the present study, *T. quinqueloba* shows a patchy distribution. It is observed maximum in the Irminger Sea and in the eastern Iceland Basin in our study. Its occurrence has no significant statistical correlation with temperature and salinity along the sampled transect. Though *T. quinqueloba* has been previously reported to vary with primary productivity (Volkmann, 2000), its abundance did not correlate with Chl-*a* concentration in the present study. Meilland et al. (2020) have also documented the same in the Barents Sea opening. This could be due to the specific habitat and food preference of the species, which cannot be represented by Chl-*a* data alone. *T. quinqueloba* has been described to be associated with water mass fronts (Hemleben et al., 1989; Husum and Hald, 2012) and are most abundant at regions of mixing of different water masses and enrichment in the nutrients (Johannessen et al., 1994; Husum and Hald, 2012).

Along the sampled transect, *N. incompta* follows the opposite trend compared to *N. pachyderma* exhibiting decreasing abundance in the subpolar waters of the Irminger and the Labrador Seas. Its abundance has strong positive correlation with temperature (r = 0.81) and salinity (r = 0.86) (Table 3.1). Also, the negative correlation of *N. incompta* percentages with water depth (bathymetry) (r = -0.61) supports its higher abundance in shallow waters of the Iceland-Faroe-Shetland Channel. This observation is coherent with other studies wherein *N. incompta* was abundant in < 100 m water depth in eastern North Atlantic (Schiebel et al., 2001; Husum and Hald, 2012). It prefers shallow stratified warm water (> 8 °C) (Ortiz et al., 1995; Schiebel et al., 2001). *N. incompta* is also related to high nutrient and Chl-*a* concentration (Ortiz et al.,1995; Kuroyanagi and Kawahata, 2004; Kretschmer et al., 2018). However, in the present study, no significant correlation of *N. incompta* abundances with Chl-*a* concentration (r = 0.05) was found. This might be due to the changing food habits of the species with respect to the availability of food in this region. Also, we have taken the superficial Chl-*a* data for the analysis, which could cause a no-correlation with species abundance as *N. incompta* thrives in 50-150 m depth of the water column.

In the present study, *G. glutinata* was most abundant in the central part of the Iceland Basin and decreased towards the western and eastern sides of the sampled transect. *G. glutinata* is a cosmopolitan species with no specific environmental limits (Schiebel et al., 2017). This species has been shown to dominate planktic foraminifera assemblages in the high latitude areas only recently (Schiebel et al., 2017; Spooner et al., 2020). In the subpolar ocean, the species abundance can increase in summer with shallow thermocline depth depending upon food availability (Stangeew, 2001). Some authors have suggested, it increases with the onset of spring bloom (Ottens, 1992) and few links it with a change in the possible food habitat (Meilland et al., 2020; Spooner et al., 2020). We found that the species occurrence has a positive correlation with temperature (r = 0.75) and salinity (r = 0.67) along the transect showing the species' affinity towards warmer and more saline water mass, but no correlation with Chl-*a*. *G. glutinata* was also reported to have a strong relationship with seasonality and food availability, especially associated with diatoms (Schiebel and Hemleben, 2000). Our data in this region shows the distribution of *G. glutinata* is related to the temperature and salinity variation rather than Chl-*a* concentration.

In the present study, temperate to subpolar species *G. bulloides* relative abundance shows a weak negative correlation (r = -0.42) with Chl-*a* concentration and also does not depend on temperature and salinity (Fig. 3.5). Here, *G. bulloides* is maximum over Reykjanes Ridge and central Iceland Basin. Generally, this species is most abundant in highly productive subpolar and tropical regions and is specifically marked as an upwelling indicator species in the tropics (Be and Tolderlund, 1971; Schiebel et al., 2001; Salguiero et al., 2010). However, a negative correlation possibly can be due to a change in the nature of food habitat in the area. Meilland et al. (2020) suggested Chl-*a* may not always represent a good indicator for foraminiferal distribution, showing no link between Chl-*a* and the productivity indicator species *T. quinqueloba* and *G. uvula* in the Barents Sea. Thus, *G. bulloides* can also be summed as a ubiquitous subpolar species and does not follow any specific trend in the SPNA ocean.

G. uvula is a temperate to polar species, constituting 0.50-2% of the assemblages (Schiebel and Hemleben, 2017), which is consistent with our data. Recently,

increased abundances of this species in surface water assemblages from subpolar to polar regions (Stangeew, 2001; Retailleau et al., 2011; Meilland et al., 2020) have been noticed, but it was not reflected in the surface sediment assemblages (Meilland et al., 2020) as also seen in our data. As the plankton tow study provides information, particularly during the sampling period, *G. uvula* abundance in the water column at that particular period can increase depending on the favourable conditions and can be different from surface sediment assemblage. The small sized-less resistant species may have low preservation potential while settling in sediment, causing an enhancement of the same in the water column and not in sediment. Moreover, the lower settling velocity of this species gives rise to a higher concentration of its tests in the water column. *G. uvula* mainly concentrated in < 100 µm fraction (Schiebel et al., 2017), might also be a reason for the low abundance of the same in > 100 µm in our study. There is no correlation of *G. uvula* percentages in our data with temperature or salinity. The occurrence of *G. uvula* presumably co-varies with primary productivity (Volkmann, 2000; Schiebel and Hemleben, 2017) and generally have a seasonal production in spring and early summer (Schiebel et al., 1995). However, it exhibits an insignificant correlation with Chl-*a* concentrations along the transect. In a recent finding, Meilland et al. (2020) have also shown no significant correlation between Chl-*a* content and *G. uvula* occurrence as they showed a more dependency on food composition rather than concentration.

G. inflata has a low abundance and is present only on the eastern side of the transect. Generally, its occurrence ranges from subpolar to subtropical waters (Schiebel et al., 2017). In the subpolar ocean, its intrusion represents the influence of warmer water coming through the North Atlantic Current (NAC). It thrives at the base of the seasonal thermocline (100-200 m) (Ganssen and Kroon, 2000; Cléroux et al., 2007). *G. inflata* abundance depends on the surface, and subsurface nutrient enrichment (Schiebel et al., 2017), i.e., eddies and frontal mixing supports its distribution. However, we found only weak positive correlation of *G. inflata* abundances with temperature ($r = 0.47$) and salinity ($r = 0.41$) but no relation to Chl-*a* concentrations ($r = -0.05$).

Abundances of the subtropical species *G. scitula* and *Orbulina* sp. are rare and very low in SPNA. However, *G. scitula* and *Orbulina* sp. have been described as subtropical species and are associated with NAC (Ottens, 1991). Hence, their presence can indicate the entrainment of warm NAC water in the study area. Moreover, the absence of correlation of planktic foraminifera with Chl-*a* in the study area is probably due to the fact that the chlorophyll data represent only the superficial layer and not the 0-100 m.

3.5.3. Faunal Assemblages

Along the sampled transect in the subpolar North Atlantic Ocean, the stations are grouped into three distinct faunal groups based on hierarchical cluster analysis.

Labrador Sea - Polar group (Cluster group I)

The Labrador Sea has the coldest water mass along the transect. It is influenced by the cold surface currents East Greenland Current (EGC), West Greenland Current (WGC), Labrador Current (LC) and relatively warmer surface current Irminger Current (IC). Also, it receives fresh Arctic water through the Canadian Arctic Archipelago. Cluster group I, associated with the Labrador Sea, comprises a single species *N. pachyderma* (100%) (Fig. 3.6). *N. pachyderma* is dominant in subpolar and polar conditions (Bé and Tolderlund, 1971; Volkmann, 2000). A decrease in species diversity and richness often occurs in regions of high environmental stress (Keller and Abramovich, 2009) which is the case in the Labrador Sea. The elevated abundance of *N. pachyderma* in the region can also be explained by the good preservation of these thick-shelled species as that is more resistant to dissolution than *T. quinqueloba* and *G. uvula* (Berger, 1973; Boltovskoy and Wright, 2013).

Study on modern-day planktic foraminifera assemblages in the Labrador Sea is rare. A previous study by Stehman (1972) documented two species, *N. pachyderma* and *G. bulloides*, in > 200 µm mesh size from the Labrador Sea. Besides, the dominance of single species in this study can be due to an underestimation of the foraminiferal species with smaller size fractions. The size range considered in the present study is > 100 µm with relative abundances of *N. pachyderma* 100%. Conversely, Stangeew (2001) reported high abundances of small-sized (> 63 µm fraction) *T. quinqueloba* (46.80%), *G. uvula* (3.50%), along with *G. glutinata* (20.80%), *N. pachyderma* (19.60%), *N. incompta* (2.60%), *G. bulloides* (6.40%), *G. scitula* (<

1%) and *G. inflata* (< 1%) in convection region of Labrador Sea in 0-200 m water column. We compared our surface sediment data of station 3 with plankton tow results of Stangeew (2001). To ascertain whether the species abundances are size-dependent, we examined the 63-100 µm size fraction in the samples of the Labrador Sea. In this fraction, compared to > 100 µm fraction, the smaller-sized species *G. uvula* was more dominant with 37-80% abundance (Fig. 3.7). The dominance of *N. pachyderma* in > 100 µm fraction and of *G. uvula* in 63-100 µm fraction infers that size plays a significant role in the analysis of planktic foraminifera assemblages, which was also observed in previous studies (Carstens et al., 1997; Husum and Hald, 2012).

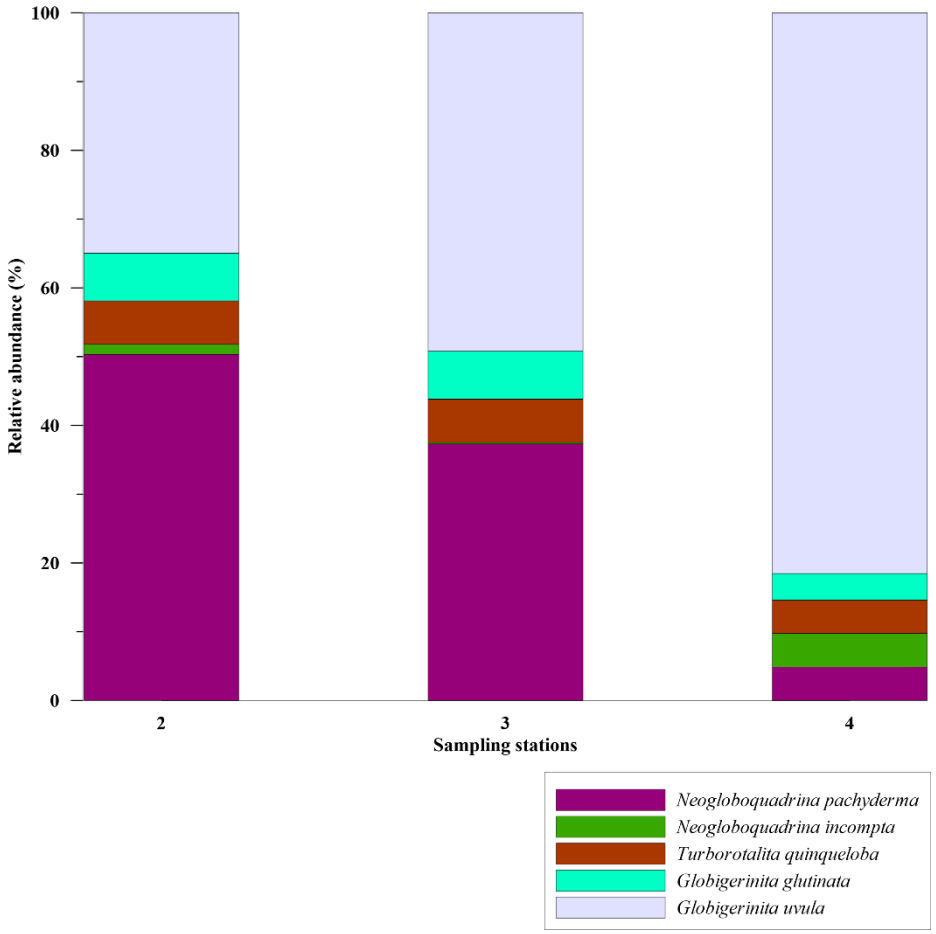

Fig. 3.7. Relative abundance (%) of planktic foraminiferal species in 63–100 µm size fraction from the stations of Labrador Sea, shown in bar plots.

In polar regions, Bé and Tolderlund (1971) reported *N. pachyderma* to be the most abundant in > 200 µm fraction. Whereas Carstens et al. (1997) and Volkmann (2000) found the species abundance to be reduced to 60% in the fraction of > 63

µm and 70% in the fraction of > 125 µm, respectively. Also, test sizes of *T. quinqueloba* in Nordic Seas have been found to differ in the past under varying climatic conditions with shell sizes becoming larger under the Atlantic water influence (Bauch, 1994). As both the size fractions in the Labrador Sea samples from our study are dominant in the cold and freshwater species *N. pachyderma* and *G. uvula*, we suggest a stronger influence of fresh melt water and EGC-influenced water than the warmer IC water in the Labrador Sea. This can be evident as the recent freshwater/meltwater flux increased in the eastern Labrador Sea (Yang et al., 2016; Zhang et al., 2021).

Irminger Sea and Iceland-Faroe-Shetland subpolar group (Cluster group II)

This group includes two areas: (1) the western side of the transect within central and northern subpolar gyre (east of Greenland, Irminger Sea and Reykjanes Ridge), (2) the eastern side of the transect in the Iceland-Faroe-Shetland Channel (IFSC) and on the northernmost Rockall Plateau between the two pathways of NAC. Cluster group II is comprised of mixed assemblages of temperate to subpolar species *N. incompta, G. glutinata* and *T. quinqueloba* and cold-water species *N. pachyderma*. On the western transect, the cold fresh water of EGC comes in contact with the relatively warm and more saline water of IC (Dickson et al., 2007). Thus, a mixed assemblage is expected in the region. The dominance of *N. pachyderma* explains this, followed by a significant abundance of *T. quinqueloba* and *N. incompta.* While, in the eastern side of the transect, assemblages consist primarily of *N. incompta* together with *T. quinqueloba* and *N. pachyderma*, mainly in the IFSC region. In the IFSC, the Arctic water (lobe of cold water north of Iceland coming in the southern Norwegian Sea) interacts with the warm Atlantic water coming with NAC. Modified North Atlantic Water (MNAW), a cooler water mass than Eastern North Atlantic Water (ENAW), is found in the upper water masses at IFSC and in some parts of the Rockall Plateau (Read, 2000). A mixed assemblage of both cold and warm species represents a mixing of cold and warm water. Planktic foraminifera assemblages of Group II reflect the greater influence of the polar water in the western SPNA.

Central North Atlantic (Iceland Basin, northwestern Rockall Plateau, off Scotland) temperate group (Cluster group III)

The region towards the east of the transect, Iceland basin, Rockall Plateau, receives warm water from NAC (Pollard et al., 2004). This group is associated with predominantly temperate and subpolar species assemblages in the central North Atlantic, which exhibit warmer-water affinity. The most abundant species of this group are *G. glutinata*, *N. incompta* and *T. quinqueloba*, while *G. bulloides* and *G. uvula* are less abundant. In the central Iceland basin, more *N. incompta* and *G. glutinata* represent a warmer water influence. Also, the presence of *G. inflata* and *Orbulina* sp. in this group shows the influence of warm subtropical water (Ottens, 1992). *G. uvula*'s contribution to the assemblage (6%) shows the presence of fresher meltwater at the surface in summer.

T. quinqueloba percentages are higher at the sites near the NAC pathways in Iceland Basin, near Scotland and the Reykjanes Ridge. NAC, in this region, acts as a frontal zone, separating the cold fresh subpolar water mass and warm saline subtropical water mass (Read, 2000; Daniault et al., 2016). *T. quinqueloba* is a front indicator species; hence, its higher abundance at the eastern Iceland basin and Reykjanes Ridge reflects the proximity of the frontal zone in the studied transect.

3.5.4. *N. pachyderma* vs *N. incompta* ratio as an indicator for change in water mass property

N. pachyderma is a subpolar to polar species with an increase in abundance poleward (Bé and Tolderlund, 1971). While *N. incompta*, reported earlier as a dextral variety of *N. pachyderma*, is preferably found in relatively warmer and more saline waters. In the present study, *N. incompta* represented its association with temperate/ subtropical characteristics of NAC in the region, as the PCA plot demonstrated (Fig. 3.5). The abundance of both species depends on physico-chemical factors such as temperature and salinity of the water mass, presence/absence of sea ice, stratification and food availability (Jonkers et al., 2010; Greco et al., 2019; Meilland et al., 2020). The highest abundances of *N. pachyderma* match with an optimum temperature range of -0.50 – 17 °C, whereas maximum percentages of *N. incompta* occur at 8.50 – 21.40 °C (Žarić et al., 2005, based on

sediment traps study; Hilbrecht, 1996, based on surface sediments study). The critical temperature for the shift from the dominance of *N. pachyderma* to *N. incompta* is at ≥ 9 °C (Žarić et al., 2005). In our study, the highest abundances of *N. pachyderma* are concentrated in the Irminger and Labrador Seas at an average temperature of 5.54 °C and an average salinity of 34.96 PSU. Contrary to this, *N. incompta* is most abundant in the eastern side of the North Atlantic, with maximum abundances at an average temperature of 6.82 °C and salinity of 35.05 PSU. The turnover in prevailing abundances of *N. pachyderma*/ *N. incompta* takes place near Reykjanes Ridge (Fig. 3.4). We suggest a change in water mass properties from the change in assemblages at the western side of Reykjanes Ridge, previously documented by authors from earlier studies (McCartney and Talley, 1982; Read., 2000). This can be illustrated by the ratio between the abundances of *N. pachyderma* and *N. incompta* along transect plotted against the temperature and salinity (average of upper 100 m water column) (Fig. 3.4B). The ratio of *N. pachyderma* and *N. incompta* was found to be > 1 in the western side with the highest values at the temperature of < 4.60 °C and salinity of < 34.80 – 35 PSU in the present study. Our results on differences in the abundances of *N. pachyderma* and *N. incompta* on the transect across SPNA are in agreement with previous data on this species ratio as an indicator of the changes in water mass distribution in Nordic Seas and SPNA (Eynaud, 2011). Updating data on the *N. pachyderma*/*N. incompta* ratio improves the use of this tool for paleoceanographic studies, as demonstrated by Eynaud et al. (2009). This is evident with the hydrographic change across the Reykjanes Ridge in the upper water masses.

3.5.5 A shift in Planktic foraminiferal assemblages in the North Atlantic

The recent trends in warming and its associated processes have led to the change in ecology and distribution of planktic foraminifera in the North Atlantic (Jonkers et al., 2019; Meilland et al., 2020). Schiebel et al. (2017) and Meillend et al. (2020) have reported a marked change in planktic foraminifera assemblages and their diversity, with an influx of temperate species increasing their dominance in the region.

We have compared our planktic foraminifera assemblage data with previously published data presenting samples collected in the North Atlantic from Matul et al.

(2018), which also includes Pflaumann et al. (2003) dataset, to see if there is any change in the planktic foraminiferal assemblages. Their dataset consists of the surface sediment assemblages from the SPNA ocean. We analyzed the average species composition for each region i.e., I. Irminger Sea II. Iceland Basin and III. Rockall Plateau and IFSC in both datasets. The assemblages observed in the dataset mentioned above and our samples are generally similar in species composition except for the absence of *Globorotalia hirsuta* and *Globorotalia truncatulinoids* in the present data.

We compared the planktic foraminifera relative abundance data for each region in both datasets (Fig. 3.8) to illustrate a possible effect of the oceanographic shift on the planktic foraminifera assemblages. The most significant faunal change within the groups was found in the Irminger Sea and Iceland basin. Irminger Sea assemblage is comprised of *N. pachyderma*, *N. incompta*, *G. glutinata, G. bulloides* and *T. quinqueloba* in our study. Whereas, the Iceland basin and Rockall Plateau-IFSC assemblage consist of all the species of the Irminger Sea assemblage along with *G. inflata* in the present study. Compared to Matul et al. (2018) data, *T. quinqueloba* percentage has increased, and percentages of *G. bulloides* and *G. glutinata* have decreased in our study area in the Irminger Sea. Likewise, in the Iceland basin, *T. quinqueloba* percentage has increased, and *G. glutinata* and *G. bulloides* percentages have decreased in this study in comparison to Matul et al. (2018) data. Moreover, the present study observed an increased relative abundance of *G. glutinata* and decreased *G. bulloides* in the Rockall Plateau-IFSC region.

Thus, an increase in subpolar species *T. quinqueloba* in the Irminger Sea and Iceland Basin from our data could indicate an increase in surface productivity and a relative increase in the cold subpolar water influx in the region. Also, a decrease in *G. inflata* percentage in both the Iceland basin and Rockall-IFSC could indicate a decrease in the influx of warm NAC water to the region (Staines-Urías et al., 2013).

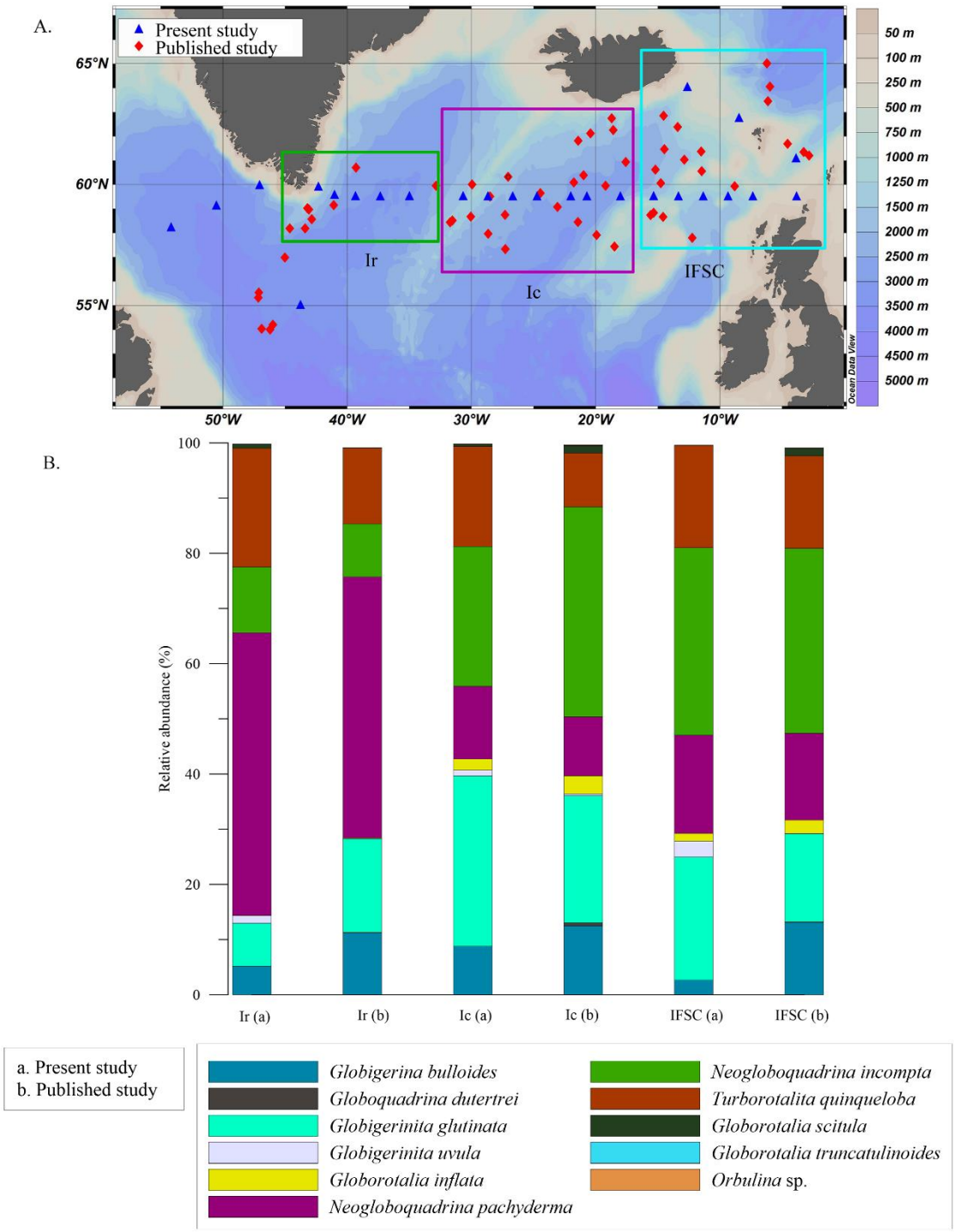

Fig. 3.8. (**A**) Map showing locations of the samples from Matul et al. (2018) (red diamond) and from our study (blue triangle). (**B**) Comparison of the relative abundance (%) of planktic species from this study (**a**) with Matul et al. (2018) (**b**), shown in the bar chart; Ir, Irminger Sea; Ic, Iceland Basin; IFSC, Rockall Plateau and Iceland-Faroe-Shetland Channel.

The abundance of *G. inflata* at the eastern side of the transect has been used as a potential indicator of the NAC water influx (Staines-Urías et al., 2013). A lower NAC influx is linked with a strengthened and expanded SPG (more eastward) and vice-versa (Hátún et al., 2005; Staines-Urías et al., 2013). Hence, a decreased influx of *G. inflata* at the eastern side of the transect, i.e., near Faroes, can be due to strengthened and expanded SPG. Moreover, an ongoing increase in the Greenland Ice sheet melt affects the Irminger Sea and the Labrador Sea the most, increasing freshwater influx (Bamber et al., 2012; Yang et al., 2016). The Labrador Sea assemblage in our study also shows an increase in cold water species *N. pachyderma* (> 100 µm), *G. uvula* and *T. quinqueloba* (> 63 µm), indicating a possible drop in temperature and salinity of the upper water column with an increased influence of SPG activity and an increase in freshwater flux. Thus, a slight shift in planktic foraminiferal assemblage in the SPNA ocean was observed in the present dataset. A further study on the present planktic foraminiferal distribution in the water column (plankton tow) in the SPNA ocean will be an important addition to this study.

3.6. Conclusions

The present study documents the planktic foraminiferal distribution and species composition in the Subpolar North Atlantic Ocean.

1. In the Subpolar North Atlantic Ocean, the recent planktic foraminifera in surface sediments show a close correlation with the surface-subsurface water mass structure.
2. Based on cluster analysis, three planktonic foraminifera groups could be identified across the transect in the Subpolar North Atlantic Ocean. The polar group is marked by the dominance of *N. pachyderma* in the Labrador Sea. The mixed group is represented by both warm and cold assemblages (*N. pachyderma, N. incompta*, *G. glutinata* and *T. quinqueloba*) from the different locations on the western and eastern sides of the transect. Lastly, a warm temperate group included stations from Reykjanes Ridge to Iceland Basin and Rockall Plateau with warm-water assemblage composed of *G. glutinata, N. incompta, T. quinqueloba, G. bulloides* and *G. uvula*.

3. The ratio *N. pachyderma* and *N. incompta* can be used as a proxy to identify the difference between cold Irminger water and relatively warmer Atlantic water in the studied transect.
4. The distribution of *N. pachyderma* in the Labrador Sea indicates the presence of cold and freshwater mass. In the Labrador Sea, *N. pachyderma* was dominant in > 100 µm fraction while *G. uvula* dominated in 63 - 100 µm fraction. It can be concluded that size is an important factor in studying the planktic foraminiferal abundances and distribution of species.
5. A comparison of our planktic foraminifera data with the previous dataset reveals a slight shift in planktic foraminiferal assemblage in the SPNA ocean.

Chapter 4

4. Surface hydrographic changes in the Subpolar North Atlantic Ocean during Holocene

4.1. Introduction

The Holocene has been documented as a relatively stable climatic period for long before the recent advancements in paleoclimatic studies (Dansgaard et al., 1993). The idea of the millennial to centennial-scale variations in the Holocene has been ascertained from numerous findings in marine, terrestrial and atmospheric records (Denton and Karlén, 1973; O'Brien et al., 1995; Bianchi and McCave et al., 1999; Bond et al., 1997, 2001; Mayewski et al., 2004). The Rapid Climate Changes, Ice rafting drifts, and Bond events are well-known from the North Atlantic Sectors (Bond et al., 2001; Jennings et al., 2002; Mayewski et al., 2004; Moros et al., 2004). These events are superimposed upon the long-term Holocene variations from early to late Holocene. The importance of these events with respect to the Subpolar North Atlantic (SPNA) Ocean hydrographic changes is a primal focus for paleoclimatic studies, given its role in global climate. The SPNA Ocean is one of the major climatic elements in shaping the global climate through Atlantic Meridional Overturning Circulation (AMOC). SPNA hydrographic changes are intricately linked with AMOC variations, evident from both modern and past records (Böning et al., 2006; Zhang, 2008; Thibodeau et al., 2018; Thornalley et al., 2018; Caesar et al., 2021). The recent Great Salinity Anomalies in the SPNA region (Dickson et al., 1988; Belkin et al., 1998), the subpolar warming hole (Drijfhout et al., 2012), and a declining AMOC (Holliday et al., 2020; Spooner et al., 2020) trend are some of the modern observations from the SPNA. Owing to its sensitivity and the complexity it holds, SPNA has caught significant attention to understand its variability and its impact on other climatic components.

Subpolar Gyre dynamics, solar insolation, and North Atlantic Oscillations (NAO) are among the different underlying mechanisms explaining the SPNA hydrographic variability during the Holocene (Bond et al., 2001; Marchal et al., 2002; Andersen et al., 2004; Staines-Urias et al., 2013; Sicre et al., 2021). The varying SPG dynamics are responsible for the variability seen in the North Atlantic Current

(NAC) attributes at the eastern SPNA (Hatun et al., 2005). Also, westerlies coupled with NAO are known to impact the heat and salt distribution in the SPNA from the subtropics (Hurrell et al., 2003; Lohmann et al., 2009). There have been different studies in both eastern and western SPNA. However, there has been an inhomogeneous evolution in hydrography between the eastern and western segments of the SPNA during the Holocene (Andersen et al., 2004; Solignac et al., 2004; Moros et al. 2004, 2006; de Vernal and Hillaire Marcel, 2006; Orme et al., 2018). The Holocene thermal maximum complexity, a temporal and spatial variability observed in the North Atlantic arose due to solar insolation and ice sheet feedback (Renssen et al., 2009). Thornalley et al. (2009) emphasized the strong influence of subsurface warm Atlantic water on SPNA inflow, which started only after 7 ka BP after the retreat of the Laurentide Ice sheet meltwater. The varying impact of Ice rafting events with cold Arctic water advance during the Holocene has reconfigured the Subpolar North Atlantic hydrography, but to different extents depending on different regional factors associated with the specific location in the SPNA. It is extremely critical to differentiate the mechanisms underlying the changing hydrography. Thornalley et al., 2009 have suggested 1500-year cycles of SPNA hydrography with alternate stratification events attributed to inherent gyre dynamics. Likewise, Staines-Urias et al. (2013) have explained the eastern SPNA hydrography with strengthened and weakened SPG conditions under positive and negative modes of NAO. Moreover, studies in the western Atlantic and north of Iceland have reported an increase in the cold freshwater inflow towards the late Holocene which further supported the influence of cold freshwater in much of western SPNA (Risebrobbaken et al., 2003; Solignac et al., 2006; Moros et al., 2006; Perner et al., 2011; Moffa-Sanchez et al., 2017; Sicre et al., 2021). Reykjanes Ridge plays an important role as it's adjacent to the subpolar front separating the cold fresh Arctic water and the warm subtropical water. Hence, this location delivers an advantage of investigating the advancement and retreat of cold water on either side of this region.

In this chapter, we illustrate the variation in hydrography near Reykjanes Ridge since the early Holocene using the planktic foraminiferal abundance and oxygen isotope composition of specific planktic foraminifera species from the core AMK 410. We would also compare the published data from the eastern and western sides

of our study site to better constrain the retreat and advance of the meltwater and the NAC.

4.2. Regional hydrography

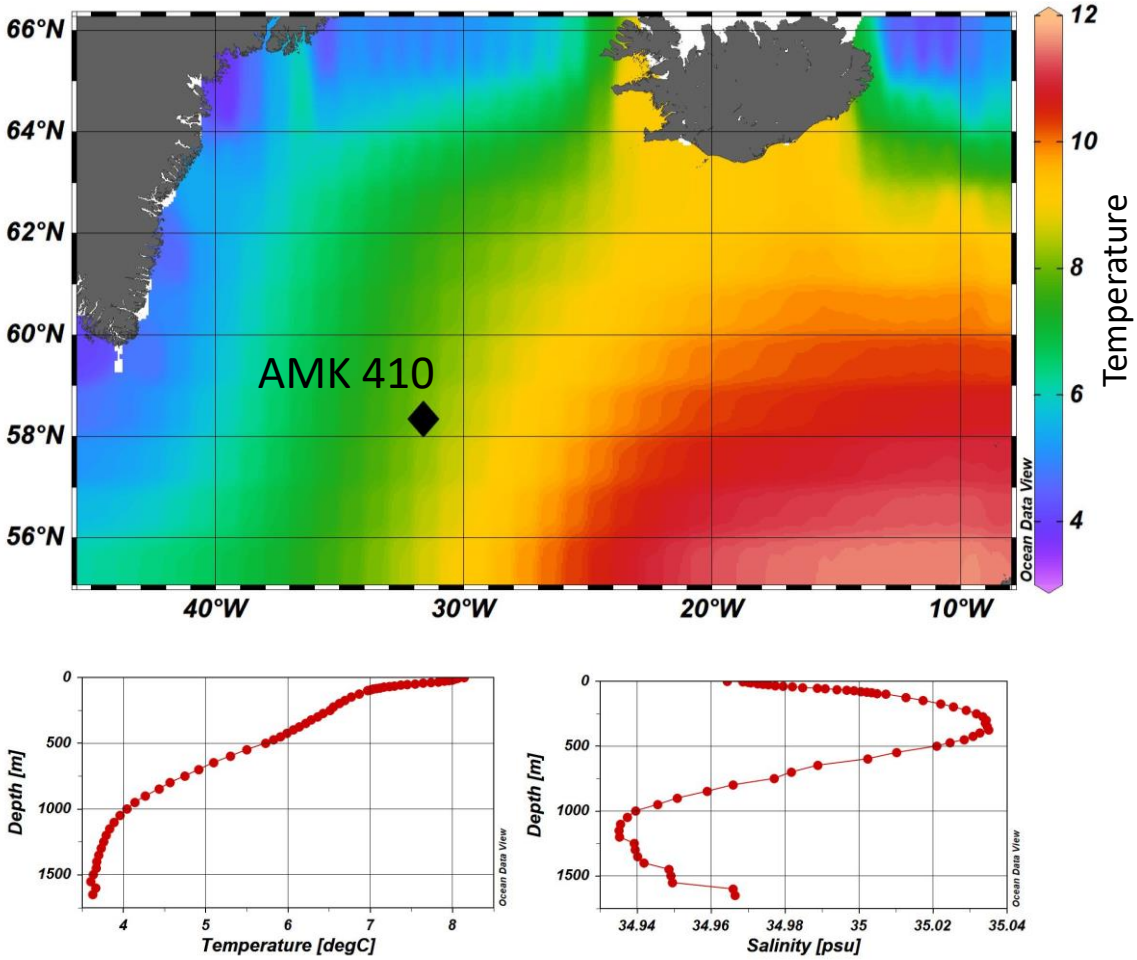

Fig. 4.1. Core location of AMK 410, shown in the map with surface temperature variation (top), below are the vertical temperature and salinity graphs (with depth) for the core site (bottom).

The hydrography over the Reykjanes Ridge depends on the relative contributions of SPG and STG. On average, during 1966-2004, SPG and STG contributed with a ratio of 44.1:55.9 to the mode water over Reykjanes Ridge, according to a model study by E. de Boisséson et al. (2012). The bathymetry of Reykjanes Ridge has shaped the hydrography of the SPNA region (Petit et al., 2018). Holocene studies near our core sites have cited the hydrographic variations in the area caused by the sensitivity toward the advancement of meltwater (Perner et al., 2018). The hydrography of this site is highly sensitive to the position of the subpolar front (SPF). The temporal and spatial variability of the SPF has been reported in recent

records (Belkin and Levitus, 1996). SPF is dependent on the subpolar gyre strength. A strengthened gyre would shift the front further east while a weakened SPG would cause a westward shift of the front. The present annual mean SST at the core site is 8 °C and SSS is 34.97 PSU (Fig. 4.1). The temperature and salinity may change depending on the variable influx of cold EGC water.

4.3. Materials and methodology

The material and methodology for this study can be found in chapter 2, 'Materials and Methods' of the thesis. The chronology of the core has also been discussed in chapter 2.

4.4. Results

4.4.1. Planktic foraminiferal assemblages during Holocene

The total planktic foraminifera (TPF) varied between $20x10^3$ and $100x10^3$ g^{-1} sediment in the core AMK 410 from 10.3 ka BP to the present. The TPF does not display a specific trend but instead fluctuates throughout the Holocene, and the lowest was seen in the last 1 ka BP (Fig. 4.2). However, a decreasing trend can be marked in the plot during the 4-2 ka BP period (Fig. 4.2). A total of eight planktic foraminifera species comprise these planktic assemblages in our studied core. *Neogloboquadrina pachyderma*, *Neogloboquadrina incompta*, *Globigerina bulloides*, *Globigerinita glutinata*, *Turborotalita quinqueloba*, *Globorotalia inflata*, *Globigerinita uvula*, *Orbulina* sp. are the major species reported in the studied core. Of these, we have documented the first seven species as the eighth species *Orbulina* sp. was very rare and found only in 3 intervals of the core, hence not included in the study. The major species found in the core are similar to the species observed in our surface sediment data (discussed in Chapter 3), and also consistent with previous studies reported from the region (Perner et al., 2018; Staines-Urias et al., 2013). The ecology of these species is described in Chapter 2, Materials and Methodology.

The relative abundance of the polar species *N. pachyderma* dropped from >60% to <20% after 10 ka BP. *N. pachyderma* percentages decreased further in the early to mid-Holocene up to 6 ka BP. After 6 ka BP to the present, the abundance of *N. pachyderma* remained low at ≤10%.

Relatively warmer species *N. incompta* percentage increased during the early-mid Holocene at a slow rate with minor fluctuations (Fig. 4.2). This trend was followed by a sharp rise in *N. incompta* percentage from 20 to <30% during 6-5 ka BP. This percentage was stable for 5 to 1.2 ka BP with a slight rise at 3 ka BP and a decrease at 2 ka BP. In the last 1 ka BP, the relative abundance of this species decreased to the minimum value, seen in its Holocene record.

The temperate to subpolar species *G. bulloides* also followed an increasing trend in the early-mid Holocene phase. The percentage of this species reached the maximum of 22% at 5 ka BP, rising from an abundance of 3% at 10.3 ka BP. Following this increasing trend, a marked decline in its abundance was observed at 4.4 ka BP. Later during the late Holocene, the abundance trend continued with a rise in *G. bulloides* percentage until present with small oscillations. However, the late Holocene values remain below the mid-Holocene maxima (Fig. 4.2).

G. glutinata, often described as temperate to subpolar species and associated with the phytoplankton productivity in the subpolar ocean (Schiebel and Hemleben, 2000), was observed to increase throughout the Holocene from 10.3 ka BP to the present. Like *N. incompta* and *G. bulloides*, this species also increased in relative abundance during the early-mid Holocene. The percentages rose from 10 to 30% during this period. Continuing with a slight decrease in 5 ka BP, the relative abundance increased with little oscillations until 1.4 ka BP. Further, *G. glutinata* percentages increased to 37% with a gentle linear trend.

T. quinqueloba, referred to as the front indicator species, exhibited the most variations in terms of amplitude in this study. The abundance of the species increased at the beginning while transitioning from 10.3 ka BP to 8 ka BP. After 8 ka BP to 5 ka BP, its percentage decreased from 40% to 4%, contrary to the trend displayed by the above-reported species. The lowest relative abundance for this species was observed at 5 ka BP. The 5-4 ka BP trend for this species was positive, with an increase in its percentage. Afterward, the percentages decreased towards 2.4 ka BP followed by a peak (50%) at 2 ka BP. From 2 ka BP to the present, the relative abundance of *T. quinqueloba* remained low with small oscillations.

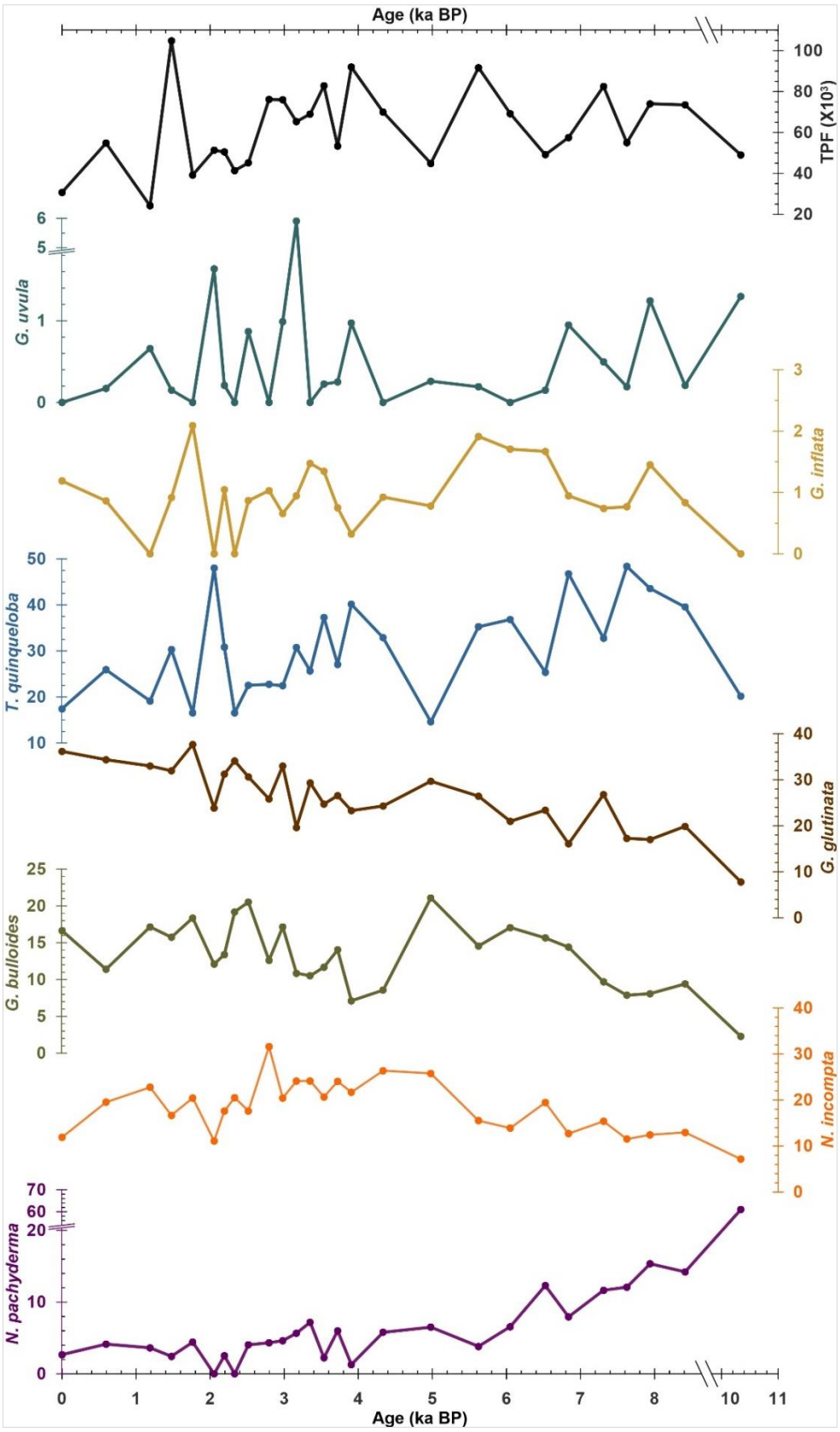

Fig. 4.2. Total planktic foraminifera (TPF, in $x10^3$ g^{-1} sediment) and relative abundance of the planktic foraminifera species (in percentage, %) of core AMK 410.

G. inflata, though comprised of smaller percentages of the assemblage, holds a significant role in subpolar ocean hydrography as it is associated with the strength of NAC (Pflauman et al., 2003). The relative abundance of this species increased after 10.3 ka BP in the early-mid Holocene phase but with a dip at 8-7 ka BP. Also, between 5-4 ka BP, *G. inflata* percentages decreased. During 4-2.2 ka BP, *G. inflata* remained at 1% on average. Around 1.8 ka BP, the abundance increased to 2.5%.

Likewise, the less abundant species in our study site, *G. uvula* displayed no constant trend in its relative abundance plot, instead fluctuating between maximum and minimum values (Fig. 4.2). The maximum percentage for the species was 6%, reached during 4-3 ka BP. In the mid-Holocene, during 7-4.4 ka BP, this species was absent from the assemblage. Compared with the trend exhibited by *G. inflata*, *G. uvula* showed a reverse trend.

Initially, all species except *N. pachyderma* increased in their relative abundance. The trend in the relative abundance of *T. quinqueloba* is the reverse of what is shown by the relatively warmer species, i.e., *G. bulloides*, *N. incompta*, and *G. glutinata*. Also, the low abundant species *G. uvula* and *G. inflata* displayed opposite trends.

4.4.2. Stable isotopic variations in planktic foraminifera

Oxygen stable isotopic composition

The stable Oxygen isotopic ratio of both species, *G. bulloides* and *N. pachyderma* ($\delta^{18}O_{bull.}$and $\delta^{18}O_{pach.}$) follow similar trends in the early Holocene. However, they slightly differ during the late Holocene (Fig. 4.3).

$\delta^{18}O_{pach.}$ ranges between 2.7 and 3.8 ‰ in our study during the Holocene, whereas the minimum $\delta^{18}O_{pach.}$ 2.7 ‰ was attained only in the last interval. The average $\delta^{18}O_{pach.}$ record except 2.7 ‰ varied between 3.2 and 3.6 ‰ (Fig. 4.3).

$\delta^{18}O_{bull.}$varied from 1.2 and 2 ‰, 1.2-1.5 ‰ less than the $\delta^{18}O_{pach.}$ values. $\delta^{18}O_{bull.}$ declines from 2 ‰ to 1.2 ‰ in the early-mid Holocene from 10.3 ka BP to 3.5 ka BP. This period also exhibited two marked dips in $\delta^{18}O_{bull.}$ at 8 ka BP and 6.5 ka BP. $\delta^{18}O_{bull.}$

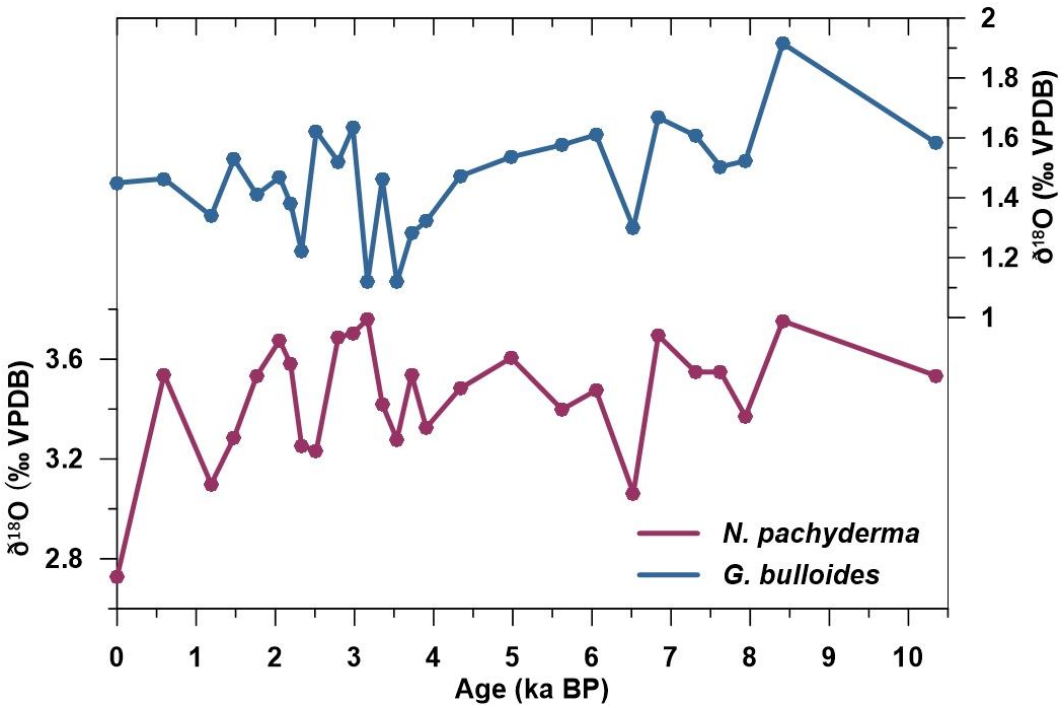

Fig. 4.3. Oxygen isotopic composition of *G. bulloides* and *N. pachyderma* (in ‰ VPDB) from the core AMK 410.

4.5. Discussion

4.5.1. $\delta^{18}O$ difference of *G. bulloides* and *N. pachyderma*: seasonal or depth stratification

G. bulloides and *N. pachyderma* are two major species making a significant part of the assemblages in the Subpolar North Atlantic (SPNA) Ocean. *G. bulloides* is described as a temperate to subpolar species in the North Atlantic and is believed to be a near-surface habitant. In tropical to subtropical oceans, the abundance of this species is a function of the increased productivity related to upwelling (Kroon and Ganssen, 1988; Naidu and Malmgren, 1996). Some studies have linked this species' occurrence to primary productivity (Ottens, 1992; Schiebel and Hemleben, 2000; Chapman, 2010). However, our study in the SPNA ocean showed no correlation between the species' abundance with the productivity factor Chl-a (Sahoo et al., 2022).

N. pachyderma is a polar species, believed to flourish when summer SST ≤ 9 °C (Bé and Tolderlund, 1971; Johannesen et al., 1994; Eynaud, 2011). This single species even comprises the total planktic foraminifera assemblage in some regions of the high-latitude oceans (Eynaud, 2011). From our surface sediment records in

the SPNA, this species was observed to dominate in the Labrador Sea with 100% abundance (Sahoo et al., 2022; chapter 3 of this thesis). *N. pachyderma* thrives in the subsurface layer (100-150m) in the SPNA Ocean and near the surface (0-50 m) in the polar ocean (Jonkers et al., 2010; Pados and Spielhagen, 2014). The abundance of the species is inversely correlated with the temperature and salinity of the upper water mass in the SPNA Ocean in our study Sahoo et al. (2022). Moreover, some studies in the Nordic Seas suggest the occurrence of this species is also dependent on sea ice cover, productivity, etc. (Greco et al., 2019).

A recent study from the Irminger Sea (Jonkers et al., 2010) has challenged the paleoceanographic significance of these two species, *G. bulloides* and *N. pachyderma* using sediment traps. This study explained that the $\Delta\delta^{18}O$ between *G. bulloides* and *N. pachyderma* is due to their seasonality flux variance and proposed a similar regional depth habitat of ~50 m. However, the values obtained from our core for both species are distinct from those observed in Jonkers et al. (2010).

G. bulloides $\delta^{18}O$ values from our study match the $\delta^{18}O$ values observed by Jonkers et al. (2013). But *N. pachyderma* values greatly differ from Jonkers et al. (2013), showing an average enrichment of ~1.5 ‰. The $\delta^{18}O$ of *G. bulloides* and *N. pachyderma* from surface sediments in the Northern North Atlantic, compiled from various published data, vary from 2.5 to 3.8 ‰ and 1.1 to 1.8 ‰, respectively (Ganssen and Kroon, 2000). This difference cannot be attributed to a seasonal influence. Additionally, the depth habitat of *N. pachyderma* may vary depending on the genotypic variation (Bauch et al., 2003) which could be attributed to this difference in $\delta^{18}O$. Additionally, in the Fram Strait, Simstich et al. (2003) suggested a change in the depth habitat of *N. pachyderma* in an east-west transect depending upon the hydrography of the region. The warm Atlantic water inflow in the Irminger Sea and the Norwegian Sea regions causes a higher offset in the *N. pachyderma* $\delta^{18}O$ than the surface values (Simstich et al., 2003). Moreover, *N. pachyderma* values in our data are comparable to the *N. pachyderma* $\delta^{18}O$ values of the surface sediment samples in Simstich et al. (2003). The isotopic difference between these two species has been documented relative to depth stratification (Risebrobakken et al., 2003; Moros et al., 2004).

4.5.2. Hydrographic changes in the SPNA during the Holocene

In the early Holocene, after 10.3 ka BP as evidenced by previous studies in the region (Moros et al., 2004), our planktic assemblage data displayed a similar pattern. After the deglacial phase at 11.7 ka BP, the cold-water species *N. pachyderma* percentages declined sharply from >60 % at 10.3 ka BP to <20 %. This reflected the retreat of the cold meltwater from the region. Simultaneously, an increase in the warmer temporal and subpolar species *N. incompta*, *G. bulloides*, *G. glutinata*, *T. quinqueloba*, and *G. inflata* supports an increase in the warm water flux in the region. A general increase in the $\delta^{18}O$ values in both species could be explained by the resume of the subtropical water influx in the region. However, the values declined during 8 ka BP, suggesting the already-known influence of the remnant Laurentide Ice Sheet meltwater in the western North Atlantic at 8.2 ka BP (Dyke and Prest, 1987; Barber et al., 1999). During this period, a minor increase in the relative abundance of the cold-water species *N. pachyderma*, and the front indicator species *T. quinqueloba* also supports the advancement of this meltwater flux. This indicates a cold and low saline water-influenced upper water column in the region. However, the NAC indicator *G. inflata* possibly indicates the NAC water influence adjacent to the site. In the early Holocene up to 8.4 ka BP, the surface-subsurface $\delta^{18}O$ difference was higher in the south of Iceland, northeast of our core location, also reflecting an influence of low saline water at the surface and stratified upper water column (Fig. 4.3, Thornalley et al., 2009). The 8.2 ka event was restricted to the western part of the North Atlantic and the warm NAC water was already activated in the eastern part of the North Atlantic (Telesinski et al., 2022).

After the decline in the meltwater influx at the 8.2 ka event, the SPG circulation in the region was reactivated following a major reorganization in the upper water column of the region (Fig. 4.3, Thornalley et al., 2009). This can be seen in the increased relative abundance of all the warm-water species and a decrease in the occurrence of *N. pachyderma*. *N. pachyderma* percentages gradually declined till 6 ka BP concurrent with an increasing trend in the warmer subpolar and temperate species *N. incompta*, *G. bulloides*, *G. glutinata*. From this, we suggest an enhanced NAC water flow to the site after 8 ka BP. However, a fluctuating but higher occurrence of *T. quinqueloba* during this period suggests a frontal influence near

the core site. The increase in warm and saline water in the area might have resulted in the enrichment in the $\delta^{18}O$ of both species since 8 ka BP. However, a sharp decline in the $\delta^{18}O$ trend of both species at 6.5 ka BP might be a result of a lower $\delta^{18}O$ influx from NAC with a strengthened SPG-like scenario. The SPNA in 8-6 ka BP has been previously observed to display a positive NAO- influenced strengthened SPG (Rimbu et al., 2003; Thornalley et al., 2009; Staines-Urias et al., 2013). In a strengthened SPG case, the NAC water gets influenced by the extended subpolar water influx, decreasing the salinity of the western SPG water (Hatun et al., 2005; Sarafanov et al., 2010). This water is represented by a lower $\delta^{18}O$ (Frew et al., 2000). A slight increase in the cold-water species *N. pachyderma* further supports a lowering of temperature and salinity in the region. The decrease in *T. quinqueloba* at 6.5 ka BP at our site might be due to the southeastward displacement of the SPF further from our core location. *T. quinqueloba* abundance at the eastern SPNA in the Iceland-Faroe-Shetland region during this period was higher than at our site (Staines-Urias et al., 2013), supporting the eastward shift of the SPF.

Between 6–4 ka BP, we have observed a major shift in the planktic foraminiferal abundances as a transition phase between the early Holocene and the late Holocene composition. The warm water species reached their maximum abundance at 5 ka BP and then declined towards 4 ka BP. At the same time, front indicator species *T. quinqueloba* and melt water species *G. uvula* were minimum and then increased. From this, we suggest a westward or a southeastward retreat of the SPF and a lower influence of the meltwater.

Moreover, a weakened NAO condition must have triggered a stratified upper water structure in the region. The period from 6–5 ka BP has been associated with one of the RCC (Rapid climatic change) events in the North Atlantic, described by Mayewski et al. (2014). This period has also been identified as an Ice rafting event (Bond et al., 1997). However, a negative NAO-induced weakened SPG could have shifted the front westward and thus prevented the meltwater influx to the region.

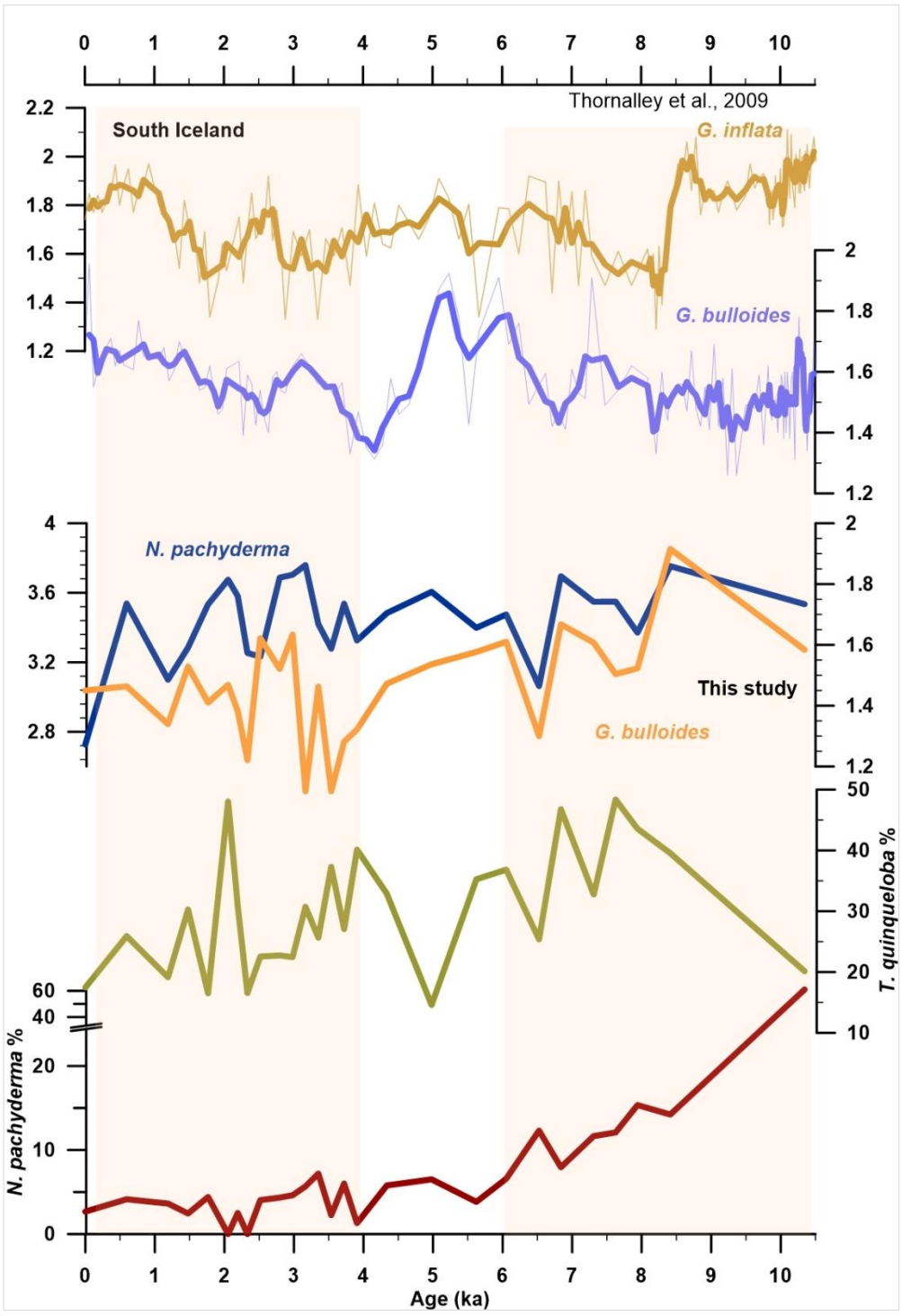

Fig. 4.4. Relative abundance of cold-water species *N. pachyderma*, front indicator species *T. quinqueloba* from this study. $\delta^{18}O$ of *G. bulloides*, *N. pachyderma* (this study) compared with the $\delta^{18}O$ of *G. bulloides* and *G. inflata* from south of Iceland (Thornalley et al., 2009).

This resulted in a dominant warm NAC water influence in our studied region, indicating a warm STG water input to the NAC. Further, a decline in the NAC indicator species *G. inflata* from our study indicates a weakened NAC influence in the region and a stratified oceanic condition. Also, a low in the total planktic foraminifera indicates a productivity decline. The oxygen isotopic data from our study reveals a minor enrichment in the $\delta^{18}O_{pach}$ values but almost constant or a minor depleted value in $\delta^{18}O_{bull}$. This further supports the presence of a stratified upper water column. This is also evident from $\delta^{18}O$ data from the south of Iceland (Thornalley et al., 2009). The near-surface salinity decreased, and subsurface salinity increased with an increase in subsurface temperature during 6–5 ka BP (Thornalley et al., 2009). A possible scenario for the decrease in near-surface salinity can be a decrease in the summer insolation in the Northern hemisphere (Moros et al., 2004). Further, a decline in $\delta^{18}O$ in both species followed towards 4 ka BP. This is accompanied by an increase in the relative abundance of *T. quinqueloba* at our site. From this, we suggest a nearness of the subpolar front to our studied region. Also, this period in the Iceland-Faroe-Shetland region has been marked by a decreased gradient in $\delta^{18}O_{bull}$ values between Iceland-Faroe and Faroe-Shetland regions, suggesting well-mixed upper water with a strengthened SPG-like condition (Staines-Urias et al., 2013). However, most studies in the eastern North Atlantic suggested warming during 6-4 ka BP (Thornalley et al., 2009; Solignac et al., 2004). This could be due to a predominance of cold subpolar water in the surface water of our region. The weakening of AMOC during 6-5 ka BP can be related to the decrease in salinity and a reduced NAC (Thornalley et al., 2009). In the present scenario, as we have seen subpolar cooling is related to a weakening of AMOC strength and a decline in NAC inflow resulting in a cooler SPNA (Sevellec et al., 2017).

The Late Holocene period from 4 ka BP to the present in SPNA is generally marked by small oscillations in the upper watermass conditions in the SPNA region. This is concomitant with our study as well, seen in the foraminiferal assemblage and oxygen isotopic data. A relatively negative NAO since 4 ka BP has been reconstructed from limnological records in western Greenland (Olsen et al., 2012). Under a negative NAO scenario, SPG strength weakens, resulting in a warmer and saline NAC inflow at the eastern side of the SPNA with an enhanced contribution

of the Subtropical Gyre (STG) (Hatun et al., 2005). This Atlantic inflow water returns to the Labrador Sea with EGC and creates an enhanced density gradient in the SPNA. This leads to a strengthened SPG by initiating a reinforced NAC (Thornalley et al., 2009). This hypothesis explains the varying hydrography seen in our data. The higher percentage of *G. uvula* in the late Holocene marks an increased influence of freshwater during this period. This variation is in accord with the other published data in this region (Perner et al., 2018). The opposite trends in percentages of the NAC indicator subsurface species *G. inflata* and the surface freshwater species *G. uvula* in the region are relevant considering the alternate retreat and advance of the freshwater during the late Holocene. The enhanced freshwater flux has also been documented in the North of Iceland and East Greenland shelf (Andrews and Giraudeau, 2003; Andersen et al., 2004; Jennings et al., 2011). Additionally, *T. quinqueloba* in our study area demonstrated a negative trend from 4-2 ka BP with small oscillations, suggesting a gradual withdrawal of frontal influence from the core site. Further, a culmination in *T. quinqueloba* percentages at 2 ka BP suggests the front was nearest to our core site during the period. This frontal shift can be explained with the help of NAO variance, documented in Olsen et al. (2012). A prominent SPF during 2.7 to 1.5 ka BP period was attributed to a strengthening in EGC strength and warming in NAC (Perner et al., 2018). This difference between EGC and NAC created a stronger gradient and hence a prominent SPF influence near Reykjanes Ridge.

As we have seen in our surface sediment study, *N. pachyderma*/*N. incompta* ratio can be used as an indicator for the change in the temperature and the SPNA hydrography in the SPNA region, as also evidenced in previous studies (Eynaud et al., 2009; Eynaud, 2011). Here, we have seen an opposite trend in the relative abundance of both species, displaying a negative relationship with each other. In the early Holocene, when the *N. pachyderma* percentages were high, *N. incompta* was relatively low. As the *N. pachyderma* percentage decreased towards the mid-Holocene, *N. incompta* abundance increased. However, from the mid-Holocene to the present, *N. pachyderma* abundance remained below 10%, indicating more of a warmer water influence in the upper water mass in this region. And this is also justified by the increased abundance of the warmer species *N. incompta* during this period. Additionally, the assemblages in the core are comparable to the assemblages

we have observed in the surface sediment samples over Reykjanes Ridge (from chapter 3).

The Holocene in the SPNA has been seen to vary with the millennial-scale to century-scale oscillations superimposed on the general Holocene trend (Bond et al., 1997; Thornalley et al., 2009). The $\delta^{18}O$ decline at 8 ka BP in our data is well recorded in our studied region, correlating with the Laurentide Ice sheet meltwater influx (Dyke and Prest, 1987). Also, a minor low-salinity event at 6.5 ka BP, correlated with the 1500-year scale oscillations, as also seen in the hydrographic data from south of Iceland (Thornalley et al., 2009).

4.6. Conclusions

- Reykjanes Ridge hydrography during the Holocene varied with the differential presence of cold polar water and warm North Atlantic water.
- Three major phases have been identified in our studied region, i) the early Holocene with the increased influence of warm Atlantic water ii) a transitional mid-Holocene from 6-4 ka BP, with some reorganization in the SPNA hydrography from thermal maximum to late Holocene, and iii) a late Holocene period from 4 ka BP with a warming trend towards present and small oscillations in its hydrography superimposed upon this trend.
- The marked feature of the early Holocene North Atlantic at 8.2 ka BP has been clearly recorded in the planktic foraminiferal assemblages and the oxygen isotopic data.
- Besides the 8.2 ka event, the small oscillations in our data throughout the Holocene reflect changing Subpolar gyre dynamics.
- The position of the Subpolar front in the region varied in the Holocene relative to our core site over the Reykjanes Ridge. The hydrography of the region was shaped by the variation of the subpolar front. The advancement of the cold polar water to our region was well-marked by the nearness of the SPF to our core site.

Chapter 5

5. NAC and EGC influence on the Subpolar North Atlantic hydrography during Holocene

5.1. Introduction

The Subpolar North Atlantic (SPNA) Ocean is an important link between tropical and northern polar oceans. The subtropical heat and salinity are transported through the SPNA toward Nordic Seas and the Labrador Sea, where deep overturning occurs forming the deep water mass, North Atlantic Deep Water (NADW). NADW then flows to the other oceans at the bottom. This meridional circulation is known as Atlantic Meridional Overturning Circulation (AMOC). AMOC has varied in the past and is known to have a greater role in the global climate (Broecker et al., 1985, 1988; Broecker and Denton, 1989; Alley et al., 2007). A changing AMOC is also observed in the modern scenario. Moreover, this has been documented to be at its minimum strength in the last millennium (Caesar et al., 2021). A recent study also shows the weakest AMOC in the last 10,000 years (Spooner et al., 2020). The observed coherency between SPNA hydrographic changes and AMOC variability has established SPNA hydrography as a potential fingerprint for the AMOC (Zhang, 2008).

SPNA surface hydrography has evolved through the Holocene with a variable influx of the North Atlantic Current (NAC) and East Greenland Current (EGC). Solar insolation variability, atmospheric phenomena and gyre dynamics together have shaped this hydrography. In spite of a still debatable cyclicity in these changes (Risebrobbaken et al., 2003; Bond et al., 2001), we have observed a dynamic variability in the Holocene SPNA hydrography. This implies a variable strength of the NAC and SPG in the SPNA. Here, we will compare our results from AMK 410 with published NAC and EGC records. Though an active AMOC was present in the early Holocene, the modern AMOC trend was only established after 7 ka BP, at the start of the active convection in the Labrador Sea following the Laurentide Ice Sheet retreat (Hillaire-Marcel et al., 2001). A relatively stable AMOC has been reconstructed since then, however, instances of decreased AMOC strength have been also observed at 5 ka BP and 2.7 ka BP (Oppo et al., 2003). These lows in

AMOC strength are majorly associated with cold freshwater advection southward in the SPNA or/and a negative NAO-like scenario (Bond et al., 2001). Additionally, a lower NAC influx linked with a weakened SPG also drives a weak AMOC (Hatun et al., 2005). A cooling in SPNA and warming in the east of Newfoundland was documented as coherent with weakened AMOC (Zhang, 2008).

With the reconstruction of near-surface temperature and salinity at our core site over Reykjanes Ridge and comparison with published records, we will understand the link between the aforementioned elements in the SPNA.

5.2. Study Area

The oceanographic settings for the core have been described in chapter 2 of the thesis.

5.3. Materials and Methodology

The methodology followed for the core has been summarized in chapter 2. Here, we will only discuss the $\delta^{18}O_{sw}$ reconstruction from combined Mg/Ca and $\delta^{18}O$ of foraminifera.

5.3.1. $\delta^{18}O_{sw}$ reconstruction

$\delta^{18}O_{sw}$ from the core has been reconstructed for the Holocene using Mg/Ca and $\delta^{18}O$ of planktic foraminifera *G. bulloides*. We have converted the Mg/Ca values (mmol/mol) of *G. bulloides* to temperature using the relation between temperature and Mg/Ca of Thornalley et al. (2009) for *G. bulloides*. Using Kim and O'Neil (1997)'s equation, these temperatures were then subtracted from the δ18O values obtained. A conversion factor of -0.27 ‰ was applied for VPDB values to VSMOW (Hut, 1987). Finally, the $\delta^{18}O_{sw}$ (VSMOW) values were corrected for the Ice-volume effect using Waelbroeck et al. (2002)'s Ice volume correction data.

As the salinity and $\delta^{18}O_{sw}$ are linearly correlated (Le Grande and Schmidt, 2006), we can interpret the $\delta^{18}O_{sw}$ variability as directly related to salinity changes.

5.4. Results

The mean Mg/Ca value varied down the core between 1.2 mmol/mol to 2.9 mmol/mol. These values were converted to water temperature using suitable calibration equation as mentioned in the Materials and Methods chapter. The

temperature derived for the upper section of the core lies well within the temperature variation observed in the region (also discussed in Chapter 2). Here, these temperature variations in the core are discussed.

Near-surface temperature and $\delta^{18}O_{sw}$ variability

The near-surface temperature of the core varied between 6 and 14 °C and the $\delta^{18}O_{sw}$ varied between -1 to 1 ‰. The top interval of the core corresponds to a temperature of 10 °C and a $\delta^{18}O_{sw}$ of 0.5 ‰. This is valid with the present-day temperature and salinity data for the region.

For the early Holocene phase, 10.3-8.5 ka BP, a moderately increasing trend in temperature and salinity was observed. However, the near-surface temperature during this period was low. After 8.5 ka BP, both temperature and $\delta^{18}O_{sw}$ (salinity) at our core site dropped significantly. During this period, the relative abundance of *N. pachyderma* also decreased while *T. quinqueloba*, *N. incompta*, and *G. inflata* increased simultaneously. Later, the temperature and $\delta^{18}O_{sw}$ reached their maximum value towards 7 ka BP, marking maxima in the early Holocene phase.

After 7 ka BP, the temperature and $\delta^{18}O_{sw}$ decreased up to 4.5 ka BP with a minor dip at 6.5 ka BP. During this cool transition period, *T. quinqueloba* also displayed a negative trend and was the minimum of the Holocene percentages in our studied region. Moreover, an increased abundance of *N. incompta* and *N. pachyderma* was exhibited whereas a decreased abundance was observed in the case of *G. inflata*.

The late Holocene trend was superimposed with regular fluctuations in both temperature and $\delta^{18}O_{sw}$ values. However, the mean values tended toward more positive values, shifting to a warmer and more saline upper watermass from 4.5 ka BP to the present. We observed regular lows in temperature and $\delta^{18}O_{sw}$ at 3.5 ka BP, 2.5 ka BP, 1.5 ka BP, and 0.5 ka BP. The species percentages also were fluctuating with a mean value throughout the Holocene. Higher *T. quinqueloba* percentages were perfectly in sync with the lower temperature and $\delta^{18}O_{sw}$ values. Further, *G. inflata* variations were coordinated with the *T. quinqueloba* variation. Additionally, these species were exhibiting a negative relation with *N. incompta* and *N. pachyderma* percentages.

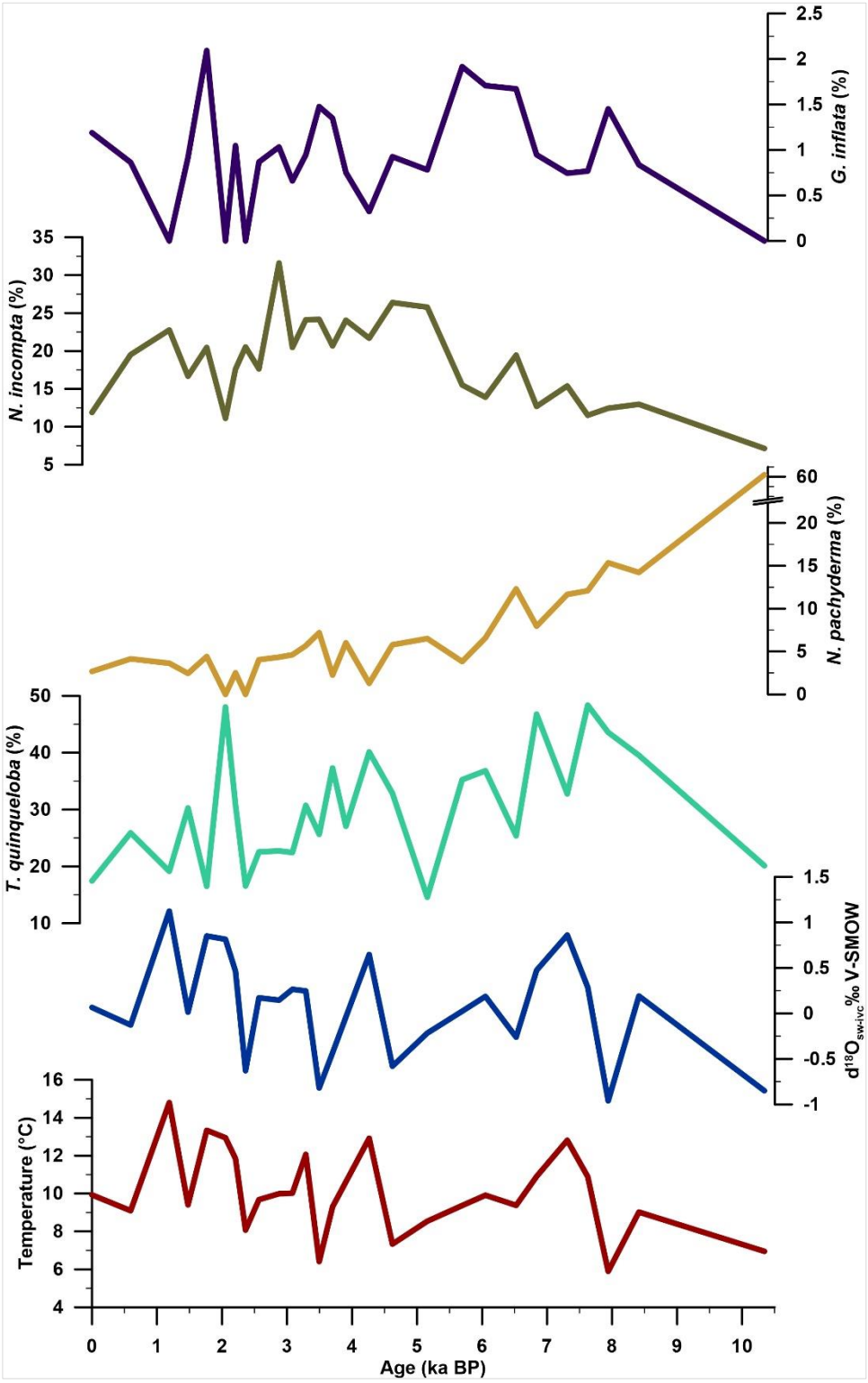

Fig. 5.1. Plots showing temperature (°C) and $\delta^{18}O_{sw\text{-}ivc}$ ‰ (V-SMOW) reconstructed from Mg/Ca and $\delta^{18}O$ of *G. bulloides* in the core AMK 410. Also, the relative abundances of the planktic foraminifera species of the same core are plotted with age (ka BP).

The trends we observed in both temperature and salinity at our core site were coherent throughout the Holocene.

5.5. Discussion

Influence of NAC and EGC on Subpolar Hydrography

The early Holocene temperatures from 10.3 ka BP increased marking a gradual decrease in the deglacial meltwater flux and a higher Northern hemispheric summer insolation. However, a lower near-surface temperature from our core reflects the presence of cold meltwater, consistent with previous studies from the western Subpolar North Atlantic (SPNA) and western Nordic Seas (Moros et al., 2004). The cold and low saline surface water at 8 ka BP in our core could be related to the 8.2 ka- event, marked by the Laurentide Ice sheet final discharge (Dyke and Prest, 1987). Only after this meltwater retreat, our core exhibited a maximum temperature which is also evident in the SST of the core near Reykjanes Ridge (LO09-14), marking the early Holocene Maxima around 10-6.5 ka BP (Moros et al., 2004). This increase in temperature represents an increase in the warm North Atlantic water influence. The increase in the *G. inflata* percentage in our core also supports an increase in the NAC influence at our core site during the Holocene. A simultaneous SST maximum was also observed in the core at North Iceland suggesting an increased NAC influence (Sicre et al., 2021). However, a decrease in the subsurface temperature and salinity (Thornalley et al., 2009) and warming at the surface can also be explained by the high summer insolation and lower winter insolation (high seasonality by orbital forcing) in the early Holocene (Liu et al., 2003).

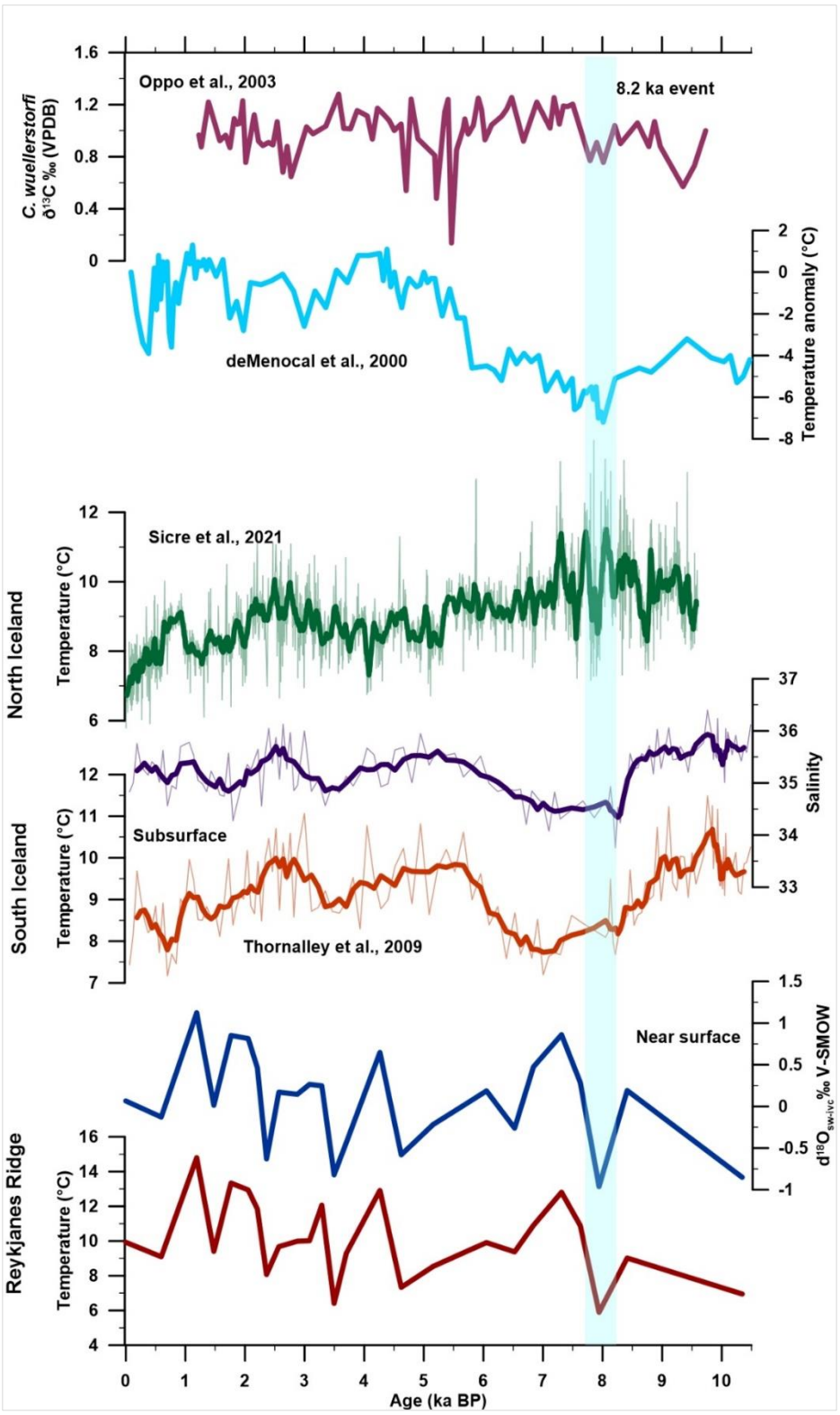

Fig. 5.2. Comparison of near-surface temperature and salinity from our core AMK 410 with *G. inflata*-based subsurface temperature and salinity from south Iceland (Thornalley et al., 2009), SST from north Iceland (Sicre et al., 2021), temperature anomaly off west Africa (deMenocal et al., 2000) and $\delta^{13}C$ ‰ (VPDB) of *Cibicides wuellerstorfi* from northeast Atlantic (Oppo et al., 2003).

In the mid-Holocene, after 7 ka BP, the temperature and salinity decreased in the near surface watermass in our studied region. However, a decrease in the subsurface salinity and temperature in the south of Iceland at the same time indicates a well-mixed upper water column (Thornalley et al., 2009). This suggests an increased low-saline SPG water influence on NAC at our site. An increase in IRD in the North Atlantic from Bond et al. (1997) is in agreement with the advection of polar water resulting in Bond event 4 at ~5.3 ka BP. Likewise, Moros et al (2004) also documented an increase in the Q/Pg percentage in the mid-Holocene from the Norwegian Sea, showing an increased IRD flux and a linked enhanced polar water flux. A mid-Holocene SST minimum is also evident from both the Reykjanes Ridge and the Norwegian Sea SST (Moros et al., 2004). Moreover, a reduced North Atlantic Current could also be the cause of this cooling. A decreased abundance of *G. inflata* in our core during the period indicates a weakened NAC. A similar observation of reduced Atlantic water since 6.9 ka BP was reported in the Barents Sea (Duplessy et al., 2001). A significant transition in the mid-Holocene from other studies (Giraudeau et al., 2000; deMenocal et al., 2000) is coherent with our study.

The late Holocene trend in our region is unstable as compared to early and mid-Holocene trends. Long-term warming in our data with multiple cold and low saline episodes during 4 ka BP-present is in accordance with the increase and decrease in the *T. quinqueloba* percentages in our studied region. The cooler and fresher episodes were coherent with higher *T. quinqueloba* percentages. These data are coherent with the earlier proposed hypothesis of an alternate advection and retreat of the polar freshwater (Solignac et al., 2004; Thornalley et al., 2009; Staines-Urias et al., 2013). This polar water flux causes enhanced stratification in the region. The stratification in our region is also supported by the decreased *G. inflata* abundance. Also, a strengthening in the EGC strength has been known during the late Holocene from various studies as a lowering in the SST in North Iceland (Sicre et al., 2021). These oscillations in the late Holocene are also accompanied by the temperature anomalies seen on the western coast of Africa (subtropical regions, deMenocal et al., 2000). Similar increased polar water advances with strengthened EGC are documented on the eastern coast of Greenland (Moros et al., 2006; Perner et al., 2013). Moreover, a decreased Irminger Current strength has been reconstructed for the late Holocene phase (Perner et al., 2016).

SPNA hydrography and AMOC during Holocene

SPNA hydrography has been associated with the Atlantic Meridional Overturning Circulation (Hakkinen and Rhines, 2004). A change in AMOC is coherent with the variation in the North Atlantic Deep Water (NADW) formation. Hence, NADW variation can be studied to monitor changes in AMOC strength. $\delta^{13}C$ of benthic foraminifera is an established proxy for the NADW and has been used to infer the NADW during Holocene (Fig.5.2, Oppo et al., 2003).

In the early Holocene, consistent with a decline in the observed temperature and salinity value, AMOC strength declined as seen from the depleted values in the $\delta^{13}C$ of *Cibicides wuellerstorfi*. The enhanced meltwater influx decreases convection by decreasing the buoyancy. However, the modern-like AMOC started after 7 ka BP after the retreat of the LIS meltwater flux (Hillaire-Marcel et al., 2001). This is in accordance with the high NAC influx and a strengthened SPG-like condition in the early Holocene, as observed from our planktic foraminiferal assemblages (discussed in Chapter 4).

Another sharp decline in the AMOC strength has been observed during 5 ka BP. This decline is generally correlated with an increased IRD flux at the same time, Bond event 4 (Bond et al., 2001; Oppo et al. 2003). However, the cooling in the near-surface temperature during the mid-Holocene can be related as a manifestation of this decline in AMOC. A weakened AMOC drives cooling in the SPNA region by weakening the NAC strength (Hakkinen and Rhines, 2004). The weakening of the NAC during this period was also indicated by a decline in the *G. inflata* abundances.

5.6. Conclusions

By comparing our near-surface temperature and salinity data from our core over Reykjanes Ridge with the published records, the following conclusions can be drawn.

- Reconstruction of near-surface and salinity in our core reflected three major phases coherent with the planktic foraminiferal species abundance data (discussed in chapter 4 of the thesis); 1. An early Holocene warming, 2. A mid-Holocene cooling and 3. A warming but oscillating late Holocene.

- The early Holocene increase in the near-surface temperature and salinity in our region was influenced by an increase in the NAC influx. Also, the 8 ka BP cooling event was clearly recognized in the near-surface attributes.
- A decline in the near-surface temperature and salinity after 7 ka BP was attributed to a decline in NAC strength.
- The late Holocene was characterized by a fluctuating trend in both temperature and salinity values with a long-term warming trend towards the present. The oscillating late Holocene trend is a result of the advance and retreat of the cold fresh polar water in the SPNA, consistent with previous studies from the region.
- The reduced deep water formation observed at 8.2 ka BP and 5 ka BP and the surface hydrography reconstructed from our data can be linked through subpolar gyre dynamics.

Chapter 6

6. Summary and Conclusion

6.1. Planktic foraminiferal assemblages from surface sediment

The present work from the Subpolar North Atlantic presents the planktic foraminifera assemblages in an east-west transect along 59.5°N latitude covering the wide region in the eastern and western subpolar North Atlantic (SPNA). Also, an attempt has been made to understand how these species are distributed from the east to west SPNA ocean using surface sediment samples. The findings from this study are as follows.

- Based on cluster analysis, three planktic foraminifera groups were found in the subpolar North Atlantic Ocean. The polar group represented by *N. pachyderma* was dominant in the Labrador Sea. A mixed group composed of both warm water and cold water species of *N. pachyderma*, *N. incompta*, *G. glutinata* and *T. quinqueloba* was dominated in the Irminger Sea but also found in some stations of the eastern transect. And a warm temperate group consisting of warm taxa *G. glutinata*, *N. incompta*, *T. quinqueloba*, *G. bulloides* and *G. uvula* was populated in the region eastward of Reykjanes Ridge, in the Iceland Basin and Rockall plateau.
- *N. pachyderma* and *N. incompta* abundances varied with increasing and decreasing trends, respectively, from east to west SPNA. Also, their ratio was in sync with the decreasing upper water column temperature. So, *N. pachyderma*/ *N. incompta* can be used to interpret the upper water temperature variation in the SPNA.
- Based a comparison with the previously published planktic foraminiferal assemblage data from the SPNA reveals a possible shift in our species assemblages.

6.2. Holocene Subpolar North Atlantic hydrography

Three major phases were identified in the Holocene based on the planktic foraminifera assemblages, Oxygen isotopic composition of planktic foraminifera and reconstructed near-surface temperature and salinity from the core AMK 410.

- The three major phases identified in the Holocene are i) the early Holocene with the increased influence of warm Atlantic water ii) a transitional mid-Holocene from 6-4 ka BP, with some reorganization in the SPNA hydrography from thermal maximum to late Holocene, and iii) a late Holocene period from 4 ka BP with a warming trend towards present and small oscillations in its hydrography superimposed upon this trend.
- The early Holocene increase in the near-surface temperature and salinity in our region was influenced by an increase in the NAC influx. A decline in the near-surface temperature and salinity after 7 ka BP was attributed to a decline in NAC strength. The oscillating late Holocene trend is a result of the advance and retreat of the cold fresh polar water in the SPNA.
- The changes in the deep water formation during the Holocene can be related to the SPNA hydrographic changes.

References

Aagaard, K. and Carmack, E.C., 1989. The role of sea ice and other fresh water in the Arctic circulation. Journal of Geophysical Research: Oceans, 94(C10), pp.14485-14498.

Aagaard, K., Swift, J.H. and Carmack, E.C., 1985. Thermohaline circulation in the Arctic Mediterranean seas. Journal of Geophysical Research: Oceans, 90(C3), pp.4833-4846.

Aldridge, D., Beer, C.J. and Purdie, D.A., 2012. Calcification in the planktonic foraminifera Globigerina bulloides linked to phosphate concentrations in surface waters of the North Atlantic Ocean. Biogeosciences, 9(5), pp.1725-1739.

Alley, R.B., 2007. Wally was right: Predictive ability of the North Atlantic "conveyor belt" hypothesis for abrupt climate change. Annu. Rev. Earth Planet. Sci., 35, pp.241-272.

Alley, R.B., Mayewski, P.A., Sowers, T., Stuiver, M., Taylor, K.C. and Clark, P.U., 1997. Holocene climatic instability: A prominent, widespread event 8200 yr ago. Geology, 25(6), pp.483-486.

AMAP, 2021. Arctic climate change update 2021: key trends and impacts. Summary for policymakers. Arctic Monitoring and Assessment Programme (AMAP), Oslo, Norway.

Anand, P., Elderfield, H. and Conte, M.H., 2003. Calibration of Mg/Ca thermometry in planktonic foraminifera from a sediment trap time series. Paleoceanography, 18(2).

Andersen, C., Koc, N., Jennings, A. and Andrews, J.T., 2004. Nonuniform response of the major surface currents in the Nordic Seas to insolation forcing: Implications for the Holocene climate variability. Paleoceanography, 19(2).

Andersson, C., Pausata, F.S., Jansen, E., Risebrobakken, B. and Telford, R.J., 2010. Holocene trends in the foraminifer record from the Norwegian Sea and the

North Atlantic Ocean. Climate of the Past, 6(2), pp.179-193.

Andersson, C., Risebrobakken, B., Jansen, E. and Dahl, S.O., 2003. Late Holocene surface ocean conditions of the Norwegian Sea (Vøring Plateau). Paleoceanography, 18(2).

Andrews, J.T. and Giraudeau, J., 2003. Multi-proxy records showing significant Holocene environmental variability: the inner N. Iceland shelf (Hunafloi). Quaternary Science Reviews, 22(2-4), pp.175-193.

Appenzeller, C., Stocker, T.F. and Anklin, M., 1998. North Atlantic Oscillation dynamics recorded in Greenland ice cores. Science, 282(5388), pp.446-449.

Arhan, M., 1990. The North Atlantic current and subarctic intermediate water. Journal of Marine Research, 48(1), pp.109-144.

Azetsu-Scott, K., Clarke, A., Falkner, K., Hamilton, J., Jones, E.P., Lee, C., et al., 2010. Calcium carbonate saturation states in the waters of the Canadian Arctic Archipelago and the Labrador Sea. Journal of Geophysical Research: Oceans, 115(C11). https://doi.org/10.1029/2009JC005917

Balestra, B., Ziveri, P., Baumann, K.H., Troelstra, S. and Monechi, S., 2010. Surface water dynamics in the Reykjanes Ridge area during the Holocene as revealed by coccolith assemblages. Marine Micropaleontology, 76(1-2), pp.1-10.

Bamber, J., Van Den Broeke, M., Ettema, J., Lenaerts, J., Rignot, E., 2012. Recent large increases in freshwater fluxes from Greenland into the North Atlantic. Geophysical Reeaserch Letters. 39(19).

Barber, D.C., Dyke, A., Hillaire-Marcel, C., Jennings, A.E., Andrews, J.T., Kerwin, M.W., Bilodeau, G., McNeely, R., Southon, J., Morehead, M.D. and Gagnon, J.M., 1999. Forcing of the cold event of 8,200 years ago by catastrophic drainage of Laurentide lakes. Nature, 400(6742), pp.344-348.

Barker, S. and Elderfield, H., 2002. Foraminiferal calcification response to glacial-interglacial changes in atmospheric CO_2. Science, 297(5582), pp.833-836.

Bauch, D., Darling, K., Simstich, J., Bauch, H.A., Erlenkeuser, H. and Kroon, D., 2003. Palaeoceanographic implications of genetic variation in living North Atlantic Neogloboquadrina pachyderma. Nature, 424(6946), pp.299-302.

Bauch, H. A., 1994. Significance of variability in *Turborotalita quinqueloba* (Natland) test size and abundance for paleoceanographic interpretations in the Norwegian-Greenland Sea. Marine Geology 121(1-2), pp.129-141. http://dx.doi.org/10.1016/0025-3227(94)90162-7

Baumann, K.H., Andruleit, H. and Samtleben, C., 2000. Coccolithophores in the Nordic Seas: comparison of living communities with surface sediment assemblages. Deep Sea Research Part II: Topical Studies in Oceanography, 47(9-11), pp.1743-1772.

Be, A. W. H., Tolderlund, D. S., 1971. Distribution and ecology of living planktonic Foraminifera in surface waters of the Atlantic and Indian oceans, in Micropalaeontology of the Oceans, Eds. B.M. Funnel, W.R. Riedel, London: Cambridge University Press, pp.105-149.

Belkin, I.M. and Levitus, S., 1996. Temporal variability of the subarctic front near the Charlie-Gibbs Fracture Zone. Journal of Geophysical Research: Oceans, 101(C12), pp.28317-28324.

Belkin, I.M., 2004. Propagation of the "Great Salinity Anomaly" of the 1990s around the northern North Atlantic. Geophysical Research Letters, 31(8).

Belkin, I.M., Levitus, S., Antonov, J. and Malmberg, S.A., 1998. "Great salinity anomalies" in the North Atlantic. Progress in Oceanography, 41(1), pp.1-68.

Berger, W. H., 1969. February. Ecologic patterns of living planktonic foraminifera. In Deep Sea Research and Oceanographic Abstracts. Vol. 16, No. 1, pp.1-24. Elsevier.

Berger, W. H., 1973. Deep-sea carbonates; Pleistocene dissolution cycles. The Journal of Foraminiferal Research, 3(4), pp.187-195. https://doi.org/10.2113/gsjfr.3.4.187

Berner, K.S., Koc, N., Divine, D., Godtliebsen, F. and Moros, M., 2008. A decadal-scale Holocene sea surface temperature record from the subpolar North Atlantic constructed using diatoms and statistics and its relation to other climate parameters. Paleoceanography, 23(2).

Bersch, M., Yashayaev, I. and Koltermann, K.P., 2007. Recent changes of the thermohaline circulation in the subpolar North Atlantic. Ocean Dynamics, 57, pp.223-235.

Bianchi, G.G. and McCave, I.N., 1999. Holocene periodicity in North Atlantic climate and deep-ocean flow south of Iceland. Nature, 397(6719), pp.515-517.

Bianchi, G.G. and McCave, I.N., 2000. Hydrography and sedimentation under the deep western boundary current on Björn and Gardar Drifts, Iceland Basin. Marine Geology, 165(1-4), pp.137-169.

Bijma, J., Hönisch, B. and Zeebe, R., 2002. Impact of the ocean carbonate chemistry on living foraminiferal shell weight: Comment on" Carbonate ion concentration in glacial-age deep waters of the Caribbean Sea" by WS Broecker and E. Clark. Geochemistry geophysics geosystems, 3 (11), 1064.

Blackmon, P.D. and Todd, R., 1959. Mineralogy of some foraminifera as related to their classification and ecology. Journal of Paleontology, pp.1-15.

Boltovskoy, E., Wright, R. C. (Eds.)., 2013. Recent foraminifera. Springer Science & Business Media.

Böhm, E., Lippold, J., Gutjahr, M., Frank, M., Blaser, P., Antz, B., Fohlmeister, J., Frank, N., Andersen, M.B. and Deininger, M., 2015. Strong and deep Atlantic meridional overturning circulation during the last glacial cycle. Nature, 517(7532), pp.73-76.

Bond, G., Kromer, B., Beer, J., Muscheler, R., Evans, M.N., Showers, W., Hoffmann, S., Lotti-Bond, R., Hajdas, I. and Bonani, G., 2001. Persistent solar influence on North Atlantic climate during the Holocene. Science, 294(5549), pp.2130-2136.

Bond, G., Showers, W., Cheseby, M., Lotti, R., Almasi, P., DeMenocal, P., Priore, P., Cullen, H., Hajdas, I. and Bonani, G., 1997. A pervasive millennial-scale cycle in North Atlantic Holocene and glacial climates. Science, 278(5341), pp.1257-1266.

Böning, C.W., Behrens, E., Biastoch, A., Getzlaff, K. and Bamber, J.L., 2016. Emerging impact of Greenland meltwater on deepwater formation in the North Atlantic Ocean. Nature Geoscience, 9(7), pp.523-527.

Böning, C.W., Scheinert, M., Dengg, J., Biastoch, A. and Funk, A., 2006. Decadal variability of subpolar gyre transport and its reverberation in the North Atlantic overturning. Geophysical Research Letters, 33(21).

Born, A., Nisancioglu, K.H. and Braconnot, P., 2010. Sea ice induced changes in ocean circulation during the Eemian. Climate dynamics, 35, pp.1361-1371.

Bova, S., Rosenthal, Y., Liu, Z., Godad, S.P. and Yan, M., 2021. Seasonal origin of the thermal maxima at the Holocene and the last interglacial. Nature, 589(7843), pp.548-553.

Brambilla, E., Talley, L.D., 2008. Subpolar mode water in the northeastern Atlantic: 1. Averaged properties and mean circulation. Journal of Geophysical Research: Oceans. 113, pp.1–18. https://doi.org/10.1029/2006JC004062

Broecker, W.S., 1994. Massive iceberg discharges as triggers for global climate change. Nature, 372(6505), pp.421-424.

Broecker, W.S., 1997. Thermohaline circulation, the Achilles heel of our climate system: Will man-made CO2 upset the current balance?. Science, 278(5343), pp.1582-1588.

Broecker, W.S., 1998. Paleocean circulation during the last deglaciation: a bipolar seesaw?. Paleoceanography, 13(2), pp.119-121.

Broecker, W.S., Andree, M., Bonani, G., Wolfli, W., Oeschger, H. and Klas, M., 1988. Can the Greenland climatic jumps be identified in records from ocean and land?. Quaternary research, 30(1), pp.1-16.

Broecker, W.S., Bond, G., Klas, M., Bonani, G. and Wolfli, W., 1990. A salt oscillator in the glacial Atlantic? 1. The concept. Paleoceanography, 5(4), pp.469-477.

Broecker, W. and Clark, E., 2001. An evaluation of Lohmann's foraminifera weight dissolution index. Paleoceanography, 16(5), pp.531-534.

Broecker, W.S. and Denton, G.H., 1990. The role of ocean-atmosphere reorganizations in glacial cycles. Quaternary science reviews, 9(4), pp.305-341.

Broecker, W.S., Kennett, J.P., Flower, B.P., Teller, J.T., Trumbore, S., Bonani, G. and Wolfli, W., 1989. Routing of meltwater from the Laurentide Ice Sheet during the Younger Dryas cold episode. Nature, 341(6240), pp.318-321.

Broecker, W.S., Peteet, D.M. and Rind, D., 1985. Does the ocean–atmosphere system have more than one stable mode of operation?. Nature, 315(6014), pp.21-26.

Broerse, A.T., Ziveri, P., van Hinte, J.E. and Honjo, S., 2000. Coccolithophore export production, species composition, and coccolith-CaCO3 fluxes in the NE Atlantic (34 N21 W and 48 N21 W). Deep Sea Research Part II: Topical Studies in Oceanography, 47(9-11), pp.1877-1905.

Buckley, M.W. and Marshall, J., 2016. Observations, inferences, and mechanisms of the Atlantic Meridional Overturning Circulation: A review. Reviews of Geophysics, 54(1), pp.5-63.

Burke, E.J., Ekici, A., Huang, Y., Chadburn, S.E., Huntingford, C., Ciais, P., Friedlingstein, P., Peng, S. and Krinner, G., 2017. Quantifying uncertainties of permafrost carbon–climate feedbacks. Biogeosciences, 14(12), pp.3051-3066.

Caesar, L., McCarthy, G.D., Thornalley, D.J.R., Cahill, N. and Rahmstorf, S., 2021. Current Atlantic meridional overturning circulation weakest in last millennium. Nature Geoscience, 14(3), pp.118-120.

Caesar, L., Rahmstorf, S., Robinson, A., Feulner, G. and Saba, V., 2018. Observed fingerprint of a weakening Atlantic Ocean overturning circulation. Nature, 556(7700), pp.191-196.

CALIB rev. 8; Stuiver, M., and Reimer, P.J., 1993, Radiocarbon, 35, pp.215-230

Carstens, J., Hebbeln, D., Wefer, G., 1997. Distribution of planktic foraminifera at the ice margin in the Arctic (Fram Strait). Marine Micropaleontology. 29(3-4), pp.257-269. https://doi.org/10.1016/S0377-8398(96)00014-X

Cattiaux, J., Vautard, R., Cassou, C., Yiou, P., Masson-Delmotte, V. and Codron, F., 2010. Winter 2010 in Europe: A cold extreme in a warming climate. Geophysical Research Letters, 37(20).

Cavalieri, D.J. and Parkinson, C.L., 2012. Arctic sea ice variability and trends, 1979–2010. The Cryosphere, 6(4), pp.881-889.

Chafik, L., Nilsen, J. E. Ø., Dangendorf, S., Reverdin, G., Frederikse, T., 2019. North Atlantic Ocean circulation and decadal sea level change during the altimetry era. Scientific Reports, 9(1), pp.1-9. https://doi.org/10.1038/s41598-018-37603-6

Chapman, M. R., 2010. Seasonal production patterns of planktonic foraminifera in the NE Atlantic Ocean: Implications for paleotemperature and hydrographic reconstructions. Paleoceanography, 25(1).

Chave, K.E., 1954. Aspects of the biogeochemistry of magnesium 1. Calcareous marine organisms. The Journal of Geology, 62(3), pp.266-283.

Clark, P.U., Pisias, N.G., Stocker, T.F. and Weaver, A.J., 2002. The role of the thermohaline circulation in abrupt climate change. Nature, 415(6874), pp.863-869.

Clarke, K. R., 1993. Non-parametric multivariate analyses of changes in community structure. Australian journal of ecology. 18(1), pp.117-143.

Cléroux, C., Cortijo, E., Duplessy, J. C., Zahn, R., 2007. Deep-dwelling foraminifera as thermocline temperature recorders. Geochemistry,

Geophysics, Geosystems. 8(4). https://doi.org/10.1029/2006GC001474

CLIMAP Project Members., 1976. The surface of the ice-age earth. Science, pp.1131-1137.

Comiso, J.C. and Nishio, F., 2008. Trends in the sea ice cover using enhanced and compatible AMSR-E, SSM/I, and SMMR data. Journal of Geophysical Research: Oceans, 113(C2).

Comiso, J.C., 2012. Large decadal decline of the Arctic multiyear ice cover. Journal of climate, 25(4), pp.1176-1193.

Comiso, J.C., 2012. Large decadal decline of the Arctic multiyear ice cover. Journal of climate, 25(4), pp.1176-1193. https://doi.org/10.1175/jcli-d-11-00113.1

Cook, E.R., D'Arrigo, R.D. and Briffa, K.R., 1998. A reconstruction of the North Atlantic Oscillation using tree-ring chronologies from North America and Europe. The Holocene, 8(1), pp.9-17.

Cunningham, S.A., Kanzow, T., Rayner, D., Baringer, M.O., Johns, W.E., Marotzke, J., Longworth, H.R., Grant, E.M., Hirschi, J.J.M., Beal, L.M. and Meinen, C.S., 2007. Temporal variability of the Atlantic meridional overturning circulation at 26.5 N. Science, 317(5840), pp.935-938.

Damon, P.E., Lerman, J.C. and Long, A., 1978. Temporal fluctuations of atmospheric 14C: causal factors and implications. Annual Review of Earth and Planetary Sciences, 6(1), pp.457-494.

Daniault, N., Mercier, H., Lherminier, P., Sarafanov, A., Falina, A., Zunino, P., et al., 2016. The northern North Atlantic Ocean mean circulation in the early 21st century. Progress in Oceanography. 146, 142–158. https://doi.org/10.1016/j.pocean.2016.06.007

Daniault, N., Mercier, H., Lherminier, P., Sarafanov, A., Falina, A., Zunino, P., Pérez, F.F., Ríos, A.F., Ferron, B., Huck, T. and Thierry, V., 2016. The northern North Atlantic Ocean mean circulation in the early 21st century. Progress in Oceanography, 146, pp.142-158.

Dansgaard, W., Johnsen, S.J., Clausen, H.B., Dahl-Jensen, D., Gundestrup, N.S., Hammer, C.U., Hvidberg, C.S., Steffensen, J.P., Sveinbjörnsdottir, A.E., Jouzel, J. and Bond, G., 1993. Evidence for general instability of past climate from a 250-kyr ice-core record. nature, 364(6434), pp.218-220.

de Boisseson, E., Thierry, V., Mercier, H., Caniaux, G. and Desbruyères, D., 2012. Origin, formation and variability of the Subpolar Mode Water located over the Reykjanes Ridge. Journal of Geophysical Research: Oceans, 117(C12).

de Carvalho Ferreira, M.L. and Kerr, R., 2017. Source water distribution and quantification of North Atlantic deep water and Antarctic bottom water in the Atlantic Ocean. Progress in Oceanography, 153, pp.66-83.

de Vernal, A. and Hillaire-Marcel, C., 2006. Provincialism in trends and high frequency changes in the northwest North Atlantic during the Holocene. Global and Planetary Change, 54(3-4), pp.263-290.

de Vries, H., 1958. Atomic bomb effect: variation of radiocarbon in plants, shells, and snails in the past 4 years. Science, 128(3318), pp.250-251.

Dekens, P.S., Lea, D.W., Pak, D.K. and Spero, H.J., 2002. Core top calibration of Mg/Ca in tropical foraminifera: Refining paleotemperature estimation. Geochemistry, Geophysics, Geosystems, 3(4), pp.1-29.

DeMenocal, P., Ortiz, J., Guilderson, T. and Sarnthein, M., 2000. Coherent high- and low-latitude climate variability during the Holocene warm period. Science, 288(5474), pp.2198-2202.

Denton, G.H. and Karlén, W., 1973. Holocene climatic variations—their pattern and possible cause. Quaternary Research, 3(2), pp.155-205.

Deser, C., Tomas, R., Alexander, M. and Lawrence, D., 2010. The seasonal atmospheric response to projected Arctic sea ice loss in the late twenty-first century. Journal of Climate, 23(2), pp.333-351.

Dickson, R., Rudels, B., Dye, S., Karcher, M., Meincke, J., Yashayaev, I., 2007. Current estimates of freshwater flux through Arctic and subarctic

seas. Progress in Oceanography. 73(3-4), pp.210-230.

Dickson, R.R., Meincke, J., Malmberg, S.A. and Lee, A.J., 1988. The “great salinity anomaly” in the northern North Atlantic 1968–1982. Progress in Oceanography, 20(2), pp.103-151.

Dong, S., Garzoli, S., Baringer, M., Meinen, C. and Goni, G., 2009. Interannual variations in the Atlantic meridional overturning circulation and its relationship with the net northward heat transport in the South Atlantic. Geophysical Research Letters, 36(20).

d'Orbigny, A.D., 1826. Methodical table of the class Cephalopoda. Annals of Natural Sciences, 1st. Series, 7, pp.245-314.

Drijfhout, S., Van Oldenborgh, G. J., Cimatoribus, A., 2012. Is a decline of AMOC causing the warming hole above the North Atlantic in observed and modeled warming patterns? Journal of Climate, 25(24), pp.8373-8379.

Dukhovskoy, D.S., Yashayaev, I., Proshutinsky, A., Bamber, J.L., Bashmachnikov, I.L., Chassignet, E.P., Lee, C.M. and Tedstone, A.J., 2019. Role of Greenland freshwater anomaly in the recent freshening of the subpolar North Atlantic. Journal of Geophysical Research: Oceans, 124(5), pp.3333-3360.

Duplessy, J.C., Ivanova, E., Murdmaa, I., Paterne, M. and Labeyrie, L., 2001. Holocene paleoceanography of the northern Barents Sea and variations of the northward heat transport by the Atlantic Ocean. Boreas, 30(1), pp.2-16.

Dyke, A.S. and Prest, V.K., 1987. Late Wisconsinan and Holocene history of the Laurentide ice sheet. Géographie physique et Quaternaire, 41(2), pp.237-263.

Eiríksson, J., Knudsen, K.L., Haflidason, H. and Henriksen, P., 2000. Late-glacial and Holocene palaeoceanography of the North Icelandic shelf. Journal of Quaternary Science: Published for the Quaternary Research Association, 15(1), pp.23-42.

Elderfield, H. and Ganssen, G., 2000. Past temperature and δ18O of surface ocean waters inferred from foraminiferal Mg/Ca ratios. Nature, 405(6785), pp.442-

445.

Ellison, C.R., Chapman, M.R. and Hall, I.R., 2006. Surface and deep ocean interactions during the cold climate event 8200 years ago. Science, 312(5782), pp.1929-1932.

Emiliani, C., 1955. Pleistocene temperatures. The Journal of geology, 63(6), pp.538-578.

Espitalié, J., Laporte, J. L., Madec, M., Marquis, F., Leplat, P., Paulet, J., Boutefeu, A., 1977. Rapid method for source rocks characterization and for determination of petroleum potential and degree of evolution. Revue De L InstitutFrancais Du Petrole, 32(1), pp.23-42.

Eynaud, F., 2011. Planktonic foraminifera in the Arctic: potentials and issues regarding modern and quaternary populations. IOP Conf. Ser. Earth Environ. Sci. IOP Publishing. Vol. 14, No. 1, p. 012005.

Eynaud, F., De Abreu, L., Voelker, A., Schönfeld, J., Salgueiro, E., Turon, J.L., Penaud, A., Toucanne, S., Naughton, F., Goñi, M.F.S. and Malaizé, B., 2009. Position of the Polar Front along the western Iberian margin during key cold episodes of the last 45 ka. Geochemistry, Geophysics, Geosystems. 10(7).

Fairbanks, R. G., Sverdlove, M., Free, R., Wiebe, P. H., Bé, A. W., 1982. Vertical distribution and isotopic fractionation of living planktonic foraminifera from the Panama Basin. Nature, 298(5877), pp.841-844.

Fairbanks, R. G., Wiebe, P. H., 1980. Foraminifera and chlorophyll maximum: vertical distribution, seasonal succession, and paleoceanographic significance. Science, 209(4464), pp.1524-1526.

Farmer, J.R., Sigman, D.M., Granger, J., Underwood, O.M., Fripiat, F., Cronin, T.M., Martínez-García, A. and Haug, G.H., 2021. Arctic Ocean stratification set by sea level and freshwater inputs since the last ice age. Nature Geoscience, 14(9), pp.684-689.

Fischer, EM, Luterbacher, J., Zorita, E., Tett, SFB, Casty, C. and Wanner, H., 2007.

European climate response to tropical volcanic eruptions over the last half millennium. Geophysical research letters, 34 (5).

Fossheim, M., Primicerio, R., Johannesen, E., Ingvaldsen, R. B., Aschan, M. M., Dolgov, A. V., 2015. Recent warming leads to a rapid borealization of fish communities in the Arctic. Nature Climate Change. 5(7), pp.673-677. https://doi.org/10.1038/nclimate2647

Frajka-Williams, E., Ansorge, I.J., Baehr, J., Bryden, H.L., Chidichimo, M.P., Cunningham, S.A., Danabasoglu, G., Dong, S., Donohue, K.A., Elipot, S. and Heimbach, P., 2019. Atlantic meridional overturning circulation: Observed transport and variability. Frontiers in Marine Science, p.260.

Francis, J.A. and Vavrus, S.J., 2012. Evidence linking Arctic amplification to extreme weather in mid-latitudes. Geophysical research letters, 39(6).

Frew, R.D., Dennis, P.F., Heywood, K.J., Meredith, M.P. and Boswell, S.M., 2000. The oxygen isotope composition of water masses in the northern North Atlantic. Deep Sea Research Part I: Oceanographic Research Papers, 47(12), pp.2265-2286.

Fu, Y., Li, F., Karstensen, J. and Wang, C., 2020. A stable Atlantic meridional overturning circulation in a changing North Atlantic Ocean since the 1990s. Science advances, 6(48), p.eabc7836.

Ganssen, G. M., Kroon, D., 2000. The isotopic signature of planktonic foraminifera from NE Atlantic surface sediments: implications for the reconstruction of past oceanic conditions. Journal of the Geological Society, 157(3), pp.693-699. https://doi.org/10.1144/jgs.157.3.693

García-Ibáñez, M.I., Bates, N.R., Bakker, D.C., Fontela, M. and Velo, A., 2021. Cold-water corals in the Subpolar North Atlantic Ocean exposed to aragonite undersaturation if the 2° C global warming target is not met. Global and Planetary Change, 201, p.103480.

García-Ibáñez, M.I., Pardo, P.C., Carracedo, L.I., Mercier, H., Lherminier, P., Ríos, A.F. and Pérez, F.F., 2015. Structure, transports and transformations of the

water masses in the Atlantic Subpolar Gyre. Progress in Oceanography, 135, pp.18-36.

Garlick, G.D., 1969. The stable isotopes of oxygen. Handbook of geochemistry, 2, p.1.

Gherardi, J.M., Labeyrie, L., Nave, S., François, R., McManus, J.F. and Cortijo, E., 2009. Glacial-interglacial circulation changes inferred from 231Pa/230Th sedimentary record in the North Atlantic region. Paleoceanography, 24(2).

Giraudeau, J., Cremer, M., Manthé, S., Labeyrie, L. and Bond, G., 2000. Coccolith evidence for instabilities in surface circulation south of Iceland during Holocene times. Earth and Planetary Science Letters, 179(2), pp.257-268.

Godwin, H., 1962. Half-life of radiocarbon. Nature, 195, pp.984-984.

Greco, M., Jonkers, L., Kretschmer, K., Bijma, J., Kucera, M., 2019. Depth habitat of the planktonic foraminifera Neogloboquadrina pachyderma in the northern high latitudes explained by sea-ice and chlorophyll concentrations. Biogeosciences 16, pp.3425–3437. https://doi.org/10.5194/bg-16-3425-2019

Grootes, P.M. and Stuiver, M., 1997. Oxygen 18/16 variability in Greenland snow and ice with 10− 3-to 105-year time resolution. Journal of Geophysical Research: Oceans, 102(C12), pp.26455-26470.

Gutjahr, M., Frank, M., Stirling, C.H., Keigwin, L.D. and Halliday, A.N., 2008. Tracing the Nd isotope evolution of North Atlantic deep and intermediate waters in the Western North Atlantic since the Last Glacial Maximum from Blake Ridge sediments. Earth and Planetary Science Letters, 266(1-2), pp.61-77.

Gyldenfeldt, A.B.V., Carstens, J. and Meincke, J., 2000. Estimation of the catchment area of a sediment trap by means of current meters and foraminiferal tests. Deep Sea Research Part II: Topical studies in Oceanography, 47(9-11), pp.1701-1717.

Haak, H., Jungclaus, J., Mikolajewicz, U. and Latif, M., 2003. Formation and

propagation of great salinity anomalies. Geophysical Research Letters, 30(9).

Hakkinen, S. and Rhines, P.B., 2004. Decline of subpolar North Atlantic circulation during the 1990s. Science, 304(5670), pp.555-559.

Hall, I.R., Bianchi, G.G. and Evans, J.R., 2004. Centennial to millennial scale Holocene climate-deep water linkage in the North Atlantic. Quaternary Science Reviews, 23(14-15), pp.1529-1536.

Hanna, E., Jones, J.M., Cappelen, J., Mernild, S.H., Wood, L., Steffen, K. and Huybrechts, P., 2013. The influence of North Atlantic atmospheric and oceanic forcing effects on 1900–2010 Greenland summer climate and ice melt/runoff. International Journal of Climatology, 33(4), pp.862-880.

Harvey, J., 1982. θ-S relationships and water masses in the eastern North Atlantic. Deep Sea Research Part A. Oceanographic Research Papers, 29(8), pp.1021-1033.

Hátún, H., Payne, M. R., Beaugrand, G., Reid, P. C., Sandø, A. B., Drange, H., et al., 2009. Large bio-geographical shifts in the north-eastern Atlantic Ocean: From the subpolar gyre, via plankton, to blue whiting and pilot whales. Progress in Oceanography. 80(3-4), pp.149-162. https://doi.org/10.1016/j.pocean.2009.03.001

Hátún, H., Sandø, A.B., Drange, H., Hansen, B. and Valdimarsson, H., 2005. Influence of the Atlantic subpolar gyre on the thermohaline circulation. Science, 309(5742), pp.1841-1844.

Heaton, T.J., Köhler, P., Butzin, M., Bard, E., Reimer, R.W., Austin, W.E., Ramsey, C.B., Grootes, P.M., Hughen, K.A., Kromer, B. and Reimer, P.J., 2020. Marine20—the marine radiocarbon age calibration curve (0–55,000 cal BP). Radiocarbon, 62(4), pp.779-820.

Heikkilä, M. and Seppä, H., 2003. A 11,000 yr palaeotemperature reconstruction from the southern boreal zone in Finland. Quaternary Science Reviews, 22(5-7), pp.541-554.

Hemleben, Ch., Spindler M., Anderson R., 1989. Modern planktonic foraminifera. New York: Springer.

Hilbrecht, H., 1996. Extant planktonic foraminifera and the physical environment in the Atlantic and Indian Oceans, in Mitteilungen Aus Dem Geologischen Institut Der Eidgen. Technischen Hochschule Und Der Universität Zürich. p. 93.

Hillaire-Marcel, C., De Vernal, A., Bilodeau, G. and Weaver, A.J., 2001. Absence of deep-water formation in the Labrador Sea during the last interglacial period. Nature, 410(6832), pp.1073-1077.

Hoerling, M.P., Hurrell, J.W. and Xu, T., 2001. Tropical origins for recent North Atlantic climate change. Science, 292(5514), pp.90-92.

Holliday, N. P., 2003. Air-sea interaction and circulation changes in the northeast Atlantic. Journal of Geophysical Research: Oceans, 108(C8). https://doi.org/10.1029/2002JC001344

Holliday, N. P., Bersch, M., Berx, B., Chafik, L., Cunningham, S., Florindo-López, C., et al., 2020. Ocean circulation causes the largest freshening event for 120 years in eastern subpolar North Atlantic. Nature Communications, 11(1), pp.1-15.

Holliday, N.P., Hughes, S.L., Bacon, S., Beszczynska-Möller, A., Hansen, B., Lavin, A., Loeng, H., Mork, K.A., Østerhus, S., Sherwin, T. and Walczowski, W., 2008. Reversal of the 1960s to 1990s freshening trend in the northeast North Atlantic and Nordic Seas. Geophysical Research Letters, 35(3).

Honjo, S., Manganini, S. J., 1993. Annual biogenic particle fluxes to the interior of the North Atlantic Ocean; studied at 34 N 21 W and 48 N 21 W. Deep Sea Research Part II: Topical studies in Oceanography 40(1-2), pp.587-607. https://doi.org/10.1016/0967-0645(93)90034-K

Hoogakker, B.A., Chapman, M.R., McCave, I.N., Hillaire-Marcel, C., Ellison, C.R., Hall, I.R. and Telford, R.J., 2011. Dynamics of North Atlantic deep water masses during the Holocene. Paleoceanography, 26(4).

Howe, J.N., Piotrowski, A.M., Noble, T.L., Mulitza, S., Chiessi, C.M. and Bayon, G., 2016. North Atlantic deep water production during the Last Glacial Maximum. Nature communications, 7(1), p.11765.

Hu, F.S., Kaufman, D., Yoneji, S., Nelson, D., Shemesh, A., Huang, Y., Tian, J., Bond, G., Clegg, B. and Brown, T., 2003. Cyclic variation and solar forcing of Holocene climate in the Alaskan subarctic. Science, 301(5641), pp.1890-1893.

Hurrell, J.W., 1995. Decadal trends in the North Atlantic Oscillation: Regional temperatures and precipitation. Science, 269(5224), pp.676-679.

Hurrell, J.W., 1996. Influence of variations in extratropical wintertime teleconnections on Northern Hemisphere temperature. Geophysical Research Letters, 23(6), pp.665-668.

Hurrell, J.W., Kushnir, Y., Ottersen, G. and Visbeck, M., 2003. An overview of the North Atlantic oscillation. Geophysical Monograph-American Geophysical Union, 134, pp.1-36.

Husum, K. and Hald, M., 2012. Arctic planktic foraminiferal assemblages: Implications for subsurface temperature reconstructions. Marine Micropaleontology, 96, pp.38-47. https://doi.org/10.1016/j.marmicro.2012.07.001

Hut, G., 1987. Consultants' group meeting on stable isotope reference samples for geochemical and hydrological investigations.

Iglesias-Rodríguez, M.D., Brown, C.W., Doney, S.C., Kleypas, J., Kolber, D., Kolber, Z., Hayes, P.K. and Falkowski, P.G., 2002. Representing key phytoplankton functional groups in ocean carbon cycle models: Coccolithophorids. Global Biogeochemical Cycles, 16(4), pp.47-1.

Iselin, C.O.D., 1936. A study of the circulation of the western North Atlantic.

Jahn, A. and Holland, M.M., 2013. Implications of Arctic sea ice changes for North Atlantic deep convection and the meridional overturning circulation in

CCSM4-CMIP5 simulations. Geophysical Research Letters, 40(6), pp.1206-1211.

Jennings, A., Andrews, J. and Wilson, L., 2011. Holocene environmental evolution of the SE Greenland Shelf North and South of the Denmark Strait: Irminger and East Greenland current interactions. Quaternary Science Reviews, 30(7-8), pp.980-998.

Jennings, A.E., Knudsen, K.L., Hald, M., Hansen, C.V. and Andrews, J.T., 2002. A mid-Holocene shift in Arctic sea-ice variability on the East Greenland Shelf. The Holocene, 12(1), pp.49-58.

Johannessen, T., Jansen, E., Flatøy, A., Ravelo, A. C., 1994. The relationship between surface water masses, oceanographic fronts and paleoclimatic proxies in surface sediments of the Greenland, Iceland, Norwegian Seas, in: Carbon cycling in the glacial ocean: constraints on the ocean's role in global change. Springer, Berlin, Heidelberg, pp.61-85. https://doi.org/10.1007/978-3-642-78737-9_4

Johns, W.E., Baringer, M.O., Beal, L.M., Cunningham, S.A., Kanzow, T., Bryden, H.L., Hirschi, J.J.M., Marotzke, J., Meinen, C.S., Shaw, B. and Curry, R., 2011. Continuous, array-based estimates of Atlantic Ocean heat transport at 26.5 N. Journal of Climate, 24(10), pp.2429-2449.

Johnson, C., Inall, M. and Häkkinen, S., 2013. Declining nutrient concentrations in the northeast Atlantic as a result of a weakening Subpolar Gyre. Deep Sea Research Part I: Oceanographic Research Papers, 82, pp.95-107. https://doi.org/10.1016/j.dsr.2013.08.007

Jonkers, L., Brummer, G.J.A., Peeters, F.J.C., Van Aken, H.M., De Jong, M.F., 2010. Seasonal stratification, shell flux, and oxygen isotope dynamics of leftcoiling *N. pachyderma* and *T. quinqueloba* in the western subpolar North Atlantic. Paleoceanography 25, pp.1–13. https://doi.org/10.1029/2009PA001849

Jonkers, L., Hillebrand, H., Kucera, M., 2019. Global change drives modern

plankton communities away from the pre-industrial state. Nature. https://doi.org/10.1038/s41586-019-1230-3

Jonkers, L., Van Heuven, S., Zahn, R. and Peeters, F.J., 2013. Seasonal patterns of shell flux, δ18O and δ13C of small and large N. pachyderma (s) and G. bulloides in the subpolar North Atlantic. Paleoceanography, 28(1), pp.164-174.

Jung, T., Vitart, F., Ferranti, L. and Morcrette, J.J., 2011. Origin and predictability of the extreme negative NAO winter of 2009/10. Geophysical Research Letters, 38(7).

Jungclaus, J.H., Haak, H., Latif, M. and Mikolajewicz, U., 2005. Arctic–North Atlantic interactions and multidecadal variability of the meridional overturning circulation. Journal of climate, 18(19), pp.4013-4031.

Jungclaus, J.H., Lohmann, K. and Zanchettin, D., 2014. Enhanced 20th-century heat transfer to the Arctic simulated in the context of climate variations over the last millennium. Climate of the Past, 10(6), pp.2201-2213.

Kandiano, E.S. and Bauch, H.A., 2002. Implications of planktic foraminiferal size fractions for the glacial-interglacial paleoceanography of the polar North Atlantic. The Journal of Foraminiferal Research, 32(3), pp.245-251. https://doi.org/10.2113/32.3.245

Kanzow, T., Send, U., Zenk, W., Chave, A.D. and Rhein, M., 2006. Monitoring the integrated deep meridional flow in the tropical North Atlantic: Long-term performance of a geostrophic array. Deep Sea Research Part I: Oceanographic Research Papers, 53(3), pp.528-546.

Katz, M.E., Cramer, B.S., Franzese, A., Hönisch, B., Miller, K.G., Rosenthal, Y. and Wright, J.D., 2010. Traditional and emerging geochemical proxies in foraminifera. The Journal of Foraminiferal Research, 40(2), pp.165-192.

Kaufman, D.S., Ager, T.A., Anderson, N.J., Anderson, P.M., Andrews, J.T., Bartlein, P.J., Brubaker, L.B., Coats, L.L., Cwynar, L.C., Duvall, M.L. and Dyke, A.S., 2004. Holocene thermal maximum in the western Arctic (0–180

W). Quaternary Science Reviews, 23(5-6), pp.529-560.

Keigwin, L.D., Sachs, J.P., Rosenthal, Y. and Boyle, E.A., 2005. The 8200 year BP event in the slope water system, western subpolar North Atlantic. Paleoceanography, 20(2). https://doi.org/10.1029/2004PA001074

Keller, G., Abramovich, S., 2009. Lilliput effect in late Maastrichtian planktic foraminifera: Response to environmental stress. Palaeogeography, Palaeoclimatology, Palaeoecology, 284(1-2), pp.47-62. https://doi.org/10.1016/j.palaeo.2009.08.029

Kennett, J. P., Srinivasan, M. S., 1983. Neogene planktonic foraminifera, Hutchinson Ross Publ. Go., Stroudsburg, Pennsylvania. pp. 265

Kim, S.T. and O'Neil, J.R., 1997. Equilibrium and nonequilibrium oxygen isotope effects in synthetic carbonates. Geochimica et cosmochimica acta, 61(16), pp.3461-3475.

Kimura, S., Nakata, H., Okazaki, Y., 2000. Biological production in meso-scale eddies caused by frontal disturbances of the Kuroshio Extension. ICES Journal of Marine Science, 57, pp.133–142. https://doi.org/10.1006/jmsc.1999.0564

Kissel, C., Van Toer, A., Laj, C., Cortijo, E. and Michel, E., 2013. Variations in the strength of the North Atlantic bottom water during Holocene. Earth and Planetary Science Letters, 369, pp.248-259.

Kleiven, H.K.F., Kissel, C., Laj, C., Ninnemann, U.S., Richter, T.O. and Cortijo, E., 2008. Reduced North Atlantic deep water coeval with the glacial Lake Agassiz freshwater outburst. science, 319(5859), pp.60-64.

Klitgaard-Kristensen, D., Sejrup, H.P. and Haflidason, H., 2001. The last 18 kyr fluctuations in Norwegian Sea surface conditions and implications for the magnitude of climatic change: evidence from the North Sea. Paleoceanography, 16(5), pp.455-467.

Knutsen, Ø., Svendsen, H., Øterhus, S., Rossby, T., Hansen, B., 2005. Direct measurements of the mean flow and eddy kinetic energy structure of the upper

ocean circulation in the NE Atlantic. Geophysical Reeaserch Letters. 32, pp.1–5. https://doi.org/10.1029/2005GL023615

Kohfeld, K. E., Fairbanks, R. G., Smith, S. L., Walsh, I. D., 1996. *Neogloboquadrina pachyderma* (sinistral coiling) as paleoceanographic tracers in polar oceans: Evidence from Northeast Water Polynya plankton tows, sediment traps, and surface sediments. Paleoceanography, 11(6), pp.679-699. https://doi.org/10.1029/96PA02617

Kretschmer, K., Jonkers, L., Kucera, M., Schulz, M., 2018. Modeling seasonal and vertical habitats of planktonic foraminifera on a global scale. Biogeosciences, 15(14). https://doi.org/10.5194/bg-15-4405-2018

Kroon, D. and Ganssen, G., 1989. Northern Indian Ocean upwelling cells and the stable isotope composition of living planktonic foraminifers. Deep Sea Research Part A. Oceanographic Research Papers, 36(8), pp.1219-1236.

Kucera, M., 2007. Chapter six planktonic foraminifera as tracers of past oceanic environments, in Methods in late Cenozoic paleoceanography, Development in Marine Geology, Eds. C. Hillaire-Marcel, A. de Vernal. (New York: Elsevier), 1, pp.213-262.

Kuhlbrodt, T., Griesel, A., Montoya, M., Levermann, A., Hofmann, M. and Rahmstorf, S., 2007. On the driving processes of the Atlantic meridional overturning circulation. Reviews of Geophysics, 45(2).

Kuroyanagi, A., Kawahata, H., 2004. Vertical distribution of living planktonic foraminifera in the seas around Japan. Marine Micropaleontology 53(1-2), pp.173-196.

Lau, N.C., 1997. Interactions between global SST anomalies and the midlatitude atmospheric circulation. Bulletin of the American Meteorological Society, 78(1), pp.21-34.

Lea, D.W., Mashiotta, T.A. and Spero, H.J., 1999. Controls on magnesium and strontium uptake in planktonic foraminifera determined by live culturing. Geochimica et Cosmochimica Acta, 63(16), pp.2369-2379.

Leduc, G., Schneider, R., Kim, J.H. and Lohmann, G., 2010. Holocene and Eemian sea surface temperature trends as revealed by alkenone and Mg/Ca paleothermometry. Quaternary Science Reviews, 29(7-8), pp.989-1004.

LeGrande, A.N. and Schmidt, G.A., 2006. Global gridded data set of the oxygen isotopic composition in seawater. Geophysical research letters, 33(12).

Li, H. and Fedorov, A.V., 2021. Persistent freshening of the Arctic Ocean and changes in the North Atlantic salinity caused by Arctic sea ice decline. Climate Dynamics, 57(11-12), pp.2995-3013.

Libby, W.F., 1981. Radiocarbon dating.

Lippold, J., Gutjahr, M., Blaser, P., Christner, E., de Carvalho Ferreira, M.L., Mulitza, S., Christl, M., Wombacher, F., Böhm, E., Antz, B. and Cartapanis, O., 2016. Deep water provenance and dynamics of the (de) glacial Atlantic meridional overturning circulation. Earth and planetary science letters, 445, pp.68-78.

Liu, Z., Brady, E. and Lynch-Stieglitz, J., 2003. Global ocean response to orbital forcing in the Holocene. Paleoceanography, 18(2).

Locarnini, R. A., A. V. Mishonov, O. K. Baranova, T. P. Boyer, M. M. Zweng, H. E. Garcia, J. R. Reagan, D. Seidov, K. Weathers, C. R. Paver, and I. Smolyar, 2018. World Ocean Atlas 2018, Volume 1: Temperature. A. Mishonov Technical Ed.; NOAA Atlas NESDIS 81, 52pp.

Loder, J.W., Boicourt, W.C. and Simpson, J.H., 1998. Western ocean boundary shelves. The Sea, 11, pp.3-28.

Lohmann, G.P., 1995. A model for variation in the chemistry of planktonic foraminifera due to secondary calcification and selective dissolution. Paleoceanography, 10(3), pp.445-457.

Lohmann, K., Drange, H. and Bentsen, M., 2009. A possible mechanism for the strong weakening of the North Atlantic subpolar gyre in the mid-1990s. Geophysical Research Letters, 36(15).

Lohmann, K., Drange, H. and Bentsen, M., 2009. Response of the North Atlantic subpolar gyre to persistent North Atlantic oscillation like forcing. Climate dynamics, 32, pp.273-285.

Lozier, M.S., Bacon, S., Bower, A.S., Cunningham, S.A., de Jong, M.F., de Steur, L., Deyoung, B., Fischer, J., Gary, S.F., Greenan, B.J. and Heimbach, P., 2017. Overturning in the Subpolar North Atlantic Program: A new international ocean observing system. Bulletin of the American Meteorological Society, 98(4), pp.737-752.

Lozier, M.S., Li, F., Bacon, S., Bahr, F., Bower, A.S., Cunningham, S.A., de Jong, M.F., de Steur, L., deYoung, B., Fischer, J. and Gary, S.F., 2019. A sea change in our view of overturning in the subpolar North Atlantic. Science, 363(6426), pp.516-521.

Lundgreen, U., 1996. Aminosa¨uren im Nordatlantik: Partikelzusammensetzung und Remineralisierung, Berichte aus dem Institut für Meereskunde an der Christian-Albrechts-Universität Kiel, 283, pp.1 – 128.

Lutjeharms, J.R.E., Walters, N.M., Allanson, B.R., 1985. Oceanic frontal systems and biological enhancement, in: W.R. Siegfried, P.R. Condy, R.M. Laws (Eds.), Antarctic Nutrient Cycles and Food Webs. Springer, Berlin, pp.11–21. https://doi.org/10.1007/978-3-642-82275-9_3

Lynch-Stieglitz, J., 2017. The Atlantic meridional overturning circulation and abrupt climate change. Annual review of marine science, 9, pp.83-104.

Mahadevan, A., D'asaro, E., Lee, C., Perry, M. J., 2012. Eddy-driven stratification initiates North Atlantic spring phytoplankton blooms. Science, 337(6090), pp.54-58.

Mallo, M., Ziveri, P., Graham Mortyn, P., Schiebel, R., Grelaud, M., 2017. Low planktic foraminiferal diversity and abundance observed in a spring 2013 west-east Mediterranean Sea plankton tow transect. Biogeosciences 14, pp.2245–2266. https://doi.org/10.5194/bg-14-2245-2017

Marchal, O., Cacho, I., Stocker, T.F., Grimalt, J.O., Calvo, E., Martrat, B., Shackleton, N., Vautravers, M., Cortijo, E., van Kreveld, S. and Andersson, C., 2002. Apparent long-term cooling of the sea surface in the northeast Atlantic and Mediterranean during the Holocene. Quaternary Science Reviews, 21(4-6), pp.455-483.

Marchitto, T.M. and Broecker, W.S., 2006. Deep water mass geometry in the glacial Atlantic Ocean: A review of constraints from the paleonutrient proxy Cd/Ca. Geochemistry, Geophysics, Geosystems, 7(12).

Marshall, J., Kushnir, Y., Battisti, D., Chang, P., Czaja, A., Dickson, R., Hurrell, J., McCartney, M., Saravanan, R. and Visbeck, M., 2001. North Atlantic climate variability: phenomena, impacts and mechanisms. International Journal of Climatology: A Journal of the Royal Meteorological Society, 21(15), pp.1863-1898.

Marshall, B.J., Thunell, R.C., Henehan, M.J., Astor, Y. and Wejnert, K.E., 2013. Planktonic foraminiferal area density as a proxy for carbonate ion concentration: A calibration study using the Cariaco Basin ocean time series. Paleoceanography, 28(2), pp.363-376.

Mashiotta, T.A., Lea, D.W. and Spero, H.J., 1999. Glacial–interglacial changes in Subantarctic sea surface temperature and δ18O-water using foraminiferal Mg. Earth and Planetary Science Letters, 170(4), pp.417-432.

Matul, A., Barash, M. S., Khusid, T. A., Behera, P., Tiwari, M., 2018. Paleoenvironment Variability during Termination I at the Reykjanes Ridge, North Atlantic. Geosciences, 8(10): 375. http://dx.doi.org/10.3390/geosciences8100375

Mayewski, P.A., Rohling, E.E., Stager, J.C., Karlén, W., Maasch, K.A., Meeker, L.D., Meyerson, E.A., Gasse, F., van Kreveld, S., Holmgren, K. and Lee-Thorp, J., 2004. Holocene climate variability. Quaternary research, 62(3), pp.243-255.

McCartney, M. S., Talley, L. D., 1982. The subpolar mode water of the North

Atlantic Ocean. Journal of Physical Oceanography, 12(11), pp.1169-1188.

McManus, J.F., Francois, R., Gherardi, J.M., Keigwin, L.D. and Brown-Leger, S., 2004. Collapse and rapid resumption of Atlantic meridional circulation linked to deglacial climate changes. nature, 428(6985), pp.834-837.

McManus, J.F., Oppo, D.W. and Cullen, J.L., 1999. A 0.5-million-year record of millennial-scale climate variability in the North Atlantic. science, 283(5404), pp.971-975.

Meilland, J., Howa, H., Hulot, V., Demangel, I., Salaün, J., Garlan, T., 2020. Population dynamics of modern planktonic foraminifera in the western Barents Sea. Biogeosciences 17, pp.1437–1450. https://doi.org/10.5194/bg-17-1437-2020

Meinen, C.S., Speich, S., Perez, R.C., Dong, S., Piola, A.R., Garzoli, S.L., Baringer, M.O., Gladyshev, S. and Campos, E.J., 2013. Temporal variability of the meridional overturning circulation at 34.5 S: Results from two pilot boundary arrays in the South Atlantic. Journal of Geophysical Research: Oceans, 118(12), pp.6461-6478.

Melling, M., Agnew, T. A., Falkner, K. K., Greenberg, D. A., Lee, C. M., Munchow, A., et al., 2008. Fresh-water fluxes via Pacific and Arctic outflows across Canadian Polar Shelf, in: R. R. Dickson, J. Meinke, and P. Rhines (Eds.), Arctic-Subarctic Ocean Fluxes, Defining the Role of the Northern Seas in Climate. Springer, Dordrecht, Netherlands, pp. 193– 247.

Meredith, M., Sommerkorn, M., Cassotta, S., Derksen, C., Ekaykin, A., Hollowed, A., Kofinas, G., Mackintosh, A., Melbourne-Thomas, J., Muelbert, M., Ottersen, G., Pritchard, H., and Schuur, E.: Polar Regions, in: IPCC Special Report on the Ocean and Cryosphere in a Changing Climate, edited by: Pörtner, H.-O., Roberts, D., Masson-Delmotte, V., Zhai, P., Tignor, M., Poloczanska, E., Mintenbeck, K., Alegría, A., Nicolai, M., Okem, A., Petzold, J., Rama, B., and Weyer, N., Cambridge University Press, Cambridge, UK and New York, NY, USA, 203–320, https://doi.org/10.1017/9781009157964.005, 2022.

Moffa-Sánchez, P. and Hall, I.R., 2017. North Atlantic variability and its links to European climate over the last 3000 years. Nature Communications, 8(1), p.1726.

Moffa-Sánchez, P. and Hall, I.R., 2017. North Atlantic variability and its links to European climate over the last 3000 years. Nature Communications, 8(1), p.1726.

Moros, M., Andrews, J.T., Eberl, D.D. and Jansen, E., 2006. Holocene history of drift ice in the northern North Atlantic: Evidence for different spatial and temporal modes. Paleoceanography, 21(2).

Moros, M., Emeis, K., Risebrobakken, B., Snowball, I., Kuijpers, A., McManus, J. and Jansen, E., 2004. Sea surface temperatures and ice rafting in the Holocene North Atlantic: climate influences on northern Europe and Greenland. Quaternary Science Reviews, 23(20-22), pp.2113-2126.

Moros, M., Jansen, E., Oppo, D.W., Giraudeau, J. and Kuijpers, A., 2012. Reconstruction of the late-Holocene changes in the Sub-Arctic Front position at the Reykjanes Ridge, north Atlantic. The Holocene, 22(8), pp.877-886.

Müller, W.A., Frankignoul, C. and Chouaib, N., 2008. Observed decadal tropical Pacific–North Atlantic teleconnections. Geophysical Research Letters, 35(24).

Naidu, P.D. and Malmgren, B.A., 1996. A high-resolution record of late Quaternary upwelling along the Oman Margin, Arabian Sea based on planktonic foraminifera. Paleoceanography, 11(1), pp.129-140.

NASA Goddard Space Flight Center, Ocean Ecology Laboratory, Ocean Biology Processing Group. Moderate-resolution Imaging Spectroradiometer (MODIS) Aqua Chlorophyll Data; 2018 Reprocessing. NASA OB.DAAC, Greenbelt, MD, USA. doi: data/10.5067/AQUA/MODIS/L3B/CHL/2018. Accessed on 24/09/2020

Nesje, A. and Johannessen, T., 1992. What were the primary forcing mechanisms of high-frequency Holocene climate and glacier variations?. The

Holocene, 2(1), pp.79-84.

Neukermans, G., Oziel, L., Babin, M. (2018). Increased intrusion of warming Atlantic water leads to rapid expansion of temperate phytoplankton in the Arctic. Global Change Biology. 24(6), pp.2545-2553. https://doi.org/10.1111/gcb.14075

Nier, A.O., 1950. A redetermination of the relative abundances of the isotopes of carbon, nitrogen, oxygen, argon, and potassium. Physical Review, 77(6), p.789.

Nummelin, A., Ilicak, M., Li, C. and Smedsrud, L.H., 2016. Consequences of future increased Arctic runoff on Arctic Ocean stratification, circulation, and sea ice cover. Journal of Geophysical Research: Oceans, 121(1), pp.617-637.

Núñez, I., Bersch, M., Haak, H., Jungclaus, J.H. and Lohmann, K., 2012. A multi-decadal meridional displacement of the Subpolar Front in the Newfoundland Basin. Ocean Science, 8(1).

Nürnberg, D., Bijma, J. and Hemleben, C., 1996. Assessing the reliability of magnesium in foraminiferal calcite as a proxy for water mass temperatures. Geochimica et cosmochimica Acta, 60(5), pp.803-814.

O'Brien, S.R., Mayewski, P.A., Meeker, L.D., Meese, D.A., Twickler, M.S. and Whitlow, S.I., 1995. Complexity of Holocene climate as reconstructed from a Greenland ice core. Science, 270(5244), pp.1962-1964.

Ólafsdóttir, S., Jennings, A.E., Geirsdóttir, Á., Andrews, J. and Miller, G.H., 2010. Holocene variability of the North Atlantic Irminger current on the south-and northwest shelf of Iceland. Marine Micropaleontology, 77(3-4), pp.101-118.

Olsen, J., Anderson, N.J. and Knudsen, M.F., 2012. Variability of the North Atlantic Oscillation over the past 5,200 years. Nature Geoscience, 5(11), pp.808-812.

Oomori, T., Kaneshima, H., Maezato, Y. and Kitano, Y., 1987. Distribution coefficient of Mg2+ ions between calcite and solution at 10–50 C. Marine

Chemistry, 20(4), pp.327-336.

Oppo, D.W., Gebbie, G., Huang, K.F., Curry, W.B., Marchitto, T.M. and Pietro, K.R., 2018. Data constraints on glacial Atlantic water mass geometry and properties. Paleoceanography and Paleoclimatology, 33(9), pp.1013-1034.

Oppo, D.W., McManus, J.F. and Cullen, J.L., 2003. Deepwater variability in the Holocene epoch. Nature, 422(6929), pp.277-277.

Orme, L.C., Miettinen, A., Divine, D., Husum, K., Pearce, C., Van Nieuwenhove, N., Born, A., Mohan, R. and Seidenkrantz, M.S., 2018. Subpolar North Atlantic sea surface temperature since 6 ka BP: Indications of anomalous ocean-atmosphere interactions at 4-2 ka BP. Quaternary Science Reviews, 194, pp.128-142.

Ortiz, J. D., Mix, A. C., 1992. The spatial distribution and seasonal succession of planktic foraminifera in the California Current off Oregon, September 1987–September 1988, in: Summerhayes, C. P., Prell, W. L., Emeis, K. C. (Eds.), Upwelling systems: Evolution since the Early Miocene. Geological Society, London, Special Publications 64(1), pp. 197-213.

Ortiz, J. D., Mix, A. C., Collier, R. W., 1995. Environmental control of living symbiotic and asymbiotic foraminifera of the California Current. Paleoceanography, 10(6), pp.987-1009.

Osman, M. B., Das, S. B., Trusel, L. D., Evans, M. J., Fischer, H., Grieman, M. M., et al., 2019. Industrial-era decline in subarctic Atlantic productivity. Nature, 569(7757), pp.551-555. https://doi.org/10.1038/s41586-019-1181-8

Ottens, J. J., 1991. Planktic foraminifera as North Atlantic water mass indicators. Oceanologica acta, 14, pp.123–140.

Ottens, J. J., 1992. April and August Northeast Atlantic surface water masses reflected in planktic foraminifera. Netherlands journal of sea research, 28(4), pp.261-283.

Otterå, O.H. and Drange, H., 2004. Effects of solar irradiance forcing on the ocean circulation and sea-ice in the North Atlantic in an isopycnic coordinate ocean general circulation model. Tellus A: Dynamic Meteorology and Oceanography, 56(2), pp.154-166.

Oziel, L., Neukermans, G., Ardyna, M., Lancelot, C., Tison, J. L., Wassmann, P., et al., 2017. Role for Atlantic inflows and sea ice loss on shifting phytoplankton blooms in the Barents Sea. Journal of Geophysical Research: Oceans, 122(6), pp.5121-5139. https://doi.org/10.1002/2016JC012582

Pados, T., Spielhagen, R.F., 2014. Species distribution and depth habitat of recent planktic foraminifera in Fram Strait, Arctic Ocean. Polar Research, https://doi.org/10.3402/polar.v33.22483

Pak, D.K., Lea, D.W. and Kennett, J.P., 2004. Seasonal and interannual variation in Santa Barbara Basin water temperatures observed in sediment trap foraminiferal Mg/Ca. Geochemistry, Geophysics, Geosystems, 5(12).

Parker, F. L., 1960. Living planktonic foraminifera from the Equatorial and Southeast Pacific. Science reports of the Tohoku University. 2nd series, Geology. Special volume, 4.

Parker, F. L., Berger, W. H., 1971, January. Faunal and solution patterns of planktonic foraminifera in surface sediments of the South Pacific. In Deep Sea Research and Oceanographic Abstracts. Elsevier. 18(1), pp.73-107.

Perner, K., Jennings, A.E., Moros, M., Andrews, J.T. and Wacker, L., 2016. Interaction between warm Atlantic-sourced waters and the East Greenland Current in northern Denmark Strait (68 N) during the last 10 600 cal a BP. Journal of Quaternary Science, 31(5), pp.472-483.

Perner, K., Moros, M., Jansen, E., Kuijpers, A., Troelstra, S.R. and Prins, M.A., 2018. Subarctic Front migration at the Reykjanes Ridge during the mid-to late Holocene: evidence from planktic foraminifera. Boreas, 47(1), pp.175-188.

Perner, K., Moros, M., Jennings, A., Lloyd, J.M. and Knudsen, K.L., 2013. Holocene palaeoceanographic evolution off West Greenland. The

Holocene, 23(3), pp.374-387.

Perner, K., Moros, M., Lloyd, J.M., Kuijpers, A., Telford, R.J. and Harff, J., 2011. Centennial scale benthic foraminiferal record of late Holocene oceanographic variability in Disko Bugt, West Greenland. Quaternary Science Reviews, 30(19-20), pp.2815-2826.

Petit, T., Mercier, H. and Thierry, V., 2018. First direct estimates of volume and water mass transports across the Reykjanes Ridge. Journal of Geophysical Research: Oceans, 123(9), pp.6703-6719.

Pflaumann, U., Sarnthein, M., Chapman, M., d'Abreu, L., Funnell, B., Huels, M., et al., 2003. Glacial North Atlantic: Sea-surface conditions reconstructed by GLAMAP 2000. Paleoceanography, 18(3).

Pickart, R.S., Spall, M.A., Ribergaard, M.H., Moore, G.K. and Milliff, R.F., 2003. Deep convection in the Irminger Sea forced by the Greenland tip jet. Nature, 424(6945), pp.152-156.

Pinto, J.G. and Raible, C.C., 2012. Past and recent changes in the North Atlantic oscillation. Wiley Interdisciplinary Reviews: Climate Change, 3(1), pp.79-90.

Pollard, R.T., Griffttths, M.J., Cunningham, S.A., Read, J.F., Pérez, F.F. and Ríos, A.F., 1996. Vivaldi 1991-A study of the formation, circulation and ventilation of Eastern North Atlantic Central Water. Progress in Oceanography, 37(2), pp.167-192. https://doi.org/10.1016/S0079-6611(96)00008-0

Pollard, R.T., Read, J.F., Holliday, N.P., Leach, H., 2004. Water masses and circulation pathways through the Iceland basin during Vivaldi 1996. Journal of Geophysical Research: Oceans, 109, pp.1–10. https://doi.org/10.1029/2003JC002067

Pörtner, H.O., Roberts, D.C., Adams, H., Adler, C., Aldunce, P., Ali, E., Begum, R.A., Betts, R., Kerr, R.B., Biesbroek, R. and Birkmann, J., 2022. Climate change 2022: Impacts, adaptation and vulnerability (p. 3056). Geneva, Switzerland: IPCC.

Praetorius, S.K., McManus, J.F., Oppo, D.W. and Curry, W.B., 2008. Episodic reductions in bottom-water currents since the last ice age. Nature Geoscience, 1(7), pp.449-452.

Rahmstorf, S., 1997. Risk of sea-change in the Atlantic. Nature, 388(6645), pp.825-826.

Rahmstorf, S., 2002. Ocean circulation and climate during the past 120,000 years. Nature, 419(6903), pp.207-214.

Rahmstorf, S., Box, J.E., Feulner, G., Mann, M.E., Robinson, A., Rutherford, S. and Schaffernicht, E.J., 2015. Exceptional twentieth-century slowdown in Atlantic Ocean overturning circulation. Nature climate change, 5(5), pp.475-480. https://doi.org/10.1038/nclimate2554

Rasmussen, T.L., Thomsen, E., Troelstra, S.R., Kuijpers, A. and Prins, M.A., 2003. Millennial-scale glacial variability versus Holocene stability: changes in planktic and benthic foraminifera faunas and ocean circulation in the North Atlantic during the last 60 000 years. Marine Micropaleontology, 47(1-2), pp.143-176.

Ravelo, A.C. and Hillaire-Marcel, C., 2007. Chapter eighteen the use of oxygen and carbon isotopes of foraminifera in paleoceanography. Developments in marine geology, 1, pp.735-764.

Read, J.F. and Pollard, R.T., 1992. Water masses in the region of the Iceland–Faeroes Front. Journal of Physical Oceanography, 22(11), pp.1365-1378.

Read, J.F., 2000. CONVEX-91: water masses and circulation of the Northeast Atlantic subpolar gyre. Progress in Oceanography. 48(4), pp.461-510. https://doi.org/10.1016/S0079-6611(01)00011-8

Rebotim, A., Voelker, A.H.L., Jonkers, L., Waniek, J.J., Meggers, H., Schiebel, R., et al., 2017. Factors controlling the depth habitat of planktonic foraminifera in the subtropical eastern North Atlantic. Biogeosciences 14, pp.827–859. https://doi.org/10.5194/bg-14-827-2017

Reimer, P.J., Baillie, M.G., Bard, E., Bayliss, A., Beck, J.W., Blackwell, P.G., Ramsey, C.B., Buck, C.E., Burr, G.S., Edwards, R.L. and Friedrich, M., 2009. IntCal09 and Marine09 radiocarbon age calibration curves, 0–50,000 years cal BP. Radiocarbon, 51(4), pp.1111-1150.

Renssen, H., Goosse, H. and Muscheler, R., 2006. Coupled climate model simulation of Holocene cooling events: oceanic feedback amplifies solar forcing. Climate of the Past, 2(2), pp.79-90.

Renssen, H., Seppä, H., Heiri, O., Roche, D.M., Goosse, H. and Fichefet, T., 2009. The spatial and temporal complexity of the Holocene thermal maximum. Nature Geoscience, 2(6), pp.411-414.

Retailleau, S., Eynaud, F., Mary, Y., Abdallah, V., Schiebel, R., Howa, H., 2012. Canyon heads and river plumes: How might they influence neritic planktonic foraminifera communities in the SE Bay of Biscay? The Journal of Foraminiferal Research 42(3), pp.257-269. https://doi.org/10.2113/gsjfr.42.3.257

Retailleau, S., Howa, H., Schiebel, R., Lombard, F., Eynaud, F., Schmidt, S., et al., 2009. Planktic foraminiferal production along an offshore–onshore transect in the south-eastern Bay of Biscay. Continental Shelf Research, 29(8), pp.1123-1135. https://doi.org/10.1016/j.csr.2008.12.021

Retailleau, S., Schiebel, R., Howa, H., 2011. Population dynamics of living planktic foraminifers in the hemipelagic southeastern Bay of Biscay. Marine Micropaleontology 80(3-4), pp.89-100.

Reynolds, L., Thunell, R.C., 1985. Seasonal succession of planktonic foraminifera in the subpolar North Pacific. The Journal of Foraminiferal Research, 15, pp.282–301. https://doi.org/10.2113/gsjfr.15.4.282

Rimbu, N., Lohmann, G., Kim, J.H., Arz, H.W. and Schneider, R., 2003. Arctic/North Atlantic Oscillation signature in Holocene sea surface temperature trends as obtained from alkenone data. Geophysical research letters, 30(6).

Rimbu, N., Lohmann, G., Lorenz, S.J., Kim, J.H. and Schneider, R.R., 2004. Holocene climate variability as derived from alkenone sea surface temperature and coupled ocean-atmosphere model experiments. Climate Dynamics, 23, pp.215-227.

Risebrobakken, B., Jansen, E., Andersson, C., Mjelde, E. and Hevrøy, K., 2003. A high-resolution study of Holocene paleoclimatic and paleoceanographic changes in the Nordic Seas. Paleoceanography, 18(1).

Roberts, N.L., Piotrowski, A.M., McManus, J.F. and Keigwin, L.D., 2010. Synchronous deglacial overturning and water mass source changes. science, 327(5961), pp.75-78.

Robson, J., Ortega, P. and Sutton, R., 2016. A reversal of climatic trends in the North Atlantic since 2005. Nature Geoscience, 9(7), pp.513-517.

Rooth, C., 1982. Hydrology and ocean circulation. Progress in Oceanography, 11(2), pp.131-149.

Rosenthal, Y., Boyle, E.A. and Slowey, N., 1997. Temperature control on the incorporation of magnesium, strontium, fluorine, and cadmium into benthic foraminiferal shells from Little Bahama Bank: Prospects for thermocline paleoceanography. Geochimica et Cosmochimica Acta, 61(17), pp.3633-3643.

Sahoo, N., Saalim, S.M., Matul, A., Mohan, R., Tikhonova, A. and Kozina, N., 2022. Planktic Foraminiferal Assemblages in Surface Sediments From the Subpolar North Atlantic Ocean. Frontiers in Marine Science, 8, p.2045.

Salgueiro, E., Voelker, A.H., de Abreu, L., Abrantes, F., Meggers, H. and Wefer, G., 2010. Temperature and productivity changes off the western Iberian margin during the last 150 ky. Quaternary Science Reviews, 29(5-6), pp.680-695.

Sarafanov, A., 2009. On the effect of the North Atlantic Oscillation on temperature and salinity of the subpolar North Atlantic intermediate and deep waters. ICES Journal of Marine Science, 66(7), pp.1448-1454.

Sarafanov, A., Falina, A., Sokov, A. and Demidov, A., 2008. Intense warming and salinification of intermediate waters of southern origin in the eastern subpolar North Atlantic in the 1990s to mid-2000s. Journal of Geophysical Research: Oceans, 113(C12).

Sarafanov, A., Mercier, H., Falina, A. and Sokov, A., 2010. Cessation and partial reversal of deep water freshening in the northern North Atlantic: observation-based estimates and attribution. Tellus A: Dynamic Meteorology and Oceanography, 62(1), pp.80-90.

Scaife, A.A., Knight, J.R., Vallis, G.K. and Folland, C.K., 2005. A stratospheric influence on the winter NAO and North Atlantic surface climate. Geophysical Research Letters, 32(18).

Schiebel, R., 2002. Planktic foraminiferal sedimentation and the marine calcite budget. Global Biogeochemical Cycles, 16(4), 3-1.

Schiebel, R., Hemleben, C., 2000. Interannual variability of planktic foraminiferal populations and test flux in the eastern North Atlantic Ocean (JGOFS). Deep Sea Research Part II: Topical studies in Oceanography 47, 1809–1852. https://doi.org/10.1016/S0967-0645(00)00008-4

Schiebel, R., Hemleben, C., 2005. Modern planktic foraminifera. Paläontologische Zeitschrift, 79(1), pp.135-148. https://doi.org/10.1007/BF03021758

Schiebel, R., Hemleben, C., 2017. Planktic foraminifers in the modern ocean. Berlin: Springer. pp. 1-358

Schiebel, R., Hiller, B., Hemleben, C., 1995. Impacts of storms on recent planktic foraminiferal test production and CaCO3 flux in the North Atlantic at 47° N, 20° W (JGOFS). Marine Micropaleontology, 26(1-4), pp.115-129.

Schiebel, R., Spielhagen, R.F., Garnier, J., Hagemann, J., Howa, H., Jentzen, A., et al., 2017. Modern planktic foraminifers in the high-latitude ocean. Marine Micropaleontology. 136, pp.1–13. https://doi.org/10.1016/j.marmicro.2017.08.004

Schiebel, R., Waniek, J., Bork, M., Hemleben, C., 2001. Planktic foraminiferal production stimulated by chlorophyll redistribution and entrainment of nutrients. Deep Sea Research Part I: Oceanographic Research Papers, 48(3), pp.721-740. https://doi.org/10.1016/S0967-0637(00)00065-0

Schlitzer, R., 2015. Ocean data view.

Schmuker, B., 2000. The influence of shelf vicinity on the distribution of planktic foraminifera south of Puerto Rico. Marine Geology 166, pp.125–143. https://doi.org/10.1016/S0025-3227(00)00014-1

Schmuker, B., Schiebel, R., 2002. Planktic foraminifers and hydrography of the eastern and northern Caribbean Sea. Marine Micropaleontology. 46(3-4), pp.387-403.

Serreze, M.C., Barrett, A.P., Stroeve, J.C., Kindig, D.N. and Holland, M.M., 2009. The emergence of surface-based Arctic amplification. The Cryosphere, 3(1), pp.11-19.

Sévellec, F., Fedorov, A.V. and Liu, W., 2017. Arctic sea-ice decline weakens the Atlantic meridional overturning circulation. Nature Climate Change, 7(8), pp.604-610.

Sgubin, G., Swingedouw, D., Drijfhout, S., Mary, Y. and Bennabi, A., 2017. Abrupt cooling over the North Atlantic in modern climate models. Nature Communications, 8(1), p.14375.

Shackleton, N., 1967. Oxygen isotope analyses and Pleistocene temperatures re-assessed. Nature, 215(5096), pp.15-17.

Shepherd, A., Ivins, E., Rignot, E., Smith, B., van den Broeke, M., Velicogna, I., Whitehouse, P., Briggs, K., Joughin, I., Krinner, G. and Nowicki, S., 2018. Mass balance of the Antarctic Ice Sheet from 1992 to 2017. Nature.

Shepherd, A., Wingham, D., Wallis, D., Giles, K., Laxon, S. and Sundal, A.V., 2010. Recent loss of floating ice and the consequent sea level contribution. Geophysical Research Letters, 37(13).

Shindell, D.T., Schmidt, G.A., Mann, M.E., Rind, D. and Waple, A., 2001. Solar forcing of regional climate change during the Maunder Minimum. Science, 294(5549), pp.2149-2152.

Shukla, P.R., Skea, J., Calvo Buendia, E., Masson-Delmotte, V., Pörtner, H.O., Roberts, D.C., Zhai, P., Slade, R., Connors, S., Van Diemen, R. and Ferrat, M., 2019. IPCC, 2019: Climate Change and Land: an IPCC special report on climate change, desertification, land degradation, sustainable land management, food security, and greenhouse gas fluxes in terrestrial ecosystems.

Sicre, M.A., Jalali, B., Eiríksson, J., Knudsen, K.L., Klein, V. and Pellichero, V., 2021. Trends and centennial-scale variability of surface water temperatures in the North Atlantic during the Holocene. Quaternary Science Reviews, 265, p.107033.

Simstich, J., Sarnthein, M., Erlenkeuser, H., 2003. Paired $\delta^{18}O$ signals of *Neogloboquadrina pachyderma* (s) and *Turborotalita quinqueloba* show thermal stratification structure in Nordic Seas. Marine Micropaleontology, 48(1-2), pp.107-125.

Smeed, D., McCarthy, G., Rayner, D., Moat, B.I., Johns, W.E., Baringer, M.O. and Meinen, C.S., 2016. Atlantic meridional overturning circulation observed by the RAPID-MOCHA-WBTS (RAPID-Meridional Overturning Circulation and Heatflux Array-Western Boundary Time Series) array at 26N from 2004 to 2015. British Oceanographic Data Centre, National Oceanography Centre, NERC, UK. doi:10.5285/8cd7e7bb-9a20-05d8-e053-6c86abc012c2

Solignac, S., de Vernal, A. and Hillaire-Marcel, C., 2004. Holocene sea-surface conditions in the North Atlantic—contrasted trends and regimes in the western and eastern sectors (Labrador Sea vs. Iceland Basin). Quaternary Science Reviews, 23(3-4), pp.319-334.

Solignac, S., Giraudeau, J. and de Vernal, A., 2006. Holocene sea surface conditions in the western North Atlantic: Spatial and temporal heterogeneities. Paleoceanography, 21(2).

Spooner, P.T., Thornalley, D.J., Oppo, D.W., Fox, A.D., Radionovskaya, S., Rose, N.L., et al., 2020. Exceptional 20th century ocean circulation in the Northeast Atlantic. Geophysical Reeaserch Letters., 47(10), e2020GL087577. https://doi.org/10.1029/2020GL087577

Srokosz, M.A. and Bryden, H.L., 2015. Observing the Atlantic Meridional Overturning Circulation yields a decade of inevitable surprises. Science, 348(6241), p.1255575.

Staines-Urías, F., Kuijpers, A. and Korte, C., 2013. Evolution of subpolar North Atlantic surface circulation since the early Holocene inferred from planktic foraminifera faunal and stable isotope records. Quaternary Science Reviews, 76, pp.66-81. https://doi.org/10.1016/j.quascirev.2013.06.016

Stangeew, E., 2001. Distribution and Isotopic Composition of Living Planktonic Foraminifera *N. pachyderma* (sinistral) and *T. quinqueloba* in the High Latitude North Atlantic. [Ph.D. Thesis]. [Kiel]: Christian-Albrechts Universität

Stehman, C. F., 1972. Planktonic foraminifera in Baffin Bay, Davis Strait and the Labrador Sea. Atlantic Geology, 8(1), pp.13-19.

Stuiver, M. and Braziunas, T.F., 1993. Modeling atmospheric 14C influences and 14C ages of marine samples to 10,000 BC. Radiocarbon, 35(1), pp.137-189.

Sundby, S. and Drinkwater, K., 2007. On the mechanisms behind salinity anomaly signals of the northern North Atlantic. Progress in Oceanography, 73(2), pp.190-202.

Swift, J.H., 1984. The circulation of the Denmark Strait and Iceland-Scotland overflow waters in the North Atlantic. Deep Sea Research Part A. Oceanographic Research Papers, 31(11), pp.1339-1355.

Swift, J.H., Aagaard, K. and Malmberg, S.A., 1980. The contribution of the Denmark Strait overflow to the deep North Atlantic. Deep Sea Research Part A. Oceanographic Research Papers, 27(1), pp.29-42.

Taylor, J. R., Ferrari, R., 2011a. Shutdown of turbulent convection as a new criterion for the onset of spring phytoplankton blooms. Limnology and Oceanography, 56(6), pp.2293-2307. https://doi.org/10.4319/lo.2011.56.6.2293

Taylor, J. R., Ferrari, R., 2011b. Ocean fronts trigger high latitude phytoplankton blooms. Geophysical Reeaserch Letters. 38(23). https://doi.org/10.1029/2011GL049312

Thibodeau, B., Not, C., Zhu, J., Schmittner, A., Noone, D., Tabor, C., Zhang, J. and Liu, Z., 2018. Last century warming over the Canadian Atlantic shelves linked to weak Atlantic meridional overturning circulation. Geophysical Research Letters, 45(22), pp.12-376.

Thornalley, D.J., Barker, S., Becker, J., Hall, I.R. and Knorr, G., 2013. Abrupt changes in deep Atlantic circulation during the transition to full glacial conditions. Paleoceanography, 28(2), pp.253-262.

Thornalley, D.J., Elderfield, H. and McCave, I.N., 2009. Holocene oscillations in temperature and salinity of the surface subpolar North Atlantic. Nature, 457(7230), pp.711-714.

Thornalley, D.J., Elderfield, H. and McCave, I.N., 2010. Intermediate and deep water paleoceanography of the northern North Atlantic over the past 21,000 years. Paleoceanography, 25(1).

Thornalley, D.J., Oppo, D.W., Ortega, P., Robson, J.I., Brierley, C.M., Davis, R., Hall, I.R., Moffa-Sanchez, P., Rose, N.L., Spooner, P.T. and Yashayaev, I., 2018. Anomalously weak Labrador Sea convection and Atlantic overturning during the past 150 years. Nature, 556(7700), pp.227-230. https://doi.org/10.1038/s41586-018-0007-4

Thunell, R. C., 1978. Distribution of recent planktonic foraminifera in surface sediments of the Mediterranean Sea. Marine Micropaleontology. 3(2), pp.147-173.

Thunell, R., Sautter, L. R., 1992. Planktonic foraminiferal faunal and stable isotopic

indices of upwelling: a sediment trap study in the San Pedro Basin, Southern California Bight. Geol. Soc. Spec. Publ. 64(1), pp.77-91.

Thunell, R.C. and Reynolds, L.A., 1984. Sedimentation of planktonic foraminifera; seasonal changes in species flux in the Panama Basin. Micropaleontology, 30(3), pp.243-262.

Tolderlund, D. S., Bé, A. W., 1971. Seasonal distribution of planktonic foraminifera in the western North Atlantic. Micropaleontology, 17(3), pp.297-329.

Trenberth, K.E., Zhang, Y., Fasullo, J.T. and Cheng, L., 2019. Observation-based estimates of global and basin ocean meridional heat transport time series. Journal of Climate, 32(14), pp.4567-4583.

Trouet, V., Esper, J., Graham, N.E., Baker, A., Scourse, J.D. and Frank, D.C., 2009. Persistent positive North Atlantic Oscillation mode dominated the medieval climate anomaly. Science, 324(5923), pp.78-80.

Trouet, V., Scourse, J.D. and Raible, C.C., 2012. North Atlantic storminess and Atlantic Meridional Overturning Circulation during the last Millennium: Reconciling contradictory proxy records of NAO variability. Global and Planetary Change, 84, pp.48-55.

Ufkes, E., Jansen, J.F. and Brummer, G.J.A., 1998. Living planktonic foraminifera in the eastern South Atlantic during spring: indicators of water masses, upwelling and the Congo (Zaire) River plume. Marine Micropaleontology, 33(1-2), pp.27-53.

Vasskog, K., Langebroek, P.M., Andrews, J.T., Nilsen, J.E.Ø. and Nesje, A., 2015. The Greenland Ice Sheet during the last glacial cycle: Current ice loss and contribution to sea-level rise from a palaeoclimatic perspective. Earth-Science Reviews, 150, pp.45-67.

Vaughan, D.G., Marshall, G.J., Connolley, W.M., Parkinson, C., Mulvaney, R., Hodgson, D.A., King, J.C., Pudsey, C.J. and Turner, J., 2003. Recent rapid regional climate warming on the Antarctic Peninsula. Climatic change, 60, pp.243-274.

Visbeck, M., Chassignet, E.P., Curry, R.G., Delworth, T.L., Dickson, R.R. and Krahmann, G., 2003. The ocean's response to North Atlantic Oscillation variability. Geophysical Monograph-American Geophysical Union, 134, pp.113-146.

Volkmann, R., 2000. Planktic foraminifers in the outer Laptev Sea and the Fram Strait—Modern distribution and ecology. Journal of Foraminiferal Research, 30(3), pp.157-176. https://doi.org/10.2113/0300157

Waelbroeck, C., Labeyrie, L., Michel, E., Duplessy, J.C., Mcmanus, J.F., Lambeck, K., Balbon, E. and Labracherie, M., 2002. Sea-level and deep water temperature changes derived from benthic foraminifera isotopic records. Quaternary science reviews, 21(1-3), pp.295-305.

Walker, M.J., Berkelhammer, M., Björck, S., Cwynar, L.C., Fisher, D.A., Long, A.J., Lowe, J.J., Newnham, R.M., Rasmussen, S.O. and Weiss, H., 2012. Formal subdivision of the Holocene Series/Epoch: a Discussion Paper by a Working Group of INTIMATE (Integration of ice-core, marine and terrestrial records) and the Subcommission on Quaternary Stratigraphy (International Commission on Stratigraphy). Journal of Quaternary Science, 27(7), pp.649-659.

Wang, M. and Overland, J.E., 2012. A sea ice free summer Arctic within 30 years: An update from CMIP5 models. Geophysical Research Letters, 39(18).

Wanner, H., Solomina, O., Grosjean, M., Ritz, S.P. and Jetel, M., 2011. Structure and origin of Holocene cold events. Quaternary Science Reviews, 30(21-22), pp.3109-3123.

Weinkauf, M.F., Kunze, J.G., Waniek, J.J. and Kučera, M., 2016. Seasonal variation in shell calcification of planktonic foraminifera in the NE Atlantic reveals species-specific response to temperature, productivity, and optimum growth conditions. PLoS One, 11(2), p.e0148363.

Winton, M., 2006. Amplified Arctic climate change: What does surface albedo feedback have to do with it?. Geophysical Research Letters, 33(3).

Woollings, T., Hoskins, B., Blackburn, M. and Berrisford, P., 2008. A new Rossby wave–breaking interpretation of the North Atlantic Oscillation. Journal of the Atmospheric Sciences, 65(2), pp.609-626.

Yang, Q., Dixon, T. H., Myers, P. G., Bonin, J., Chambers, D., Van Den Broeke, M. R., et al. (2016). Recent increases in Arctic freshwater flux affects Labrador Sea convection and Atlantic overturning circulation. Nature Communications, 7(1), pp.1-8. https://doi.org/10.1038/ncomms10525

Žarić, S., Donner, B., Fischer, G., Mulitza, S., Wefer, G. (2005). Sensitivity of planktic foraminifera to sea surface temperature and export production as derived from sediment trap data. Marine Micropaleontology. 55, pp.75–105. https://doi.org/10.1016/j.marmicro.2005.01.002

Zhang, J., Weijer, W., Steele, M., Cheng, W., Verma, T. and Veneziani, M., 2021. Labrador Sea freshening linked to Beaufort Gyre freshwater release. Nature Communications,12(1), pp.1-8.

Zhang, R., 2008. Coherent surface-subsurface fingerprint of the Atlantic meridional overturning circulation. Geophysical Research Letters, 35(20).

Ziveri, P., Thunell, R. C., Rio, D., 1995. Export production of coccolithophores in an upwelling region: results from San Pedro Basin, Southern California Borderlands. Marine Micropaleontology, 24(3-4), pp.335-358.

Zweng, M. M., J. R. Reagan, D. Seidov, T. P. Boyer, R. A. Locarnini, H. E. Garcia, A. V. Mishonov, O. K. Baranova, K. Weathers, C. R. Paver, and I. Smolyar, 2018. World Ocean Atlas 2018, Volume 2: Salinity. A. Mishonov Technical Ed.; NOAA Atlas NESDIS 82, pp.50.